8-8-2017

Analysis of a Non-canonical Antiviral Mechanism in West Nile Virus-infected Mouse Cells

Dan Cui

ANALYSIS OF A NON-CANONICAL ANTIVIRAL MECHANISM IN WEST NILE VIRUS-INFECTED MOUSE CELLS

by

DAN CUI

Under the Direction of Margo Brinton, Ph.D.

ABSTRACT

Upon viral infection, host cells produce type I interferon (IFN), which activates the JAK-STAT signaling pathway and induces the expression of hundreds of interferon-stimulated genes (ISGs) to establish an antiviral state. In West Nile virus (WNV)-infected cells, the JAK-STAT signaling pathway is blocked by viral proteins. However, the expression of a subset of ISGs, which includes 2′-5′-oligoadenylate synthetase 1a (*Oas1a*), *Oas1b,* interferon regulatory factor 7 (*Irf7*), *Mx1*, and interferon-induced proteins with tetratricopeptide repeats 1 (*Ifit1*), is still upregulated by an IFN-independent mechanism in WNV-infected mouse embryonic fibroblasts (MEFs). Studies in cells with one or more components of RNA-sensing pathway knocked out

showed that the alternative ISG upregulation is activated through RIG-I or MDA5, and the downstream adaptor IPS-1. In cells with IRF3, 5 and 7 knocked out, the alternative ISG upregulation by WNV infection is reduced but not eliminated. As an initial means of discovering the transcription factors involved in this non-canonical ISG upregulation, the critical regulatory regions in the promoters of two representative ISGs, *Oas1b* and *Ifit1*, were mapped using a dual luciferase assay system with a NanoLuc luciferase promoter reporter in WNV-infected *Ifnar1*$^{-/-}$ MEFs. The region from -299 to -28 in the *Oas1b* promoter, and the region from -192 to -50 in the *Ifit1* promoter were identified as being important for upregulating non-canonical gene expression after WNV infection. Fine mapping identified enhancer and repressor sub-regions as well as transcription factor binding sites (TFBSs) putatively involved in the IFN-independent antiviral mechanism. Mutation of one identified TFBS in the ISG promoters reduced *Oas1b* and *Ifit1* promoter activities. In electrophoretic mobility shift assays (EMSAs), a unique band, which was detected in WNV-infected but not in mock-infected *Ifnar1*$^{-/-}$ MEF nuclear extracts, was not observed when a probe with the identified TFBS mutated was used, suggesting that a unique complex forms at the identified TFBS when it is in the context of the adjacent flanking regions. The unique complex appears to contain NF-κB components and IRF3, IRF5 or IRF7. Our findings provide new insights into the mechanism involved in non-canonical upregulation of ISGs after WNV infection.

INDEX WORDS: West Nile virus, IFN-independent signaling, Transcription factors, Interferon-stimulated genes, Interferon-stimulated response element, NF-κB

ANALYSIS OF A NON-CANONICAL ANTIVIRAL MECHANISM IN WEST NILE VIRUS-INFECTED MOUSE CELLS

by

DAN CUI

A Dissertation Submitted in Partial Fulfillment of the Requirements for the Degree of

Doctor of Philosophy

in the College of Arts and Sciences

Georgia State University

2017

ANALYSIS OF A NON-CANONICAL ANTIVIRAL MECHANISM IN WEST NILE VIRUS-INFECTED MOUSE CELLS

by

DAN CUI

Committee Chair: Margo Brinton

Committee: Richard Plemper

Casonya Johnson

Electronic Version Approved:

Office of Graduate Studies

College of Arts and Sciences

Georgia State University

August 2017

DEDICATION

To my parents, Yongsheng Cui and Ping Zheng

To my husband, Jiafeng Geng

With love

ACKNOWLEDGEMENTS

I would love to give my deepest gratitude to my PhD advisor and mentor, Dr. Margo Brinton, for her guidance, patience, encouragement, and support over the years on my PhD study. She is my role model of being a scientist. She not only teaches me how to properly perform scientific research but also provides me valuable training opportunities in scientific writing and presentation. She gives me enough freedom to explore the unknowns in my own way while providing indispensable guidance towards the right path.

I would love to thank my dissertation committee members, Dr. Richard Plemper and Dr. Casonya Johnson, for the invaluable insights and constructive suggestions on my research project. I am also grateful to Dr. Jae Hyung Lim for the scientific training and career advice that she provided to me during my first year at Georgia State University.

I would love to thank the Brinton lab members, past or present, Dr. Mausami Basu, Dr. Sean Courtney, Dr. Heather Vatter, Dr. Hsuan Liu, Dr. Han Di, Esther Morantz, Joe Madden, Ayisha Mclntyre, Heena Sadhwani, Jessica Siemer, Bronislava Stockman, and Fred Ede, for the technical assistance, encouragement, support, and friendship during the past years. The positive, collaborative environment we built together means a lot.

The journey of my PhD study would not be so enjoyable without the friendship along the way. I would love to thank my Bio-girls, Yin-Yin, Alex, Ashley, Chelsea, and Jessica, for all the wonderful memories inside and outside of school. I am thankful to my GSU friends, especially Jie, Jing, Nan, Hesong, Chen, and Xiaojun, for their support, care and encouragement.

Most importantly, I would love to express my heartfelt gratitude to my family members. It is the unconditional love, support, and faith from my mom, dad, and husband that make it happen. Love y'all.

TABLE OF CONTENTS

LIST OF TABLES

LIST OF FIGURES

LIST OF ABREVIATIONS

Dengue virus (DENV)

Yellow fever virus (YFV)

Japanese encephalitis (JEV)

Tick-borne encephalitis viruses (TBEV)

West Nile virus (WNV)

Zika virus (ZIKV)

Untranslated regions (UTR)

Capsid (C)

Premembrane (prM)

Envelop (E)

subgenomic RNA (sfRNA)

Dendritic cells (DCs)

Blood brain barrier (BBB)

Central neural system (CNS)

Interferon (IFN)

Multiple sclerosis (MS)

Pattern recognition receptors (PPRs)

Interferon-stimulated genes (ISGs)

Pathogen-associated molecular patterns (PAMPs)

Toll-like receptors (TLRs)

Double-stranded RNA (dsRNA)

TIR domain-containing adaptor inducing IFN-β (TRIF)

Tumor necrosis factor (TNF)

TNF receptor-associated factor 3 (TRAF3)

IκB kinase ε (IKKε)

TANK-binding kinase 1 (TBK1)

Myeloid differentiation primary response gene 88 (MyD88)

RIG-I like receptors (RLRs)

Retinoic acid inducible gene I (RIG-I)

Melanoma differentiation-associated gene 5 (MDA5)

Laboratory of genetics and physiology-2 (LGP2)

Caspase activation and recruitment domains (CARDs)

Mitochondrial antiviral signaling (MAVS)

Mitochondria-associated membranes (MAMs)

cGAS (cyclic GAMP-AMP synthase)

Stimulator of interferon genes (STING)

Type I IFN receptor (IFNAR)

IFN- γ receptor (IFNGR)

Gamma-activated sequence (GAS)

Gamma-activated factor (GAF)

dsRNA-activated protein kinase (PKR)

2′-5′ oligoadenylate synthestase (OAS)

Interferon-induced proteins with tetratricopeptide repeats (IFIT)

OAS-like (OASL)

Chikungunya virus (CHIKV)

Phosphoprotein phosphatase 1α (PP1α)

Tripartite motif protein 25 (TRM25)

RNA-binding domain (RBD)

Receptor-interacting protein 1 (RIP1)

Suppressors of cytokine signaling 1 (SOC1)

IFN-stimulated response element (ISRE)

IFN-stimulated genes (ISGs)

Interferon regulatory factor 9 (IRF9)

IRF-binding element (IRF-E)

Janus tyrosine kinase (JAK)

Mouse embryo fibroblasts (MEFs)

Fetal bovine serum (FBS)

Dulbecco's modified Eagle's medium (DMEM)

Non-essential amino acid (NEAA)

Transcription start site (TSS)

Transcription factor binding sites (TFBSs)

Caffeic Acid Phenethyl Ester (CAPE)

Vesicular stomatitis virus (VSV)

Electrophoretic mobility shift (EMSA)

CCAAT/enhancer-binding protein beta (CEBP/β)

1 INTRODUCTION

1.1 Flaviviruses

1.1.1 Genus Flavivirus

The family *Flaviviridae* currently contains four genera: *Flavivirus*, *Hepacivirus*, *Pestivirus*, and *Pegivirus*. The genus *Flavivirus* includes viruses transmitted by blood-feeding arthropods, several of which are emergent or re-emergent pathogens that are found on six continents. Viruses in this genus include dengue virus (DENV), yellow fever virus (YFV), Japanese encephalitis (JEV), tick-borne encephalitis viruses (TBEV), West Nile virus (WNV), and the recently emerged pathogen, Zika virus (ZIKV). Flavivirus infections in humans are responsible for significant morbidity and mortality (Fields *et al.*, 2013; Daep *et al.*, 2014).

1.1.2 Flavivirus genome characteristics and replication

Flaviviruses are enveloped viruses with an ~11-kb positive-sense, single-stranded RNA genome that encodes a single open reading frame with highly structured 5′ and 3′ flanking untranslated regions (UTR). The flavivirus genome has a 5′ type 1 cap structure, as do eukaryotic cell mRNAs. However, unlike the eukaryotic host mRNA, the flavivirus genome RNA does not contain a 3′ poly-A. The flavivirus replication life cycle begins with virion attachment to cell surface receptors, endocytosis, and fusion with the endosomal membrane resulting in the release of the viral genome RNA into the cytoplasm. The genome is translated by host machinery as a single polyprotein, which is subsequently cleaved by host and viral proteases to generate three structural [capsid (C), premembrane (prM), and envelop (E)] and seven non-structural (NS1, NS2A, NS2B, NS3, NS4A, NS4B, NS5) proteins. The non-structural proteins form the replication complex that is required for viral RNA synthesis on ER membrane. The nascent genome RNA is encapsidated by ER-membrane associated structural proteins. Following virion

assembly and transport through the host cellular secretory pathway, mature viral particles are released by exocytosis from an infected cell (Brinton, 2002). All tested viruses in the genus *Flavivirus*, including WNV, DEVN, TBEV, and YFV, also produce a unique 3′ noncoding subgenomic RNA (sfRNA) in infected cells, which is generated by cellular 5′ to 3′ exonuclease XRN1 digestion of genome RNA that is terminated by an RNA structure located RNA 3′ UTR (Funk *et al.*, 2010; Chapman *et al.*, 2014). The role of the sfRNA in the flavivirus replication cycle is not clear. However, it was shown that sfRNA contributes to flavivirus pathogenicity and evasion of the host immune response (Roby *et al.*, 2014).

1.1.3 Enzootic cycle and pathogenicity of WNV

WNV is a mosquito-borne virus that is present in Africa, Eastern Europe and the Mediterranean region, Russia, the Middle East, India, Australia, and the Americas. It was first discovered in the West Nile district of Uganda in 1937 (Kramer *et al.*, 2008). WNV emerged in New York City in the summer of 1999, then spread throughout the United States within four years and has continued to cause seasonal outbreaks (Komar, 2003; Reisen, 2013). In nature, WNV is maintained in a transmission cycle between birds and mosquitos, predominantly *Culex* mosquito species that prefer to bite birds over humans. However, WNV is sometimes transmitted to a person by a mosquito bite. Unlike DENV- or ZIKV-infected humans, humans infected with WNV are dead-end hosts and not part of the enzootic cycle because they have low viremia levels. Although WNV infections in humans are usually asymptomatic, some people develop fever and flu-like symptoms and less than 1 % of WNV-infected patients develop neurological diseases, such as encephalitis, meningitis, or poliomyelitis. Older adults are at greater risk of developing severe symptoms (Dauphin and Zientara, 2007). The central nervous system damage caused by a WNV infection is non-reversible. The study of WNV-host interactions provides

valuable insights for the development of vaccines and the identification of targets for antiviral drug development.

WNV infections in human are usually the result of a mosquito bite. During blood-feeding, mosquitos inject their saliva into human skin, which contains WNV particles and some molecules that reduce inflammation and alter host immunity (Titus *et al.*, 2006). WNV pathogenesis in humans is not well characterized, but studies in rodent models have provided some insights. Following a mosquito bite, WNV replicates in local skin cells, including keratinocytes, dermal dendritic cells (DCs), and Langerhans cells. After DC migration, viral particles infect the regional draining lymph node, and subsequently migrate in the blood to the spleen, cross the blood brain barrier (BBB) and infect the central neural system (CNS) causing neuron damage (Suthar *et al.*, 2013). Host innate and adaptive immune responses work together to clear a WNV infection and limit possible damage due to an immune response.

1.1.4 WNV strain diversity

Based on the comparison of the amino acid sequences of the envelope protein, WNV isolates have been divided into lineage1 and lineage 2 (Berthet *et al.*, 1997). Lineage 1 consists of strains that are often associated with outbreaks of human encephalitis and meningitis, including NY99 and Eg101 (Lanciotti *et al.*, 1999; Brinton, 2002). A WNV strain that is endemic to Australia and Asia, Kunjin virus, also belongs to lineage 1 but has an attenuated phenotype in humans (Beasley *et al.*, 2005). Lineage 2 strains are restricted to Africa and are usually less pathogenic, but several recent neuroinvasive cases associated with endemic lineage 2 WNV suggest that the virulence of WNV strains in this linage may be underestimated (Venter and Swanepoel, 2010). Recent studies of the genome sequences of additional WNV isolates suggest that some WNV isolates cannot be grouped into lineage 1 or 2. A phylogenetic analysis

that used partial genome sequences (C-prM-E) added three additional genetic lineages for WNV strains (Bakonyi *et al.*, 2005; Bondre *et al.*, 2007). Because only a few isolates have recently been found for lineages 3, 4, and 5, little is known about their phenotypes (Suthar *et al.*, 2013).

1.1.5 WNV replication cycle

The cell surface receptor(s) used for WNV attachment and entry is unknown (Brinton, 2002; 2014). WNV particles enter cells via receptor-mediated endocytosis, and viral RNA is released into the cell cytoplasm following fusion of the viral and cellular endosomal membranes. The WNV genome encodes three structural proteins (C, prM, E) and seven non-structural proteins (NS1, NS2A, NS2B, NS3, NS4A, NS4B, NS5). Many of the non-structural proteins have multiple functions, but all contribute to facilitate virus RNA replication. The 3′ and 5′ terminal regions of the WNV genome has been shown to interact with each other to regulate viral minus strand RNA replication, and interaction between some cell proteins and the terminal viral RNAs may promote virus RNA replication (Brinton and Basu, 2015).

1.2 Host cell interferon (IFN) antiviral response

The IFN response serves as an essential component of mammalian cell innate antiviral defense. IFN was first described by Alick Isaacs and Jean Lindenmann in 1957 as a phenomenon of "conditions that disrupted virus information" (Isaacs and Lindenmann, 1957). In the 1970s, it was found that there is a family of IFN proteins. During the next two decades, it was demonstrated that IFNs were not only effective in defending against virus diseases and cancer but also for treating multiple sclerosis (MS). As the intercellular molecular events involved in the production of IFN as well as the intercellular networks stimulated by IFN being elucidated, it became clear that IFNs are fundamental components of the innate immune system (Borden *et al.*, 2007). To date, three types of IFNs (type I, III, III) have been identified.

Either the incoming virion or viral genome or viral molecules produced in infected cells are sensed by host cell sensors, called pattern recognition receptors (PPRs). These membrane-bound or cytoplasmic PPRs activate downstream signaling pathways that lead to the production of different kinds of cytokines and chemokines. Secreted IFNs are important cytokines that bind to cell surface IFN receptors, activate signaling pathways and induce an antiviral state in infected and uninfected cells by upregulating the expression of hundreds of interferon-stimulated genes (ISGs). The antiviral function of these ISGs establishes an antiviral state, forming the first line of immune response to virus infection. The IFN response in host cells is classified into three phases: induction of IFN expression, activation of the IFN effector pathway, and expression of ISGs.

1.2.1 Host PPRs that induce IFN expression after a flavivirus infection

The membrane-bound and cytoplasmic PRRs in mammalian cells serve as a sophisticated immune surveillance network to sense unique features of invading viral pathogens. Unique features of viruses, termed pathogen-associated molecular patterns (PAMPs), include viral nucleic acids, proteins and carbohydrates (Brennan and Bowie, 2010; Wilkins and Gale, 2010). Three major classes of PPRs have been shown to contribute to efficient detection of a flavivirus infection. IFNs are induced through the signaling pathways downstream of an activated PRR after virus infection.

1.2.1.1 Toll-like receptors (TLRs)

TLRs are transmembrane proteins that serve as membrane-bound PRRs. There are 10 TLR family members encoded by the human genome and 12 by the mouse genome. TLR3, TLR7, TLR8, and TLR9 detect viral nucleic acids in endosomal compartments. Except for TLR9, which recognizes CpG-rich regions of viral DNA, the other TLRs, TLR3, TRL7, and TL8, are of importance in sensing a flavivirus infection. The RNA ligands detected by the three

flavivirus-activated TLRs differ. TLR3 recognizes double-stranded RNA (dsRNA) or a stem-loop in a ssRNA; TLR7 and TLR8 recognize GU-rich ssRNA (Akira *et al.*, 2006; Uematsu and Akira, 2007).

TLR3 is expressed in immune cells as well as in non-immune cells, such as fibroblasts, epithelial cells, and endothelial cells. Following ligand binding, TLR3 recruits the adaptor molecule TIR domain-containing adaptor inducing IFN-β (TRIF) and signals through TNF receptor-associated factor 3 (TRAF3) and TRAF6 to activate the kinase IκB kinase ε (IKKε) and TANK-binding kinase 1 (TBK1), which activates the transcription factors IRF3, IRF7 and NF-κB that trigger the transcription of IFN and pro-inflammatory cytokine genes (Akira *et al.*, 2006; Wang *et al.*, 2011). The role of TLR3 in the innate immune response against a WNV infection is complicated and controversial. In a study of WNV infections in TLR3-/- mice, two independent research groups demonstrated distinct outcomes of a WNV infection (Wang *et al.*, 2004; Daffis *et al.*, 2008). One study showed that TLR3-/- mice were more resistant to WNV infection suggesting that impaired TLR3-dependent pro-inflammatory cytokine production leads to increased penetration of the blood brain barrier and higher incidence of lethal infection (Wang *et al.*, 2004). The other study found that TLR3-/- mice were more susceptible to WNV infection as evidenced by increased viral burdens in the brain, suggesting that TLR3 contributes to restrict the viral infection and replication in neurons (Daffis *et al.*, 2008). Interestingly, there is no difference in the IFN levels produced between WNV-infected TLR3-/- and wild-type fibroblasts, dendritic cells, or mice (Daffis *et al.*, 2008), indicating that TLR3 is dispensable for IFN induction in response to a WNV infection, and different PRRs are responsible for the induction of IFN after WNV infection. The results from a study of human susceptibility to WNV infection

suggested that higher levels of TLR3 in macrophages from aged donors leads to elevated levels of pro-inflammatory cytokines and increased central nervous system disease (Kong *et al.*, 2008).

The expression of TLR7 and TLR8 is mainly restricted to dendritic cells, macrophages, and B cells. TLR7 and TLR8 transmit signals through the adaptor molecule myeloid differentiation primary response gene 88 (MyD88), activating IRF7 and NF-κB, which activate the expression of IFNs and pro-inflammatory cytokines (Akira *et al.*, 2006; Wang *et al.*, 2011). TLR7 and its adaptor molecule MyD88 play a protective role against WNV-induced encephalitis in mice. TLR7-/- mice and Myd88-/- mice both showed increased susceptibility to lethal WNV infection, which appears to be linked to increased viral burden in the brain (Town *et al.*, 2009; Szretter *et al.*, 2010). It is suggested that TLR7 and MyD88 provide protection against a WNV infection by reducing immune cell migration to infected cell target sites. However, after WNV infection, MyD88-/- mice showed a reduced IFN response while TLR7-/- mice showed an elevated level of IFN in the blood, suggesting that the activation of IFN production occurs through cross talk between signal pathways downstream of multiple PRRs.

1.2.1.2 RIG-I like receptors (RLRs)

The cytosolic RNA sensors, RLRs, are considered to be key intracellular PRRs for the detection of a flavivirus infection. RLRs family receptors, which include the retinoic acid inducible gene I (RIG-I), melanoma differentiation-associated gene 5 (MDA5, also known as IFIH1) and laboratory of genetics and physiology-2 (LGP2, also known as DHX58), are expressed in most cell types. All three RLRs contain a DExD/H helicase domain and a C-terminal domain, which are both essential for binding viral RNA. In addition, RIG-I and MDA5 have two N-terminal caspase activation and recruitment domains (CARDs), which are protein-protein interaction domains that are required for mediating antiviral signaling downstream of

RNA recognition (Wilkins and Gale, 2010). In contrast, LGP2 lacks both CARDs and the signaling effector domain and has been suggested to function as a regulator of RIG-I and MDA5; however, its mode of action could be positive or negative regulation (Satoh *et al.*, 2010; Wang *et al.*, 2011; Bruns and Horvath, 2012; Malur *et al.*, 2012).

In the cytoplasm of a virus infected cell, the recognition of viral RNA activates the enzymatic functions of RIG-I and MDA5 and initiates signal transduction pathways via the adaptor protein mitochondrial antiviral signaling (MAVS), which is also called IPS-1, VISA, or Cardif, localizing at the mitochondria, mitochondria-associated membranes (MAMs) and peroxisomes (Barral *et al.*, 2009; Gack, 2014). The activation of RIG-I or MDA5 and their subsequent transportation to IPS-1 are tightly controlled by an interplay of ubiquitination and phosphorylation modifications (Gack, 2014). IPS-1 transduces signaling that activates transcription factors such as NF-κB, IRF3, IRF7, and ATF2/c-Jun, resulting in the production of antiviral IFNs for the establishment of a broadly effective cellular antiviral state.

RLRs recognize pathogen patterns that are highly specific to viral RNAs and distinct from host 5′-capped mRNA. Although RIG-I and MDA5 are structurally similar, they have distinct ligand preferences that enable them to recognize the RNAs of different viruses. Early studies suggested that the viral pathogens detected by RIG-I and MDA5 were non-overlapping. However, new evidence suggests that both of RIG-I and MDA5 contribute to efficient detection of VSV, Sendai virus, DENV and WNV infections (Wilkins and Gale, 2010; Gack, 2014). A significant amount of research has been focused on understanding the molecular signatures that are required for recognition by RLRs. Results from experiments with synthetic or purified viral RNAs showed that RIG-I recognizes ssRNA with a 5′-triphosphate or short blunt-end dsRNA to distinguish non-self from self RNA (Kell and Gale, 2015). The 5′-triphosphate moiety that

stimulates RIG-I could be from the viral RNAs produced during replication or the RNA of incoming virions (Weber *et al.*, 2013). In addition, particular sequence compositions of the RNA ligand play a role in RIG-I recognition. The poly-U/UC motifs in HCV genomic RNA activate RIG-I in combination with a 5′-triphosphate moiety (Saito *et al.*, 2008). In contrast, the characteristics of MDA5 RNA ligands have not yet been well defined. The current thought is that MDA5 recognizes long dsRNA (greater than 1 kb in length) and synthesized RNAs, such as poly (I:C). Recognition by MDA5 does not require a 5′-triphosphalation on RNA (Schlee, 2013).

In the context of detecting a WNV infection, RLR signaling is crucial for activating the innate and adaptive immune responses. Moreover, the roles of RIG-I and MDA5 are essential and non-redundant in detecting WNV infection. Studies with WNV-infected RIG-I or MDA5 knockout cells showed that at early times of infection, RIG-I is activated to contribute to innate immune protection, while at later times, MDA5 sustains and amplifies the antiviral response. IPS-1 was indispensable for the RIG-I and MDA5 downstream signaling that controls WNV infection (Fredericksen *et al.*, 2008; Errett *et al.*, 2013). Both RIG-I-/- and MDA5-/- mice showed increased mortality after WNV challenge and double knock out RIG-$I^{-/-}$ /$MDA5^{-/-}$ mice developed severe pathogenesis after WNV infection, similar to what was observed in IPS-1-/- mice (Suthar *et al.*, 2010; Errett *et al.*, 2013). Additional studies showed that the exposed 5′ triphosphate and dsRNA structure activating RIG-I and MDA5 were produced during WNV genome replication rather than those present on the incoming virion RNA (Shipley *et al.*, 2012; Errett *et al.*, 2013). LGP2 is not essential for inducing an innate immune response to a WNV infection. The elevated susceptibility of LGP2-/- mice to WNV infection is linked to a defect in T cell expansion, which is not virus specific (Suthar *et al.*, 2012). A study of WNV-infected IPS-1-/- cells and mice suggested that the RLR signaling is not only important for inducing an innate

immune response but also plays a role in regulating inflammation and modulating the adaptive immune response (Suthar *et al.*, 2010).

1.2.1.3 cGAS-STING-dependent sensors

cGAS (cyclic GAMP-AMP synthase) is a cytosolic DNA sensing enzyme. cGAS is known to be triggered by DNA viruses and activates the production of IFN through stimulator of interferon genes (STING, also known as MITA, MPYS or ERIS) and downstream IRF3 (Barber, 2015). STING, which was also shown to transduce signaling downstream of RIG-I, is associated with the ER. cGAS-STING signaling was recently shown to be able to restrict DENV and WNV infections, which is surprising because cGAS is a DNA-sensing PRR (Gack and Diamond, 2016). Ectopically expressed cGAS restricts WNV replication in human cells. In cGAS-/- cells, WNV replicates to a higher level compared to WT control cells and cGAS-/- mice exhibited elevated susceptibility to lethal WNV infection (Schoggins *et al.*, 2014). The mechanism by which cGAS protects the host from a WNV infection seems to be through maintaining a basal immune response. Consistent with characteristics of the cGAS-/- mice, STING-/- mice are more susceptible to lethal WNV infection (You *et al.*, 2013). The cGAS-STING induced immune response is effective against DNA viruses and only some of positive-sense single-stranded RNA viruses, but how it is activated during an RNA virus infection has not yet been elucidated. Possible ligands for cGAS activation in cells infected with a positive-sense, single-stranded RNA virus infection include viral genome RNA, cDNA, dsRNA, and host cell-derived DNA. It was suggested that STING could be activated by virus-induced ER membrane remodeling or by fragments of mitochondrial DNA released from focal areas of virus-induced mitochondrial fragmentation (Holm *et al.*, 2012; Maringer and Fernandez-Sesma, 2014).

1.2.2 IFNs

The expression of IFN genes in response to a stimulus is tightly controlled by some gene-specific transcription repressors and sequence-specific transcription factors, which is the main controlling level of IFN production (Levy *et al.*, 2011). To date, three types of IFNs have been identified. Type I IFNs, which include IFN-α, IFN-β, IFN-ε, IFN-κ, and IFN-ω, are secreted by almost all cell types in mammals. Each of the type I IFNs is encoded by a single gene except for IFN-α of which there are 13 subtypes in humans. Type I IFNs interact with the type I IFN receptor (IFNAR) that is composed of the IFNAR1/IFNAR2 heterodimer on the cell surface. Nearly every cell type expresses receptors for type I IFNs (Takaoka and Yanai, 2006; Maher *et al.*, 2007). Type II IFN, which includes only one species, IFN-γ, is produced by activated T lymphocytes, monocytes, and NK cells, and binds to the IFN- γ receptor (IFNGR) composed of an IFNGR1/IFNGR2 heterodimer (Takaoka and Yanai, 2006). IFN- γ plays a crucial role in bridging the innate and adaptive responses (Schroder *et al.*, 2004). Type III IFNs, which include IFN-λ1 (IL-29), IFN-λ2 (IL-28A), IFN-λ3 (IL-28B), and IFN-λ4, bind to the IFN-λ receptor composed of IFNLR1/IL-10Rβ (Fox *et al.*, 2009; Levy *et al.*, 2011). Expression of the IFN-λ receptor is not well characterized with respect to cell type. It was originally thought to be limited primarily to epithelial cells. Later studies demonstrated that hepatocytes express IFNLR1 and respond to IFN-λ treatment (Sommereyns *et al.*, 2008; Muir *et al.*, 2010).

1.2.3 IFN signaling: The JAK-STAT pathway

The binding of IFN to receptors located on both infected and adjacent uninfected cells activates the JAK kinases that are associated with the cell surface IFN receptors, leading to the JAK-STAT pathway signaling that activates ISG expression. Four mammalian JAKs were discovered: JAK1, JAK2, JAK3, and TYK2. In the absence of a stimulus, the JAK proteins are

in an inactivate conformation. After type I IFN binding to the IFNAR1/2 heterodimer, the JAK1/TYK2 kinases become activated and phosphorylate STAT1 and STAT2 on specific tyrosines. The phosphorylated STATs interact with IRF9 to form the transcription factor complex ISGF3 that translocates into the nucleus and binds to the ISRE of ISG promoters to activate their expression (Takaoka and Yanai, 2006; Borden *et al.*, 2007; Wilkins and Gale, 2010; Stark and Darnell, 2012). Type III IFN also activates JAK1 and TYK2 to activate the formation of ISGF3 to induce ISG expression. However, type II IFN activates JAK1 and JAK2, which activate tyrosine phosphorylation and dimerization of STAT1 that induces the expression of ISGs through the gamma-activated sequence (GAS) promoter element. The STAT1 homodimer responding to type II IFN is also called gamma-activated factor (GAF) (Borden *et al.*, 2007).

The JAK-STAT pathway was defined in the 1990s. The trimeric ISGF3 complex is an essential component of JAK-STAT signaling activated by type I and type III IFN. It was subsequently discovered that in addition to the canonical ISGF3 complex with both STAT1 and STAT2 tyrosine phosphorylated, there are another two forms of ISGF3 with transcription factor function. In one, only STAT1 is tyrosine phosphorylated and binds to non-phosphorylated STAT2 and IRF9, which forms in response to IFN-γ (Morrow *et al.*, 2011). The other is non-phosphorylated STAT1 and STAT2 binding to IRF9, which forms in response to type I IFNs to prolong the expression of a subset of ISGs (Cheon and Stark, 2009; Stark and Darnell, 2012). All three forms of ISGF3 can bind to the ISRE (Fink and Grandvaux, 2013; Majoros *et al.*, 2017). The versatile functions of STAT1 are tightly regulated by its post-translational modifications. Besides tyrosine phosphorylation, phosphorylation of STAT1 on serine 708 induced by IKKε can regulate the expression of some ISGs (Tenoever *et al.*, 2007; Perwitasari *et al.*, 2011).

Moreover, this serine phosphorylation inhibits the homodimerization of STAT1 but does not disrupt ISGF3 formation, thus distinguishing type II IFN signaling activation from type I and type III IFN (Ng *et al.*, 2011). During the early stages of ISG induction, STAT1 is tyrosine phosphorylated, but unphosphorylated STAT1 functions during the late stages of ISG expression prolongation after virus infection (Levy and Darnell, 2002; Stark and Darnell, 2012).

The mammalian STAT protein family consists of 7 members: STAT1, STAT2, STAT3, STAT4, STAT5A, STAT5B, and STAT6. They are expressed in different tissues and respond to various cytokines. For example, STAT6 is mainly distributed in bone-marrow-derived cells; STAT3 gets tyrosine phosphorylated in response to IL-6, while STAT1 and STAT2 respond to IFNs (Aaronson and Horvath, 2002; Cheon *et al.*, 2011). In addition to the well-studied ISGF3 complex and STAT1 dimer, increasing numbers of reports suggest that additional STAT proteins play a role in the IFN response. Some other STAT containing complexes, including a STAT3 homodimer, a STAT5 homodimer, a STAT2/STAT1 heterodimer, and a STAT5/CRKL heterodimer, can be induced by IFNs to mediate gene transcription (Brierley and Fish, 2005). In response to different subtypes of type I IFNs, different human leukocyte subsets employ signaling mediated by different STAT proteins, suggesting a cell-type specificity of the IFN response. In addition, the cell-type specific responses to type I IFNs might be activated by several different kinases besides JAKs, including PI3K and p38 kinase (van Boxel-Dezaire *et al.*, 2006; van Boxel-Dezaire *et al.*, 2010).

1.2.4 The IFN response elements of ISG promoters

The two major DNA regulatory elements, ISRE and GAS, on the promoters of ISGs have been shown to mediate the gene expression as a result of the activation of the JAK-STAT pathway.

1.2.4.1 ISRE consensus

The ISRE, with the consensus sequence 5′-A/GNGAAANNGAAACT-3′ (Darnell *et al.*, 1994), is the DNA motif that the trimeric factor ISGF3 complex, which is composed of STAT1, STAT2, and IRF9, binds to in response to type I and type III IFN binding to their cell surface receptors. The binding of the ISGF3 complex to the ISRE site leads to expression of ISGs required for the innate antiviral immune response. The exact DNA binding contacts of the ISGF3 complex are not known, as no co-crystal structure of ISGF3-ISRE has been solved.

Recent studies suggested some non-canonical proteins can bind to the ISRE downstream of type I IFN binding to its receptor. An ISGF3-like complex containing STAT6, STAT2 and IRF9 was observed binding to the ISRE element in type I IFN-stimulated B cells (Gupta *et al.*, 1999; Fink and Grandvaux, 2013). In the absence of STAT1, STAT2 and IRF9 alone can form a complex that binds to the ISRE sequence to regulate the expression of some ISGs and establish an antiviral response to DENV infection (Kraus *et al.*, 2003). Similar STAT1-independent resistance has been reported against other kinds of virus infections (Perry *et al.*, 2011; Blaszczyk *et al.*, 2015; Majoros *et al.*, 2017).

The consensus sequence of the ISRE partially overlaps that of the IRF-binding elements (IRF-E) which have the consensus sequence 5′-AANNGAAANNGAAA-3′. The IRF-E site is recognized by proteins from the IRF family (Fujii *et al.*, 1999; Taniguchi *et al.*, 2001). The exact nucleotide sequence of the binding site for each IRF family member is slightly different. Studies show that besides ISGF3, IRF7 can bind to the ISRE and regulate ISG expression. ISREs can be grouped into IRF7-specific, ISGF3-specific, and universal ISREs (Schmid *et al.*, 2010).

1.2.4.2 GAS consensus

The GAS site, with the canonical consensus sequence 5′-TTCNNNGAAA-3′, is the DNA motif that the STAT1 homodimer binds to in response to type II IFN (Aaronson and Horvath, 2002). Recent studies have reported that some other STAT complexes can recognize GAS-like elements after type I IFN treatment. A STAT2 homodimer can modulate expression of a subset of ISGs through binding to a GAS-like site with a palindromic sequence of TTNNNNAA in response to type I IFN; a STAT1/STAT2 heterodimer can bind to another GAS-like site with the consensus sequence ATTCCCNGAAA, which is found in the promoter of IRF1 (Ghislain *et al.*, 2001; Brierley *et al.*, 2006). The binding affinity between a STAT dimer and a DNA sequence is determined by the nucleotide sequence as well as by cooperative interactions between the STAT dimer and adjacent proteins on the promoter (Aaronson and Horvath, 2002).

1.2.5 The antiviral functions of ISGs

ISGs are a diverse group of hundreds of genes, whose expression establishes an antiviral state in infected cells. Each type of IFN induces a different set of ISGs, and these sets of ISGs partially overlap (Der *et al.*, 1998). The ISGs can inhibit almost every step of a virus life cycle in the host cells, including virus entry, translation, viral genome replication and transcription, viral particle assembly and escape (de Veer *et al.*, 2001; Schneider *et al.*, 2014). The antiviral functions of some of the proteins encoded by ISGs have been studied in recent years using a siRNA library screen to knock down or a vector to overexpress single ISG. A number of ISGs were found to have antiviral functions against influenza viruses, flaviviruses or alphaviruses (Itsui *et al.*, 2006; Zhang *et al.*, 2007; Jiang *et al.*, 2008; Brass *et al.*, 2009; Brehin *et al.*, 2009; Jiang *et al.*, 2010). Proteins encoded by ISGs known to have antiviral functions include dsRNA-activated protein kinase (PKR), MX1, 2′-5′ oligoadenylate synthetase (OAS1 and OAS3),

ISG15, ISG20, IFITM-1, -2 and -3, and viperin (also known as RSAD2). A screen of more than 380 ISGs against six viruses confirmed the antiviral functions of IFITM, OAS, ISG15, ISG20, viperin, MX, and IRF7 proteins, and identified additional antiviral proteins encoded by ISGs, including interferon-induced proteins with tetratricopeptide repeats (IFIT) proteins and IRF1. Most of the ISGs that have direct antiviral functions show antiviral activities against a wide range of viruses (Schoggins *et al.*, 2011). Among the >300 known ISGs, some are components of the IFN induction and JAK-STAT pathways, such as RIG-I, MDA5, IRF7, IRF9, and STAT1. However, the functions of the majority of the >300 ISGs have still not been fully described. It is suggested that the combined functions of multiple ISGs increase the magnitude of the antiviral activity (Schoggins and Rice, 2011; Schneider *et al.*, 2014). However, a small subset of ISGs was shown to be able to enhance the replication of a particular virus species, indicating the complexity of the IFN system (Schoggins and Rice, 2011).

1.2.5.1 OAS family

Once an OAS protein is activated by double-stranded RNA, it catalyzes the formation of unique 2′-5′ linked oligoadenylates from ATP, which serve as second messengers for the dimerization and activation of endonuclease RNase L. Activated RNase L degrades both cellular and viral ssRNA (Silverman, 2007). Expression of the OAS gene is activated by IFN signaling and regulated by the ISRE in the OAS gene promoter (Rutherford *et al.*, 1988). Moreover, the OAS-RNase L system is an important IFN-induced antiviral pathway for several types of viruses, including flaviviruses, picornaviruses, alphaviruses, and herpesviruses (Austin *et al.*, 2005; Silverman, 2007; Brehin *et al.*, 2009; Hornung *et al.*, 2014).

The human OAS family contains four genes: OAS1, OAS2, OAS3, and OAS-like (OASL). The OAS1, OAS2, OAS3 proteins all have the 2′-5′ oligoadenylate synthase activity,

whereas the OASL protein provides antiviral activity by enhancing the activation of RIG-I signaling (Zhu *et al.*, 2014). In contrast, the mouse OAS family contains eight Oas1 genes (Oas1a to Oas1h), one Oas2, one Oas3, and two Oasl genes (Oasl1 and Oasl2) (Justesen *et al.*, 2000). The mouse Oas1 isoforms were generated by gene duplication (Perelygin *et al.*, 2006). Among the eight mouse Oas1 proteins, only Oas1a and Oas1g have been reported to have OAS enzymatic activity (Kakuta *et al.*, 2002). The non-enzymatic Oas1b has a specific antiviral activity against members of the genus *Flavivirus* that is independent of the OAS/RNase L pathway (Scherbik *et al.*, 2007a; Elbahesh *et al.*, 2011). Oas1d, which also encodes a non-enzymatic OAS protein, was reported to be involved in germline development (Yan *et al.*, 2005). The mouse Oas12 has OAS enzymatic activity, but Oasl1 does not (Eskildsen *et al.*, 2003). Mouse Oas1l has been shown to negatively regulate the production of type I IFN by inhibiting the translation of IRF7, the transcription factor that positively regulates the expression of IFN genes (Lee *et al.*, 2013).

1.2.5.2 IFIT family

Interferon-induced proteins with tetratricopeptide repeats (IFIT) are highly induced by type I or type III IFN treatment or by a viral infection. Proteins of the IFIT family, which have no known enzymatic activities, inhibit viral replication in host cells through binding to viral RNA together with other host proteins, and decrease virus transcription and translation (Fensterl and Sen, 2015).

The human IFIT family consists of four members: IFIT1 (ISG56), IFIT2 (ISG54), IFIT3 (ISG60 or IFIT4), and IFIT5 (ISG58). The genes encoding human IFIT proteins are clustered together on chromosome 10. A human pseudogene *IFIT1B* has been identified on human chromosome 13, but it remains uncharacterized (Diamond, 2014). The mouse Ifit family consists

of three characterized members: Ifit1 (Isg56), Ifit2 (Isg54), and Ifit3 (Isg49). The murine *Ifit* genes are clustered on chromosome 19qC1. The same locus also contains three additional uncharacterized members: *Ifit1b*, *Ifit1c*, and *Ifit3b* (Fensterl and Sen, 2015). All human and mouse *IFIT* genes, except for human *IFIT1B*, have one or two ISREs within 200 bp upstream of the transcription start site, which drives their stimulus-dependent expression (Fensterl and Sen, 2011).

Antiviral functions have been demonstrated for several IFIT proteins. IFIT proteins localize in the cytoplasm and inhibit cellular translation initiation by interaction with eIF3, which is a large protein complex consisting of 13 different subunits termed eIF3a-m (Damoc *et al.*, 2007). In human cells, IFIT1 and IFIT2 both bind to the eIF3e subunit, and IFIT2 additionally binds to eIF3c; in mouse, Ifit1 and Ifit2 selectively bind to eIF3c subunit. The binding of IFIT proteins to eIF3 subunits prevents the formation of the preinitiation complex 48S (Hui *et al.*, 2005; Terenzi *et al.*, 2005; Terenzi *et al.*, 2006). IFIT proteins block viral protein translation as well as cell protein translation in infected cells.

Mammalian cellular mRNAs contain a 5′ N-7 methylated guanosine cap linked by a 5′-to-5′ triphosphate bridge to the first base, the ribose of which is further modified by methylation at the 2′-O position (Decroly *et al.*, 2011). These modifications assist in translational control as well as in distinguishing self from non-self RNA. Both human IFIT1 and mouse Ifit1 recognize 2′-O unmethylated RNA and 5′-ppp RNA as non-self RNA. IFIT1 recognizes viral RNAs with these types of 5′ ends and acts as an effector molecule to suppress viral translation. The full antiviral function after IFIT1 binding to 5′-ppp RNA requires the binding of IFIT2 and IFIT3 to IFIT1 (Pichlmair *et al.*, 2011; Diamond, 2014). Human IFIT5 also binds to 5′-ppp RNA, but it is not in the same complex with IFIT1, IFIT2, and IFIT3. The exact antiviral function of IFIT5 is

not clear, but the protein was shown to co-localize with the cellular cytosolic sensor RIG-I (Katibah *et al.*, 2013; Vladimer *et al.*, 2014).

Besides binding to host proteins and viral nucleic acids, IFIT1 protein has been demonstrated to directly bind to a viral protein E1, which is a viral helicase encoded by human papillomavirus (HPV) (a double-stranded DNA virus). The binding of IFIT1 to E1 sequesters this viral helicase in the cytoplasm thus preventing it from aiding viral replication within the nucleus (Terenzi *et al.*, 2008).

1.2.5.3 IRF family

The interferon regulatory factor (IRF) family consists of nine members in mammals: IRF1, IRF2, IRF3, IRF4 (also known as PIP or ICSAT), IRF5, IRF6, IRF7, IRF8 (also known as ICSBP), and IRF9 (also known as ISGF3γ) (Taniguchi *et al.*, 2001). IRF proteins do not have direct antiviral activities, but most of them function as transcription factors for type I IFN pathway genes. All of the IRF proteins have an N-terminal helix-turn-helix DNA-binding domain (Ikushima *et al.*, 2013). The DNA sequence that IRFs bind to is called the IRF binding element (IRF-E) with the sequence 5′-AANNGAAANNGAAA-3′, which is recognized by all of the IRF proteins, from IRF1 to IRF9 (Paun and Pitha, 2007). However, each IRF protein possesses slightly different DNA binding specificities within the IRF consensus sequence (Schmid *et al.*, 2010). IRF4 and IRF8 are mainly expressed in lymphocytes, macrophages, B cells and dendritic cells while the other IRFs are more ubiquitously expressed in almost all cell types (Paun and Pitha, 2007).

IRF1, which was the first IRF protein discovered, has a prominent antiviral role against numerous viruses, including WNV, YFV, human immunodeficiency virus (HIV) and chikungunya virus (CHIKV) (Schoggins *et al.*, 2011). IRF1 enhances the expression of the IFN-

β gene but its precise role is not clear (Escalante *et al.*, 1998). IRF1 was also shown to induce the expression of many ISGs in the absence of IFN (Pine, 1992). Overexpression of IRF1 in human STAT1-/- MEFs transcriptionally activates a set of ISGs without inducing the expression of IFN (Schoggins *et al.*, 2011). Therefore, IRF1 appears to activate an antiviral program in the absence of STAT1 signaling and IFN gene induction.

IRF2 binds to the same DNA motif as IRF1, but it represses IRF1-induced transcriptional activation (Hida *et al.*, 2000). Moreover, it does not induce the expression of the IFN-α and IFN-β genes but acts as a negative regulator of the expression of type I IFNs as well as of IFN signaling (Honda *et al.*, 2004; Kuo and Calame, 2004).

IRF3 and IRF7 are the main transcription factors that induce the expression of type I IFNs in virus-infected cells. IRF3 and IRF7, which are highly homologous, both have an N-terminal DNA binding domain and phosphorylation sites in the C-terminus that can be phosphorylated in response to a virus infection (Taniguchi *et al.*, 2001). IRF3 is constitutively expressed and locates in the cytoplasm in a latent form. Upon viral infection, it is phosphorylated, dimerizes, translocates to the nucleus and binds to its target DNA sequence on the gene promoters switching on gene expression (Grandvaux *et al.*, 2002; Mori *et al.*, 2004). Unlike IRF3, IRF7 is expressed at low levels in cells and its expression is upregulated by type I IFNs. IRF7 regulates the expression of the IFN-α and IFN-β genes (Honda and Taniguchi, 2006). Similar to IRF3, cytosolic IRF7 undergoes phosphorylation, dimerization and nuclear translocation to become an active transcription factor. IRF3 and IRF7 can form homodimers and heterodimers, and each of these dimers differently acts to regulate the expression of type I IFN genes. An IRF3 homodimer and IRF3/IRF7 heterodimers regulate the early phase of IFN-β

production, while the IRF-7 homodimer appears to be responsible for maintaining the expression levels of type I IFNs (Sato *et al.*, 1998; Honda *et al.*, 2005).

IRF5 has roles in the immune response to pathogens and apoptosis. It responds to TLR as well as RLR signaling. The antiviral role of IRF5 is different from that of IRF7, mainly for the set of genes it induces (Barnes *et al.*, 2004). IRF5 is involved in the induction of some ISGs and in IFN-β gene induction after WNV infection of dendritic cells (Lazear *et al.*, 2013). In WNV-infected mice, IRF5 protects the host through shaping the early innate immune response, which includes controlling the type I IFN responses and regulating the expression of other cytokines and chemokines (Thackray *et al.*, 2014). IRF6 is closely related to IRF5 with respect to amino acid sequence, but it does not have an antiviral function. IRF6 is a key regulator controlling the keratinocyte proliferation-differentiation switch (Richardson *et al.*, 2006).

IRF9 is a component of the tertiary complex ISGF3 that is formed in response to type I IFN binding to its receptor. It is essential for the antiviral response of type I IFN because it is the major DNA-binding subunit of the transcription factor complex ISGF3, which also contains p-STAT1 and p-STAT2 (Taniguchi *et al.*, 2001). IRF9 can also form ISGF3-like complexes with a STAT1 homodimer or with STAT2 alone, which have similar DNA binding affinities as ISGF3 (Kraus *et al.*, 2003).

1.3 Viruses antagonize the host IFN response at the cellular and molecular levels

Although the IFN response is critical for controlling virus infection, both RNA viruses and DNA viruses have evolved multiple ways to invade the host IFN system. Viruses inhibit IFN production, block the JAK-STAT signaling, or disrupt the action of ISGs.

1.3.1 Virus infections that inhibit IFN production

Virus infections activate the host cell RLR-IPS-1 pathway, TLR-MyD88/TRIF pathway or cGAS-STING pathway to induce the expression of type I IFNs. In the RLR-IPS-1 pathway, the binding of viral RNA to cytosolic RLRs, mainly RIG-I and MDA5, causes a conformational change in RIG-I and MDA5, which reveals the N-terminal CARD domain. In addition to a conformational change, RIG-I and MDA5 undergo dephosphorylation by cellular phosphoprotein phosphatase 1α (PP1α) and PP1γ before being released from the auto-repression state. Lys63-linked ubiquitination by tripartite motif protein 25 (TRM25) and Riplet (also known as RNF135 or REUL) is essential for RIG-I activation, while the requirement for Lys63-linked ubiquitin chains for MDA5 activation is still being debated (Chiang *et al.*, 2014). Active RIG-I and MDA5 separately bind to IPS-1, which also has a CARD domain, through a CARD-CARD interaction. This eventually leads to activation of IRF3, IRF7 (via IKKε and TBK1) and NF-κB (via the IKKα/β/γ complex), which is required for the transcription of the IFN-β gene. The TLR-MyD88/TRIF pathway and cGAS-STING pathway also ultimately lead to the activation of IKKε, TBK1 and the IKKα/β/γ complex, thereby activating the transcription factors IRF3, IRF7 and NF-κB needed for induction of type I IFN gene expression. The induction of IFN signaling can be divided into three phases: recognition of viral RNAs by PRRs, signaling transduction from PRRs via adaptor proteins, and activation of the IRF and NF-κB transcription factors. Each of these three phases can be a target for virus antagonism against IFN induction.

1.3.1.1 The counteraction to IFN production by non-flaviviruses

Both RNA viruses and DNA viruses encode proteins that can antagonize IFN production. A well-characterized IFN antagonist is the influenza A virus non-structural protein NS1. This protein blocks IFN induction through multiple mechanisms. NS1 binds to dsRNA via its N-

terminal RNA-binding domain (RBD), thus potentially protecting viral RNA from detection by cellular sensors (Donelan *et al.*, 2003). In addition, NS1 binds to TRIM25 and Riplet to block their mediation on Lys63-linked polyubiquitination of RIG-I (Gack *et al.*, 2009). In the nucleus, NS1 interacts with host protein CPSF30 via its C-terminal effector domain (ED), which results in inhibition of host gene expression including the IFN genes (Garcia-Sastre, 2011).

Paramyxoviruses, which have single-stranded negative-sense RNA genome, have been well studied for IFN production antagonism. The non-structural proteins V, W, and C, which are produced from the single P/V/C gene through an RNA-editing mechanism, play important roles in IFN antagonism (Goodbourn and Randall, 2009). Among them, V proteins are considered the principal IFN antagonists. The V proteins have been shown to directly inhibit MDA5, to indirectly inhibit RIG-I via LGP2, and also to inhibit the IRF3/IRF7 kinase IKKε and TBK1, to prevent IFN gene expression. However, the inhibition mechanisms of the V proteins of different members of this family are not the same (Andrejeva *et al.*, 2004; Goodbourn and Randall, 2009; Chiang *et al.*, 2014; Hoffmann *et al.*, 2015). The paramyxovirus W protein and C protein have also been shown to inhibit the activation of IRF3 by mislocalizing the IRF3 protein inside the nucleus (Shaw *et al.*, 2005; Sparrer *et al.*, 2012). DNA viruses encode specific proteins that antagonize IFN production by targeting cGAS, nuclear translocation or the transcriptional activity of IRF3 (Hoffmann *et al.*, 2015).

1.3.1.2 The counteraction to IFN production by Flaviviruses

1.3.1.2.1 Prevention of recognition of viral components by PRRs

Flaviviruses have evolved ways to sequester or modify viral RNA to dampen recognition by cell sensors. In infected cells, some of the small non-structural proteins of DENV and WNV induce invaginations in the ER membrane that are the sites for exponential replication of genome

RNA. These invaginations have been proposed to act as a physical barrier to conceal replicated viral RNA from cellular cytosolic sensors (Welsch *et al.*, 2009; Gillespie *et al.*, 2010). Many flaviviruses, including WNV, DENV, JEV, ZIKV, and YFV, add a 5′ cap structure to their genomic RNAs, which is N7 and 2′-O methylated by the viral methyltransferases encoded in the NS5 protein, thereby creating a mimic of the eukaryotic cell cap structures. Recombinant WNV, JEV, and DENV with a mutation in the 2′-O-methyltransferase show growth attenuation in IFN-competent cells (Daffis *et al.*, 2010; Kimura *et al.*, 2013; Li *et al.*, 2013). A mutant WNV lacking the 2′-O-methyltransferase was inhibited by murine Ifit1, but wild-type WNV was not. In addition, the same mutant WNV was avirulent in wild-type mice but virulent in Ifit1-/- mice (Daffis *et al.*, 2010).

1.3.1.2.2 Inhibition of PRRs or their adaptor proteins

Lys63-linked polyubiquitination of RIG-I that is regulated by TRIM25 is required for RIG-I activation. Host protein TRIM25 is a target of flavivirus sfRNA, which is a non-coding RNA derived from the 3′UTR of the viral genomic RNA. The sfRNA of an epidemic DENV strain was shown to bind to TRIM25, thus disrupting the stability of TRIM25 and weakening the RIG-I mediated IFN response (Manokaran *et al.*, 2015). The translocation of activated RIG-I to interact with IPS-1, which is presented on mitochondria, mitochondria-associated membranes, and peroxisomes, has been shown to be a target of flavivirus counteraction of IFN production. The DENV and WNV NS3 proteins interact with a human cell protein, 14-3-3ε, which is the chaperone for RIG-I translocation to mitochondria (Chan and Gack, 2016). The interaction between NS3 and 14-3-3ε prevents the translocation of RIG-I to mitochondria; thus RIG-I cannot interact with IPS-1(MAVs) to transduce downstream signaling.

In the cGAS-STING pathway, STING transduces signaling downstream of the cell sensor cGAS to activate the transcription factor IRF3. The DENV NS2B/3 protease cleaves human STING, thus inhibiting cGAS mediated type I IFN induction. Murine STING is not a target of DENV NS2B/3 because the cleavage site for DENV NS2B/3 is not present in the murine ortholog (Aguirre *et al.*, 2012; Yu *et al.*, 2012a). WNV NS2B/3 has a structure very similar to that of DENV NS2B/3, but WNV NS2B/3 shows more strict cleavage site specificities than DENV NS2B/3 (Shiryaev *et al.*, 2007). It is not known whether WNV NS2B/3 cleaves human STING. Moreover, STING cleavage was not observed during JEV and YFV infection, which was investigated with isolated JEV NS2B/3 protein or NS2B/3 protein of the YFV vaccine strain 17D (Yu *et al.*, 2012b; Maringer and Fernandez-Sesma, 2014). Nevertheless, YFV NS4B is known as an antagonist of STING since it binds and colocalizes with STING in transient transfection experiments (Ishikawa *et al.*, 2009).

WNV structural protein E has been shown to target the kinase, receptor-interacting protein 1 (RIP1), which is downstream of TLR3-TRIF signaling for type I IFN induction. The inhibition of RIP1 requires a particular glycosylation profile on the E protein. Only mosquito cell-derived, but not mammalian cell-produced, WNV have this type of glycosylation profile on E protein (Arjona *et al.*, 2007).

1.3.1.2.3 Antagonism of signaling proteins and transcription factors downstream of PRRs

The kinases IKKε and TBK1 are required for activation of the transcription factors IRF3 and IRF7. DENV NS2B/3 protease binds to IKKε and blocks its kinase activity, thus inhibiting IRF3 mediated IFN expression (Anglero-Rodriguez *et al.*, 2014). Ectopically expressed DENV NS2A and NS4B, as well as WNV NS4B (NY99 strain), inhibit the activation of TBK1 but the exact mechanism involved is not known. The inhibition of TBK1 by NS2A and NS4B may

require other factors because NS2A and NS4B do not directly interact with TBK1 (Dalrymple *et al.*, 2015). A study of NS2A from the WNV Kunjin strain demonstrated that a single amino acid substitution (Ala30 to Pro) in this nonstructural protein controls its antagonism on IFN-β promoter activity but the targeted cell protein is not known. Recombinant WNV_{Kunjin} with a mutant NS2A had attenuated viral replication in cells and reduced virulence in mice (Liu *et al.*, 2004; Liu *et al.*, 2006).

1.3.2 Viruses inhibit the IFN signaling pathway

Secreted type I IFNs bind to the IFNAR1/2 heterodimer receptor. The kinases that are associated with the receptor, JAK1 and TYK2, then become activated through *trans*- and auto-phosphorylation and catalyze the phosphorylation of STAT1 and STAT2 which then form the transcription factor complex ISGF3 with IRF9. The ISGF3 complex translocates into the nucleus, binds to the ISRE in ISG promoters, and activates the expression of ISGs establishing an antiviral state. Type III IFN activates the same kinases and transcription factor complex as type I IFNs, while type II IFN activates JAK1 and JAK2 kinases and uses a p-STAT1 dimer as the transcription factor (Schneider *et al.*, 2014). Viruses have evolved several ways of interfering with the IFN-induced JAK-STAT pathway to sustain high levels of infection. The viral antagonizing strategies of the IFN signaling pathway fall into two major categories: inhibition of kinase activities and direct targeting of STAT1 and/or STAT2.

1.3.2.1 The counteraction of the JAK-STAT pathway by non-flaviviruses

Paramyxovirus V proteins antagonize the JAK-STAT pathway through several different mechanisms. Measles virus (MeV) V protein interacts with JAK1, which inhibits phosphorylation of STAT1 and STAT2 (Caignard *et al.*, 2007). V proteins of particular paramyxoviruses (rubulaviruses) target STAT1 or STAT2 for proteasomal degradation. In

rubulavirus-infected cells, a V-degradation complex (VDC) is formed, which contains the V protein, STAT1, STAT2, and components of an E3 ubiquitin ligase complex. This VDC complex mediates the polyubiquitination of the STAT proteins that results in their degradation. Although both STAT1 and STAT2 are present in the VDC, only one of the two STAT proteins is degraded, and which one is degraded differs among the viruses (Parisien *et al.*, 2001; Andrejeva *et al.*, 2002; Hoffmann *et al.*, 2015). Some other V proteins disrupt the JAK-STAT pathway by sequestering STAT1 and STAT2 in the cytoplasm, thus preventing their nuclear translocation and transcription factor function (Rodriguez *et al.*, 2002; Rodriguez *et al.*, 2003; Horvath, 2004). The non-structural C proteins of the paramyxovirus, Sendai virus (SeV), have been found to bind to STAT1 and STAT2 and interfere with STAT1 and STAT2 phosphorylation, while the C protein of another paramyxovirus, human parainfluenza virus type 1 (hPIV1), binds to phosphorylated STAT1 and sequesters it in cytoplasmic perinuclear aggregates (Komatsu *et al.*, 2002; Gotoh *et al.*, 2003; Schomacker *et al.*, 2012). Since STAT1 is involved in type I, II, III IFN signaling, and STAT2 is involved in type I and III IFN signaling, the inhibition of both STAT1 and STAT2 by paramyxovirus non-structural V and C proteins weakens type I, II, and III IFNs signaling.

Another highly pathogenic virus, Ebola virus (EBOV), which belongs to the family *Filoviridae*, can also interfere with IFN signaling. The VP24 protein of EBOV interacts with the host karyopherin-α protein, which is a nuclear importer, and thus inhibits nuclear translocation of phosphorylated STAT1 by this importer (Reid *et al.*, 2006; Reid *et al.*, 2007). However, the VP24 protein of another highly pathogenic filovirus, Marburg virus (MARV), does not block STAT1 nuclear import. Instead, the MARV VP40 protein acts as an antagonist against IFN

signaling by preventing the function of JAK1 thus inhibiting the phosphorylation of STAT1 and STAT2 (Basler and Amarasinghe, 2009; Valmas *et al.*, 2010; Valmas and Basler, 2011).

1.3.2.2 The counteraction of the JAK-STAT pathway by flaviviruses

1.3.2.2.1 Inhibition of JAK1 or TYK2 activity

Non-structural protein NS4B of WNV is the antagonist that inhibits the activation of both JAK1 and TYK2 in human cells, thereby blocking STAT activation (Keller *et al.*, 2006; Evans and Seeger, 2007). Both the DENV and YFV NS4B proteins function by blocking the activation of STAT1 (Munoz-Jordan *et al.*, 2005). In cells infected by JEV, the viral NS5 protein blocks phosphorylation of TYK2 and STAT1 (Lin *et al.*, 2006). WNV also blocks IFN signaling by upregulating the expression of suppressors of cytokine signaling 1 (SOC1) and SOC3 that blunt JAK1 activity. Another neuroinvasive flavivirus, TBEV, shares the same invasion strategy against IFN signaling (Mansfield *et al.*, 2010). Furthermore, WNV-induced depletion of IFNAR1 dampens IFN signaling (Evans *et al.*, 2011).

1.3.2.2.2 Direct targeting of STAT1 and STAT2

Flavivirus infections target STAT1 and STAT2 by directly blocking their phosphorylation or by sequestering these STAT proteins in the cytoplasm or by targeting STATs for degradation (Lin *et al.*, 2006; Munoz-Jordan and Fredericksen, 2010). DENV NS5 targets human STAT2 for proteasomal degradation but does not interact with murine STAT2 (Ashour *et al.*, 2010). In addition, ectopically expressed DENV NS5 binds to human STAT2, but not to TYK2 or STAT1 and inhibits the phosphorylation of STAT2 (Mazzon *et al.*, 2009). JEV NS5 blocks the phosphorylation of STAT1, thus inhibiting STAT1 nuclear translocation (Lin *et al.*, 2006). NS5 protein from WNV NY99 prevents the phosphorylation of STAT1 in human cells (Laurent-Rolle *et al.*, 2010). WNV Eg101 NS5 protein blocks phosphorylation of STAT proteins

in primate cells, but in infected MEFs, STAT1 and STAT2 are phosphorylated, but their nuclear translocation is blocked by an unknown mechanism (Pulit-Penaloza *et al.*, 2012b). WNV-induced redistribution of cellular cholesterol was also shown to block STAT1 phosphorylation and nuclear translocation, thus dampening IFN signaling (Mackenzie *et al.*, 2007).

Studies of ZIKV from two different labs showed that ZIKV infection blocks the JAK-STAT pathway in host cells. The ZIKV NS5 protein targets human STAT2, which causes its degradation, but it does not target mouse STAT2. This finding is similar to what was observed for DENV NS5. However, unlike DENV NS5, ZIKV NS5-mediated STAT2 degradation does not require the E3 ubiquitin ligase UBR4 (Grant *et al.*, 2016). In A549 and human dendritic cells, ZIKV infection inhibits the phosphorylation of STAT1 and STAT2 but the mechanism was not studied (Bowen *et al.*, 2017).

1.3.3 Virus escape of ISG antiviral functions

Although the functions of most of the ISGs are unknown, some proteins encoded by ISGs have direct antiviral functions, for example, viperin and Ifit1, while some ISG proteins have regulatory effects on the IFN system, for example, IRF3, IRF7, and STAT1. Viruses have evolved ways to escape the antiviral functions of particular ISGs. One well-characterized example is how viruses escape the antiviral function of Ifit1, which acts as a sensor of non-self RNA as well as an antiviral effector. Flaviviruses use their own enzymes to generate a 5′ cap on the viral genome to escape detection by Ifit1 as described previously. Alphavirus, which also has positive-sense single-stranded RNA genome but no cap 1 structure, use a particular secondary structure within the 5′ UTR of their genome RNA to alter Ifit1 binding and function, thereby avoiding inhibition by Ifit1 protein (Hyde *et al.*, 2014).

GOAL OF THE DISSERTATION

Although WNV has the ability to inhibit the IFN signaling pathway, efficient upregulation of a subset of ISGs, including Oas1a, Oas1b, and Irf7, was still observed in WNV-infected cells and cells deficient in IFN signaling (Pulit-Penaloza *et al.*, 2012b). However, it was not known which host cellular sensors were used to detect a WNV infection and signal the initiation of this IFN-independent ISG upregulation mechanism. It was also not known which transcription factors were involved in activating the ISGs or to which binding sites in the ISG promoters these TFs bound. The goals of this study were to increase understanding of this non-canonical IFN-independent mechanism of ISG upregulation with studies designed to address the following aims.

Aim 1. Analysis of the host cellular factors involved in the WNV-induced IFN-independent ISG upregulation mechanism.

Aim 2. Functional analysis of the promoters of representative ISGs in WNV-infected MEFs that do not respond to IFN.

The data obtained under Aims 1 and 2 are described in Chapter 2.

2 IDENTIFICATION OF HOST CELLULAR FACTORS AND TRANSCRIPTION FACTOR BINDING SITES INVOLVED IN A NON-CANONICAL INTERFERON-STIMULATED GENE UPREGULATION MECHANISM

2.1 Introduction

In response to a virus infection, host cells produce type I IFNs that serve as the first line of antiviral defense. Secreted type I IFNs bind to their receptors, which are heterodimers of IFNAR1 and IFNAR2, located on the surfaces of both infected and adjacent uninfected cells. The binding of IFNs to their receptors activates the receptor-associated kinases inside the cells, which phosphorylate STAT1 and STAT2. The transcription factor complex ISGF3 composed of phosphorylated STAT1, phosphorylated STAT2 and interferon regulatory factor 9 (IRF9), forms and translocates into the nucleus, binds to the IFN-stimulated response element (ISRE) in the promoters of IFN-stimulated genes (ISGs) and activates ISG expression. The proteins encoded by hundreds of ISGs target different steps of virus replication cycles, and their actions establish an antiviral state.

Viruses have evolved various ways of evading the host IFN response by targeting either IFN production or IFN signaling (Hoffmann *et al.*, 2015; Gack and Diamond, 2016). In WNV-infected host cells, the induction, expression, and secretion of type I IFN occur normally, but the canonical Janus tyrosine kinase (JAK)-STAT signaling pathway is blocked by the virus infection. However, the Brinton lab previously discovered a backup antiviral response characterized by the upregulation of a subset of ISGs when the canonical IFN-induced antiviral signaling is blocked in WNV-infected mouse embryo fibroblasts (MEFs) (Scherbik *et al.*, 2007b). This subset of ISGs includes Oas1a, Oas1b, and Irf7. Each of these ISGs has a known antiviral function. Oas1a, which is an enzymatically active synthetase, can synthesize 2′-5′

oligoadenylates (2-5A) from ATP and 2-5A activates the latent endonuclease RNase L, leading to RNase L-mediated cellular and viral RNA degradation (Scherbik *et al.*, 2006; Silverman, 2007). Oas1b, which is an inactive synthetase, has antiviral activity that specifically targets members of the genus *Flavivirus* and is independent of the OAS/RNase L pathway (Scherbik *et al.*, 2007a; Elbahesh *et al.*, 2011). Irf7 is a "master regulator" that is an important regulator of the production of type I IFNs after virus infection (Honda *et al.*, 2005). The IFN independence of the upregulation of a subset of ISGs was confirmed in WNV-infected Ifnar1-/- MEFs as well as in WNV-infected STAT1-/- MEFs and STAT2-/- MEFs (Pulit-Penaloza *et al.*, 2012b). These results showed that the IFN-independent ISG upregulation mechanism still occurs in response to a WNV infection when canonical IFN-dependent signaling is blocked. However, the finding that the level of virus replication in Ifnar1-/- MEFs is higher than in wild-type MEFs indicates that the broader IFN-induced canonical ISG response provides a more robust antiviral response against WNV infection than the non-canonical upregulation of a subset of ISGs. Recent studies suggest that the IFN-independent ISG upregulation mechanism is not limited to WNV-infected MEFs. Influenza A virus was demonstrated to induce a set of ISGs in the absence of ISGF3 activation, suggesting that an IFN-independent ISG upregulation mechanism exists in influenza A virus-infected cells (Schmid *et al.*, 2010). A study screening over 380 ISGs for their antiviral functions in a transient gene overexpression system showed that some ISG proteins could trigger an antiviral program in human STAT1-/- fibroblasts (Schoggins *et al.*, 2011). This result suggests that an IFN-independent ISG upregulation mechanism also exists in human cells. Although the IFN-independent ISG upregulation mechanism is a backup antiviral response, further study of this mechanism is expected to broaden knowledge of host antiviral mechanisms and to provide insights for future research in the host-virus interaction field.

Several recent studies suggest that some ISGs can be upregulated in response to a virus infection through pathways that are independent of the JAK-STAT signaling pathway (Kalvakolanu, 2003; Schmid *et al.*, 2010; Schoggins *et al.*, 2011). A hypothesized mechanism of alternative ISG upregulation is the activation of cell pathogen pattern receptors (PRRs) by viral components activates signaling pathways, ultimately leading to the activation of transcription factors and the induction of ISG expression. The cell cytosolic RNA sensors, RIG-I and MDA5, can detect a WNV infection (Suthar *et al.*, 2013; Lazear and Diamond, 2015). Signaling from RIG-I or MDA5 is transduced through the downstream adaptor IPS-1. However, the Brinton lab previously showed that in cells with RIG-I or MDA5 knocked out, IFN-independent ISG upregulation still occurs (Pulit-Penaloza *et al.*, 2012b). In contrast, when IPS-1 was knocked out, ISGs were upregulated at 8 h post infection with WNV, but the mRNA levels decreased progressively at later times, suggesting that IPS-1 is required for the IFN-independent mechanism at later times after WNV infection when the viral proteins have inhibited canonical IFN signaling (Pulit-Penaloza *et al.*, 2012b). Transcription factors IRF3 or IRF7 can induce an IFN-like transcriptome response in the absence of type I IFN signaling (Schmid *et al.*, 2010). However, IFN-independent ISG upregulation still occurred in WNV-infected IRF3-/-, IRF7-/- and IRF3/7-/- MEFs indicating that IRF3 and IRF7 are dispensable for the IFN-independent ISG upregulation mechanism (Pulit-Penaloza *et al.*, 2012b). These results suggest that the alternative IFN-independent ISG upregulation mechanism is working through cell sensors, but how this mechanism regulates ISG expression is not fully understood.

In the present study, Mx1 and Ifit1 were identified as additional members of the subset of ISGs that can be upregulated by WNV infection in an IFN-independent manner. The cellular cytosolic sensors, RIG-I and MDA5, were found to be redundantly involved in detection of

WNV infection that leads to the activation of the IFN-independent upregulation of ISGs. The transcription factors IRF3, IRF5, and IRF7, were redundantly involved in mediating the alternative upregulation of ISGs. A dual-luciferase assay system was established to map critical DNA regulatory elements in the promoters of ISGs upregulated by the IFN-independent ISG upregulation mechanism. By mapping the promoters of two representative ISGs, Ifit1 and Oas1b, the ISRE, which is the regulatory element that mediates ISG upregulation in the canonical JAK-STAT pathway, was also found to be involved in mediating IFN-independent ISG upregulation after WNV infection in mouse cells by interacting with a new protein complex. This novel ISRE-binding transcription factor complex appears to contain NF-κB components, IRF3, IRF5 or IRF7, and additional protein factors. The promoter regions flanking the ISRE also contribute to the regulation of ISG expression in the IFN-independent mechanism.

2.2 Materials and methods

2.2.1 Cells and viruses

Primary IFNAR-/- (Ifnar1-/-), IRF1-/-, RIG-I/MDA5-/-, IRF5-/-, IRF3/5/7-/- and wild-type C57BL/6 MEFs (provided by Michael Diamond, Washington University School of Medicine, St. Louis, MO) were cultured in high glucose Dulbecco's modified Eagle's medium (DMEM) supplemented with 10% fetal bovine serum (FBS), 1% L-glutamine, 1% non-essential amino acid (NEAA), and penicillin (100 U/ml)/streptomycin (100 µg/ml). Primary MEFs were used for experiments between passage 3 and passage 7. IFNAR-/- and wild-type C57BL/6 MEF cell lines transformed by the 3T3 protocol were grown in DMEM supplemented with 3% FBS, 5% newborn bovine serum, 1% L-glutamine, and penicillin (100 U/ml)/streptomycin (100 µg/ml). tSTAT1-/- and wild-type t129/SvEv MEF cell lines (provided by Karen Mossman, McMaster University, Hamilton, Ontario, Canada) were cultured in MEM supplemented with

10% FBS, 1% L-glutamine and penicillin (100 U/ml)/streptomycin (100 µg/ml). These cells were maintained at 37°C in an incubator in a 5% CO_2 atmosphere.

A WNV Eg101 virus stock was prepared by infecting baby hamster kidney (BHK) cells at a multiplicity of infection (MOI) of 0.1 and harvesting culture fluid at about 40 hours post infection (hpi). The culture fluid was clarified by centrifugation at 2,000 rpm for 5 min, aliquoted and stored at -80°C. A stock of WNV W956IC was made by transfecting *in vitro* transcribed W956IC RNA into BHK cells (1 µg/2 × 10^6 cells) with the transfection reagent DMRIE-C according to the manufacturer's protocol (Invitrogen) (Basu and Brinton, 2011). At 72 h after transfection, a time when BHK cells were rounded up but still attached, cell culture fluid was harvested, clarified, aliquoted and stored at -80°C. Virus titers were assessed by plaque assay on BHK monolayers as previously described (Emara *et al.*, 2008).

2.2.2 Extraction of total cell RNA and quantification of cellular mRNAs

MEFs were cultured in 6-well plates and infected with WNV at the indicated MOI. At the indicated times, cell lysates were collected with TRI-reagent (Molecular Research Center), and total RNA was extracted following the manufacturer's protocol. The purity and integrity of the RNA were determined using a NanoVue Plus spectrophotometer (GE Healthcare) (at A_{260}/A_{280} and A_{260}/A_{230}) and by RNA gel electrophoresis. One-step real-time quantitative (q) RT-PCR was performed using the TaqMan RNA-to-Ct 1-step Kit (ThermoFisher Scientific) for each target gene and the endogenous control gene in a singleplex format with 300 ng of total RNA. The following TaqMan gene expression assays (20 × primer and FAM/MGB probe mixes) were used: Mn00836412_m1 for Oas1a, Mn00449297_m1 for Oas1b, Mn00516793_m1 for Irf7, Mm00515153_m1 for Ifit1, Mm00487796_m1 for Mx1, Mm00488995_m1 for Mx2, Mm00491265_m1 for Rsad2 (Applied Biosystems). Glyceraldehyde-3-phosphate dehydrogenase

(GAPDH) mRNA was detected as an endogenous control for each sample with mouse GAPDH primers and probe (Applied Biosystems). The cycling reactions were run on an Applied Biosystems 7500-Fast Real-time PCR System with the following parameters: reverse transcription at 48°C for 15 min, AmpliTaq activation at 95°C for 10 min, denaturation at 95°C for 15 sec, and annealing/extension at 60°C for 1 min (cycle repeated 40 times). Each experiment was repeated at least twice and all samples were analyzed in triplicate. Triplicate threshold cycle (Ct) values were used to calculate comparative fold change for the expression of the targeted gene using the $2^{-\Delta\Delta Ct}$ method provided by Applied Biosystems software. To estimate gene induction by WNV infection, the transcript level obtained for each gene was normalized to the GAPDH transcript level in the same sample and the relative fold change (RQU) was calculated over the 8 h mock-infected sample. For the type I IFN treatment samples, the RQU was calculated over the untreated sample value.

2.2.3 Plasmid construction and site-directed mutagenesis

2.2.3.1 Ifit1 promoter mapping constructs

The mouse Ifit1 gene promoter region analyzed consisted of sequence 1,000 bp upstream and 66 bp downstream from the transcription start site (TSS). This region was amplified from C57BL/6 genomic DNA using primers designed based on the C57BL/6J mouse genomic sequence [(NCBI) Genbank ID: NC_000085.6]. The amplified PCR product was then cloned into a Topo vector (Invitrogen) and sequenced. After digesting the Topo vector DNA with SacI and HindIII, the insert fragment was subcloned into the Nanoluc (Nluc) luciferase reporter vector pNL4.17 to generate the (-1000, +66) reporter construct. Additional Ifit1 promoter truncation constructs were made using the Topo-Ifit1 promoter vector as a template and the primers listed

in Table 2-1. Each of the PCR products was digested with SacI and HindIII and then ligated into the Nluc luciferase reporter. All of the constructs were sequenced for verification.

Table 2.1 Primer sequences used for construction of Ifit1 promoter fragments of different lengths

	Forward primers	Reverse primers
Ifit1-1000, +66	CTCAAGAGCTCTGAGCCCCACTGTCTGTAGTTC[a]	CTCACAAGCTTGAACTCCTCAGAAACCTGCCTT[b]
Ifit1 -700, +66	CTCAAGAGCTCCATGACTATGATTGGTGGAAAG	CTCACAAGCTTGAACTCCTCAGAAACCTGCCTT
Ifit1 -500, +66	CTCAAGAGCTCGACACACAACAAACCAGCTAG	CTCACAAGCTTGAACTCCTCAGAAACCTGCCTT
Ifit1 -350, +66	CTCAAGAGCTCGCTTGGAAGAAAGAACAACAC	CTCACAAGCTTGAACTCCTCAGAAACCTGCCTT
Ifit1 -192, +66	CTCAAGAGCTCTGTATCCGTTTCAGAGCCTTC	CTCACAAGCTTGAACTCCTCAGAAACCTGCCTT
Ifit1 -132, +66	CTCAAGAGCTCCCACAGTGCGTCTCCCTG	CTCACAAGCTTGAACTCCTCAGAAACCTGCCTT
Ifit1 -50, +66	CTCAAGAGCTCCTGACTGAAAAGAGCACACC	CTCACAAGCTTGAACTCCTCAGAAACCTGCCTT

[a] Underlined letters indicate the SacI restriction site included in all forward primers.
[b] Underlined letters indicate the HindIII restriction site included in all reverse primers.

2.2.3.2 Oas1b promoter mapping constructs

Six Oas1b truncation promoter constructs were previously made by inserting promoter fragments of various lengths into the pGL-4.17 firefly luciferase reporter plasmid DNA (Pulit-Penaloza *et al.*, 2012b). These constructs were modified by replacing the reporter gene with the Nluc luciferase gene using HindIII/BamHI sites. The Nluc gene was amplified from pNL1.1 CMV-Nluc DNA with the forward primer 5′-GCCAAGCTTGGCAATCCG-3′ and the reverse primer 5′-CGACGGATCCTTATCG-3′ containing HindIII and BamHI restriction digest sites, respectively (the restriction sites are underlined in the primer sequences). A promoter-less Nluc luciferase reporter vector pNL-4.17 plasmid was also made using the same strategy for replacing the firefly luciferase gene in the pGL-4.17 plasmid with the Nluc luciferase gene. Additional Oas1b promoter fragments of different lengths were amplified by PCR with the primers listed in Table 2-2 using the longest Oas1b promoter construct as a template. Internal deletion fragments were made using a "double-joint PCR" strategy (Kim *et al.*, 2009). For the fragment (-299/-202, -93/+50) that has an internal deletion, two sub fragments were amplified with the primer pairs (-299,-202) and (-93, +50)-1 respectively in the first-round PCR with the longest Oas1b promoter construct used as a template, and then the two amplified sub fragments (ratio of 1:1) were fused together in a second-round PCR. The fused product was then amplified with the primer pair (-299/-202, -93/+50) in the third-round PCR. The other fragment (-299/-144, -93/+50) was generated using the same strategy with primer pairs (-299, -144) and (-93, +50)-2 in the first-round PCR and primer pair (-299/-144, -93/+50) in the third-round PCR. The amplified promoter fragments were next inserted into the pNL-4.17 plasmid at NheI/BglII sites. All of the constructs were sequenced for verification.

Table 2.2 Primer sequences used for construction of Oas1b promoter fragments of different lengths

	Forward primer	Reverse primer
(-299, +50)	CTAGCTAGCAGGAGATGGAAGCCGAGCTC[a]	GAAGATCTCCTCTGCAGCCAGCAG[b]
(-251, +50)	CTAGCTAGCCCTGATTCCGTTTCCCTTC	GAAGATCTCCTCTGCAGCCAGCAG
(-134, +50)	CTAGCTAGCCCTGGGCCGGATCTTAAG	GAAGATCTCCTCTGCAGCCAGCAG
(-93, +50)	CTAGCTAGCGTACCTGTTCAGAAGCCCTAAC	GAAGATCTCCTCTGCAGCCAGCAG
(-54, +50)	CTAGCTAGCCCTGGATGATTTGCATATC	GAAGATCTCCTCTGCAGCCAGCAG
(-28, +50)	CTAGCTAGCTTCCCGGGAAATGGAAACTG	GAAGATCTCCTCTGCAGCCAGCAG
(-299, -202)	CTAGCTAGCAGGAGATGGAAGCCG	CAGGTACTACGTTTTAGGAACAATCTGTG[c]
(-93, +50)-1	CTAAAACGTAGTACCTGTTCAGAAGCC	GAAGATCTCCTCTGCAGCCAGCAG
(-299/-202, -93/+50)	CTAGCTAGCAGGAGATGGAAGCCG	GAAGATCTCCTCTGCAGCCAGCAG
(-299, -144)	CTAGCTAGCAGGAGATGGAAGCCG	GTAAGGAAACTGACCTGGCTTTCTCG
(-93, +50)-2	GTTTCCTTACGTACCTGTTCAGAAGCC	GAAGATCTCCTCTGCAGCCAGCAG
(-299/-144, -93/+50)	CTAGCTAGCAGGAGATGGAAGCCG	GAAGATCTCCTCTGCAGCCAGCAG

[a] Underlined letters indicate the NheI restriction site included in all forward primers.
[b] Underlined letters indicate the BglII restriction site included in all reverse primers.
[c] Double underlined letters indicate a linker sequence to connect the two sub fragments in the internal deletion promoter fragment.

2.2.3.3 Site-directed mutagenesis of ISREs

The software tool MatInspector (Genomatix) was used to predict transcription factor binding sites (TFBSs) in the Oas1b and Ifit1 promoter fragment sequences, and two ISREs were identified in each gene promoter within 350 bp upstream of TSS. Specific mutations were introduced into each of the ISREs of the Oas1b promoter constructs (-251, +50) and (-93, +50), as well as into those of the Ifit1 promoter construct (-192, +66). Mutations were introduced using the primers listed in Table 2-3 and a QuickChange II Site Directed Mutagenesis Kit (Agilent Technologies) following the manufacturer's protocol. The mutant construct sequences were analyzed with MatInspector to ensure that the substitutions disrupted the ISRE but did not create any new transcription factor binding sites. All of the constructs were verified by DNA sequencing.

Table 2.3 Primer sequences used for ISRE motif mutation

		Promoter sequence
Oas1b mISRE1	F[a]	GTGCACGTAGAAGAAGGGTACCGGAATCAGGAAACCACA[b]
	R	TGTGGTTTCCTGATTCCGGTACCCTTCTTCTACGTGCAC
Oas1b mISRE2	F	CAGAAATGGGACTTTCAGGTACCATTTCCCGGGAAGGGC
	R	GCCCTTCCCGGGAAATGGTACCTGAAAGTCCCATTTCTG
Ifit1 mISRE1	F	GGATAAACTGCAGGCTTCAGGTACACTTTCCAGTCTCAGTTTC
	R	GAAACTGAGACTGGAAAGTGTACCTGAAGCCTGCAGTTTATCC
Ifit1 mISRE2	F	GTACACTTTCCAGTCTCAGGTACAGTTTCTCACTGCTGACT
	R	AGTCAGCAGTGAGAAACTGTACCTGAGACTGGAAAGTGTAC

[a] F, forward primer; R, reverse primer.
[b] Underlined letters indicate mutated nts.

2.2.4 Transient transfection and dual luciferase assay

In the study of mapping the promoters of Ifit1 and Oas1b, IFNAR-/- MEFs were seeded at 6×10^4 cells/well in 24-well plates. After 24 h, cells were mock-infected or infected with WNV W956 at a MOI of 3 and cultured with the antibiotic-free medium. At 3 hpi, 0.4 μg Oas1b or Ifit1 promoter Nluc luciferase construct DNA was co-transfected with 0.1 μg firefly luciferase

vector pGL 4.53 DNA (Promega) using Lipofectamine LTX with PLUS (Invitrogen) according to the manufacturer's protocol. At 28 hpi, cells were harvested with 150 µl Passive Lysis Buffer (Promega) per well. The Nanoluc and firefly luciferase activities were measured separately with the Dual-Glo® luciferase assay system (Promega) according to the manufacturer's protocol using a Victor 3 plate reader (Perkin Elmer). The Nanoluc luciferase activity was normalized to the firefly luciferase activity in each sample.

In the study of investigating ISRE activation in an IFN-independent manner, a luciferase reporter containing three copies of the ISRE consensus sequence (Stratagene) was co-transfected with the pGL-TK Renilla luciferase reporter at a ratio of 20:1 using Lipofectamine LTX with PLUS (Invitrogen) into mock-infected and WNV-infected IFNAR-/- MEFs. Firefly and Renilla luciferase activities were measured with the Dual-Luciferase® reporter assay system (Promega) according to manufacturer's protocol using the Victor 3 plate reader (Perkin Elmer). The firefly luciferase activity was normalized to the Renilla luciferase activity in each sample.

2.2.5 Electrophoretic mobility shift assay (EMSA) and supershift assay

IFNAR-/- MEFs were infected with WNV W956 at a MOI of 3 or mock-infected. At 21 hpi, cells were lysed, and nuclear extracts were collected with a Nuclear Fraction Kit (Active Motif). The forward and reverse strands of the double-stranded Ifit1 oligonucleotide DNA probes listed in Table 2-4 were synthesized with a 3′-biotin label (Integrated DNA Technologies). After being reconstituted, 50 pmol of each strand were mixed with TE buffer and annealed using a thermocycler with the following parameters: 95°C for 5 min, 95°C (-1°C/cycle) for 1 min (cycle repeated 47 times), and held at 4°C. Annealed probes were aliquoted and stored at -20°C. The same probe without a 3′-biotin label was used for cold probe competition experiments. Nuclear extracts (3 µg) prepared from IFNAR-/- MEFs that were either mock- or

WNV-infected were incubated with 20 fmol of labeled DNA probe for 1 h at 22°C. The 20 µl binding reactions also included 50 ng/µl herring sperm DNA (non-specific nucleotide competitor), 2.5% glycerol and 0.05% NP-40. To ensure specific binding between the DNA probe and the proteins in the nuclear extract, 0.2 to 4 pmol of the unlabeled probe was added to the reaction for specific competition with the biotin-labeled probe. For supershift assays, nuclear extracts (3 µg) were incubated with 2 to 10 µg of anti-RelA antibody (Santa Cruz Biotechnology, Cat#sc-8008x) for 30 min at 4°C prior to adding the DNA probe into the reaction. After incubation for 1 h at 22°C, 5× loading buffer (ThermoFisher Scientific) was added and the samples were electrophoresed on a 6% native polyacrylamide gel (ThermoFisher Scientific). Electrophoresis was stopped when the front dye had migrated to about ¾ of the way to the bottom of the gel. The DNA-protein complexes that were separated on the native polyacrylamide gel were then transferred to a positively charged nylon membrane (GE Healthcare), where the labeled probe was detected using a Chemiluminescent Nucleic Acid Detection Kit (ThermoFisher Scientific) and a LAS4000 CCD camera with high-resolution increment exposure. For supershift assays, the band intensities were measured three times with different parameters for band detection and background removal using ImageQuant TL software.

Table 2.4 Ifit1 promoter probe sequences used for EMSA

	Probe sequence
FT66F[a]	5′-GATGATAAACTGCAGGCTTCAGTTTCACTTTCCAGTCTCAGTTTCAGTTTCTCACTGCTGACTGAAAAG-3′ bio
FT66R[b]	5′-CTTTTCAGTCAGCAGTGAGAAACTGAAACTGAGACTGGAAAGTGAAACTGAAGCCTGCAGTTTATC-3′bio
FTmutF	5′-GATGATAAACTGCAGGCTTCAGGTACACTTTCCAGTCTCAGGTACAGTTTCTCACTGCTGACTGAAAAG-3′ bio[c]
FTmutR	5′-CTTTTCAGTCAGCAGTGAGAAACTGTACCTGAGACTGGAAAGTGTACCTGAAGCCTGCAGTTTATC-3′-bio

[a] Forward strand.
[b] Reverse strand.
[c] Underlined letters indicate mutated nts.

2.2.6 Inhibition of the NF-κB pathway

The NF-κB inhibitor, Caffeic Acid Phenethyl Ester (CAPE) (Santa Cruz Biotechnology), was dissolved in DMSO to make a 25 mg/ml stock solution. The effect of CAPE on the alternative ISG upregulation mechanism was assayed by the dual luciferase assay with the Ifit1 (-192, +66) Nluc luciferase construct. CAPE was added to the cell culture medium to final concentrations of 3, 5, 10, or 15 μg/ml right after virus absorption, while 0.05% DMSO treatment was used as controls. Significant differences were determined with a one-way ANOVA with multi-comparisons to the DMSO treatment sample and Tukey's post hoc test.

2.2.7 Detection of proteins by Western blotting in nuclear fractions

Nuclear and cytoplasmic extracts were prepared from IFNAR-/- MEFs using a Nuclear Fraction Kit (Active Motif) following the manufacturer's protocol. The protein concentrations in these fractions were measured using a BCA assay (ThermoFisher Scientific). Equivalent amounts (45 μg) of nuclear and cytoplasmic samples were used for SDS-polyacrylamide gel electrophoresis (PAGE). The separated proteins were electrophoretically transferred to a nitrocellulose membrane. The membrane was blocked with Tris-buffered saline (TBS, pH 8) containing 5% nonfat dried milk or 5% bovine serum albumin (BSA) and 0.1% Tween-20 for 1 h at room temperature and then incubated with a primary antibody overnight at 4℃. The membrane was then incubated with anti-rabbit or anti-mouse antibody conjugated with horseradish peroxidase (HRP) (Cell Signaling Technology) for 1 h at room temperature, washed with TBS containing 0.1% Tween-20, and processed for chemiluminescence using a SuperSignal West Pico Substrate kit (Thermo Fisher Scientific). The primary antibodies used were: anti-alpha-tubulin (Cell Signaling Technology, Cat#3873) and anti-Histone H3 (Cell Signaling Technology, Cat#4499), anti-p65 (RelA) (Santa Cruz Biotechnology, Cat#sc-8008x), anti-p50 (Cell Signaling

Technology, Cat#12540), anti-IRF3 (Cell Signaling Technology, Cat#4302), anti-IRF5 (Cell Signaling Technology, Cat#4950), and anti-IRF7 (Invitrogen, Cat#PA5-20280).

2.3 Results

2.3.1 Mx1 but not Mx2 expression is induced by WNV in an IFN-independent manner

To identify additional ISGs in the subset that is induced by WNV infection in an IFN-independent manner, the mRNA expression levels of ISGs with known antiviral functions were analyzed in WNV-infected IFNAR-/- MEFs. Mx proteins have been shown to have evolutionarily conserved antiviral activities towards several families of viruses, among which the majority studied were negative-strand RNA viruses. The expression of Mx genes is typically strictly dependent on type I and III IFNs (Verhelst *et al.*, 2013). Two Mx proteins are encoded by the human (MxA and MxB) as well as the mouse (Mx1 and Mx2) genomes. Human MxA is a cytoplasmic protein. Polymorphisms in the human MxA gene have been associated with HCV infection outcomes (Knapp *et al.*, 2003; Garcia-Alvarez *et al.*, 2017). Mouse Mx1 localizes to the nucleus and inhibits viruses that replicate in the nucleus, such as influenza virus, whereas mouse Mx2 is cytoplasmic and protects against viruses that replicate in the cytoplasm, such as vesicular stomatitis virus (VSV) (Haller *et al.*, 2007). Rsad2 (also known as cig5 and viperin) has antiviral activity against a wide variety of viruses (Helbig and Beard, 2014). Rsad2 has been shown to be induced by all three types of IFN, and its expression is tightly regulated by ISGF3 (Severa *et al.*, 2006). However, infection with another flavivirus, Japanese encephalitis virus (JEV), directly activates Rsad2 expression through activating the transcription factors IRF3 and AP-1 (Chan *et al.*, 2008). The induction of Rsad2 in an IRF-3 dependent but an IFN-independent manner was observed in cells infected with an alphavirus, Chikungunya virus (CHIKV) (White

et al., 2011). Mice lacking Rsad2 showed increased mortality after WNV infection (Szretter *et al.*, 2011).

The mRNA expression levels of Mx1, Mx2, and Rsad2 were measured by real-time quantitative (q) RT-PCR in the total cellular RNA samples collected from WNV Eg101-infected IFNAR-/- MEFs. At 34 hpi, Mx1 was upregulated in WNV Eg101-infected IFNAR-/- MEFs. Neither Mx2 nor Rsad2, which are induced by IFN-β treatment in wild-type MEFs, were detected in the WNV-infected IFNAR-/- MEFs (Figure 2-1 A). The IFN-independent induction of Mx1 was next investigated in RNA samples of WNV Eg101-infected IFNAR-/- MEFs collected at different times after infection. Mx1 mRNA expression was induced by WNV Eg101 infection of IFNAR-/- MEFs, and the peak transcript level was observed at 32 hpi (Figure 2-1 B). The kinetics of Mx1 upregulation were similar to those of the other ISGs in this subset after WNV Eg101 infection in IFNAR-/- MEFs (Pulit-Penaloza *et al.*, 2012b). The data indicate that Mx1 is another member in the subset of ISGs that can be induced by WNV in an IFN-independent manner. The data also confirmed that only a subset of ISGs could be induced by the alternative mechanism.

The human MxA and mouse Mx1 proteins have antiviral activity against negative-strand RNA viruses but are not very effective in inhibiting flaviviruses. The cytoplasmic human MxA protein was reported to sequester WNV capsid protein that was ectopically expressed from a vector, but this potential inhibitory effect on replication was not observed in the context of a virus infection (Hoenen *et al.*, 2014). Constitutive expression of murine Mx1 protein protects against influenza virus infection but not WNV infection in mice (Moritoh *et al.*, 2009).

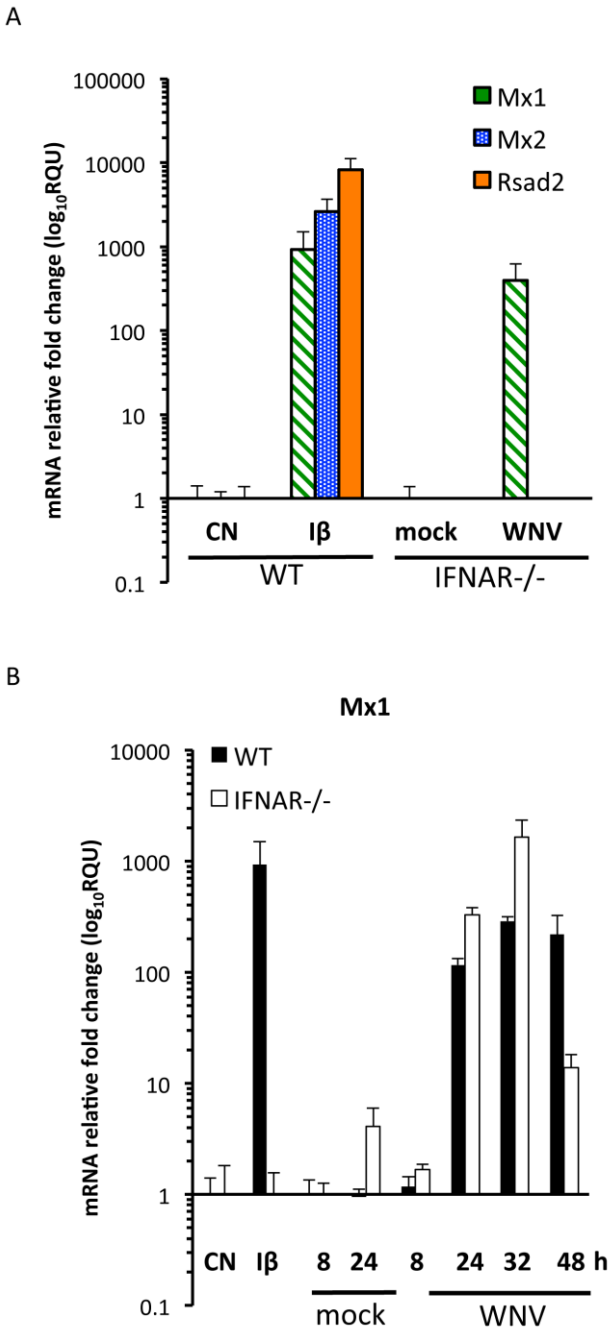

Figure 2.1 Mx1, but not Mx2 and Rsad2, is upregulated in an IFN-independent manner.

Primary IFNAR-/- MEFs and wild-type C57BL/6 MEFs were mock-infected or infected with WNV Eg101 at a MOI of 5 for the indicated times, or treated with IFN-β (1000 U/ml) for 3 h. (A) Mx1, Mx2 and Rsad2 mRNA levels were measured by real-time qRT-PCR in cellular RNA samples from mock- or WNV-infected IFNAR-/- MEFs collected at 34 hpi or from control- or IFN-treated wild-type C57BL/6 MEFs (positive control). (B) The Mx1 mRNA levels in IFNAR-/- or wild-type MEFs at different times after WNV infection were analyzed by real-time qRT-PCR. The transcript level of each gene was normalized to the GAPDH transcript level

in the same sample and is shown as the relative fold change over the amount in 34 h mock-infected samples. For the IFN-treated sample, the relative fold change was calculated over the amount in an untreated MEF sample. Each sample was assayed in triplicate, and representative data from one of three independent experiments are shown. The error bars represent standard deviation (SD). CN, untreated control. Iβ, IFN-β treatment.

2.3.2 Ifit1 is an additional ISG in the subset that is induced by WNV infection in an IFN-independent manner

IFIT proteins (interferon-induced proteins with tetratricopeptide repeats) are known to be induced by type I or type III IFN treatment or viral infection. IFIT proteins have no known enzymatic activities but inhibit virus transcription and translation in host cells (Fensterl and Sen, 2015). The Ifit1 gene is conserved among mammals. Cytoplasmic Ifit1 protein recognizes non-self RNA structures, such as 2′-O unmethylated RNA and 5′-ppp RNA and acts as an effector molecule to suppress viral translation (Pichlmair *et al.*, 2011; Diamond, 2014). To escape the antiviral function of Ifit1, flaviviruses have evolved their own capping machinery to modify the 5′ end of the viral RNA in the same way that host mRNA is modified. A WNV with a mutation inhibiting the viral 2′-O-methyltransferase activity showed reduced pathogenesis in wild-type mice due to the action of the Ifit1 protein (Szretter *et al.*, 2012).

To determine whether Ifit1 can be induced by WNV infection in an IFN-independent manner, the transcript level of Ifit1 was assayed in WNV Eg101-infected MEFs by real-time qRT-PCR. After WNV infection, Ifit1 was highly induced in primary wild-type C57BL/6 MEFs as well as in IFNAR-/- MEFs (Figure 2-2 A). The data indicate that Ifit1 can be induced by WNV infection in an IFN-independent manner as well as in an IFN-dependent manner. IFN-independent induction of Ifit1 was also observed in WNV-infected tSTAT1-/- MEFs, which lack a fundamental component of the JAK-STAT signaling pathway. The tSTAT1-/- MEFs and control wild-type t129 MEFs used were transformed cell lines. As expected, Ifit1 gene

expression was induced by WNV infection in both wild-type t129 and tSTAT1-/- MEFs (Figure 2-2 B). The data indicate that Ifit1 is also a member of the subset of ISGs that are induced by WNV infection by an IFN-independent mechanism.

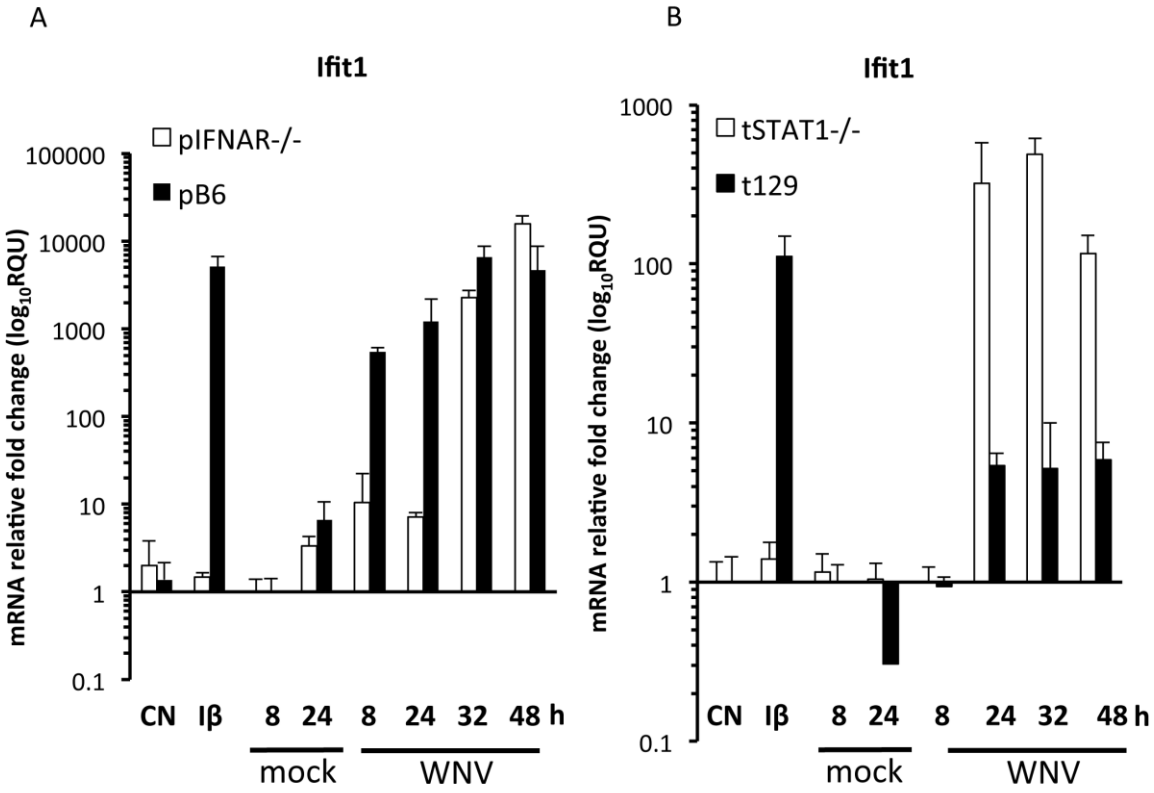

Figure 2.2 Ifit1 is upregulated in an IFN-independent manner by WNV infection.

Ifit1 mRNA expression was measured by qRT-PCR in WNV Eg101-infected (MOI of 5) (A) primary IFNAR-/- MEFs and (B) transformed STAT1-/- MEFs. MEFs were mock-infected or infected with WNV strain Eg101 at the indicated times post infection, or treated with IFN-β (1000 U/ml) for 3 h. The Ifit1 transcript level was normalized to the transcript level of GAPDH in the same sample and is shown as the relative fold change over the amount in the 8 h mock-infected samples. Each sample was assayed in triplicate, and representative data from one of three independent experiments are shown. The error bars represent SD. CN, control. Iβ, IFN-β treatment.

2.3.3 Comparison of the alternative ISG upregulation mechanism induced by WNV Eg101 and WNV W956IC

WNV Eg101 was used in the initial study that discovered the IFN-independent upregulation of ISGs after WNV infection (Pulit-Penaloza *et al.*, 2012b). W956IC (referred as W956 hereafter) is an engineered chimeric WNV. The majority of the W956 genome is from the lineage II WNV strain B956, with the 1,496 nts from the 3′ end from the lineage I WNV strain Eg101 (Yamshchikov *et al.*, 2001). Compared to the natural virus strain Eg101, the chimeric virus produces higher levels of "unprotected" viral RNA at early times after infection, which activate the cellular RNA sensors inducing elevated levels of IFN-β. Because more RNA replication than genome translation is occurring at early times after infection, fewer viral proteins that inhibit the canonical IFN signaling are produced. Consequently, W956-infected cells rapidly produce high levels of ISGs that reduce the yield of W956 virus in type I IFN-competent cells (Scherbik *et al.*, 2013). Therefore, it was hypothesized that a WNV W956 infection would induce the IFN-independent expression of ISGs to a higher level than a WNV Eg101 infection.

To test this hypothesis, the extent of upregulation of some representative ISGs induced by the IFN-independent mechanism by these two WNVs was compared. IFNAR-/- MEFs, which do not have canonical IFN signaling, were infected with WNV W956 or WNV Eg101 at a MOI of 5. Total cellular RNA samples were collected from W956-infected cells at 8, 16, 24, 32 and 48 hpi. Total cellular RNAs were only collected at 8, 24 and 32 hpi after WNV Eg101 infection because this was a repeat of previously published data.

Oas1a, Oas1b, and IRF7 mRNA expression level were analyzed by real-time qRT-PCR. In response to WNV Eg101 infection, the transcription of Oas1a and Oas1b mRNA increased since 8 hpi and reached a peak level of more than a 1000-fold change at 32 hpi in IFNAR-/-

MEFs (Figure 2-3 A and B). Irf7 was induced by only about 100 fold at 32 hpi after WNV Eg101 infection of IFNAR-/- MEFs (Figure 2-3 C). The WNV Eg101 data obtained are consistent with previously published data (Pulit-Penaloza *et al.*, 2012b).

In WNV W956-infected IFNAR-/- MEFs, high levels of Oas1a, Oas1b, and Irf7 expression levels were observed by 16 hpi, which were similar to the levels reached by 32 hpi in WNV Eg101-infected cells. Although the expression levels of Oas1a and Oas1b progressively decreased with time after infection starting at 24 hpi, the Irf7 levels did not decline (Figure 2-3 D to F). These data demonstrate that WNV W956 induces more robust IFN-independent expression of the subset of ISGs at early times after virus infection than WNV Eg101, which is likely due to the strong activation of the cellular RNA sensors by the high levels of "unprotected" viral RNA produced at early times in WNV W956-infected cells.

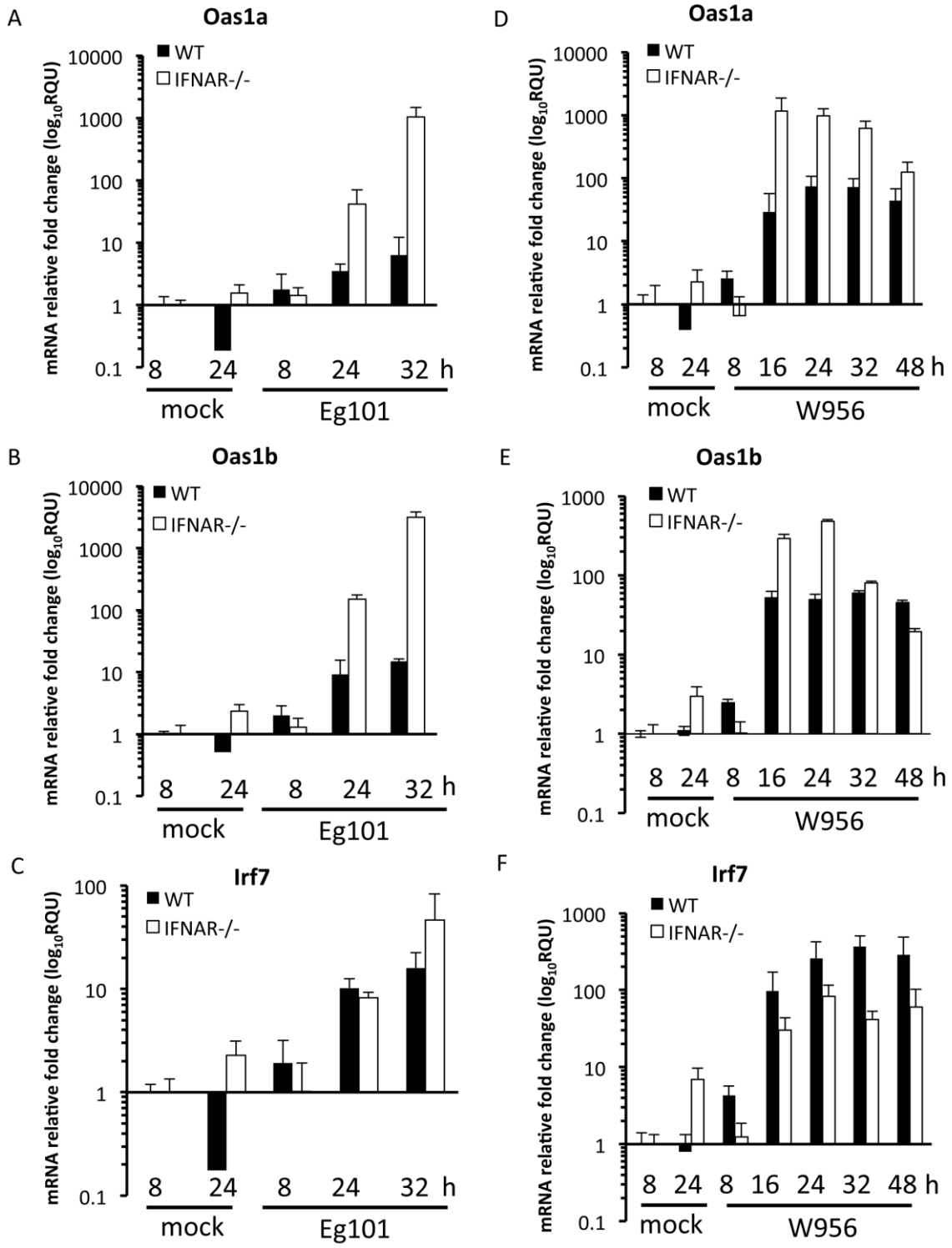

Figure 2.3 WNV W956 induces the alternative mechanism of ISG expression to a higher level than WNV Eg101 at early times after infection.

Transformed (3T3) IFNAR-/- and wild-type C57B/6 MEFs were infected with WNV Eg101 or WNV W956 at a MOI of 5, and total cellular RNA was collected at the indicated times

after infection. The mRNA expression levels of Oas1a, Oas1b, and Irf7 were measured by real-time qRT-PCR in WNV Eg101-infected MEFs (A to C) and WNV W956-infected MEFs (D to F). The transcript level of each gene was normalized to the GAPDH transcript level in the same sample and is shown as relative fold change over the amount in the 8 h mock-infected samples. Each sample was assayed in triplicate. Representative data from one of three independent experiments are shown. The error bars represent SD.

To compare the yields produced by WNV Eg101 and WNV W956 in IFN-incompetent MEFs, IFNAR-/- MEFs were infected (MOI of 1), and the extracellular virus titers were measured by plaque assay. At 12 hpi, WNV W956-infected IFNAR-/- MEFs produced 10 times more virus than the WNV Eg101-infected cells. The virus yields were similar at 24 hpi and after that were slightly lower from the W956-infected cells (Figure 2-4). The observation that higher yields of W956 are produced at an early time after infection but not at later times was similar to what was observed in BHK cells, which also have a defective IFN system (Scherbik *et al.*, 2013). Overall, these data suggest that in W956-infected IFN-incompetent cells, the "unprotected" viral RNA produced at early times after infection (around 12 h) rapidly activates IFN-independent antiviral signaling.

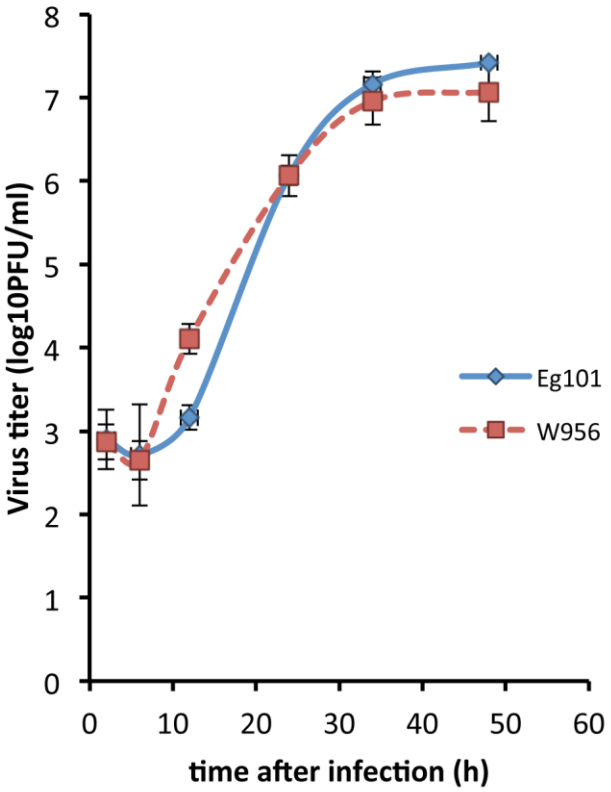

Figure 2.4 Comparison of virus production by WNV Eg101 and W956 virus infections in IFNAR-/- MEFs.

Confluent monolayers of 3T3-transformed IFNAR-/- MEFs were infected with WNV Eg101 or WNV W956 at a MOI of 1. At the indicated times after infection, culture fluids were collected, and infectivity was determined by plaque assay. The values are averages of duplicate titrations of each sample from two independent biological repeats. The error bars represent SD (n=4).

2.3.4 The alternative ISG upregulation mechanism is activated by viral RNA sensor RIG-I or MDA5

The RLR family of cytosolic sensors, RIG-I and MDA5, are both essential for the induction of IFN expression and control pathogenesis after a WNV infection (Errett *et al.*, 2013). After viral RNA binds to RIG-I or MDA5, signaling is transduced through the adaptor molecule IPS-1 to activate downstream signaling leading to the induction of IFN-β gene expression. In WNV-infected cells, the expression and secretion of type I IFN are normal, but signaling induced

by secreted IFN binding to its cell surface receptor is blocked by viral nonstructural proteins. A previous study in the Brinton lab showed that in MEFs lacking IPS-1, the IFN-independent subset of ISGs is upregulated at 8 hpi but is progressively decreased thereafter (Pulit-Penaloza *et al.*, 2012b). These data suggest that IPS-1 is involved in regulating this subset of ISGs in the IFN-independent manner. IPS-1 is the downstream adaptor molecule of RIG-I and MDA5. In MEFs lacking either RIG-I or MDA5, the alternative ISG upregulation mechanism was still observed in WNV Eg101-infected MEFs (Pulit-Penaloza *et al.*, 2012b). However, the lack of RIG-I resulted in a slight reduction in gene upregulation levels (Pulit-Penaloza *et al.*, 2012b). It was not known whether RIG-I and MDA5 redundantly sense WNV RNA or whether viral RNA was detected by a different cell sensor during the induction of the IFN-independent upregulation of ISGs. Toll-like receptor 3 (TLR3), TLR7, and TLR8 have been shown to be involved in sensing a WNV infection (Gack and Diamond, 2016). The cyclic GAMP-AMP synthase (cGAS), which senses DNA, was shown to be activated by both a WNV and a dengue virus (another flavivirus) infection. cGAS signaling is transduced through stimulator of interferon genes (STING) which can associate with IPS-1 (Ishikawa *et al.*, 2009; Kell and Gale, 2015).

The characteristic of producing high levels of early viral RNAs that activate the cell sensors makes WNV W956 a better virus than WNV Eg101 for studying the involvement of cell sensors in the IFN-independent mechanism. MEFs lacking both RIG-I and MDA5 were used to determine whether RIG-I and MDA5 function redundantly in sensing viral RNA during the initiation of IFN-independent upregulation of ISGs. RIG-I$^{-/-}$/MDA5$^{-/-}$ MEFs were infected with WNV W956 at a MOI of 5 to ensure that all of the cells were infected and total cellular RNA was harvested at the indicated times. ISG transcripts levels were assayed by real-time qRT-PCR. In WNV W956-infected RIG-I$^{-/-}$/MDA5$^{-/-}$ MEFs, Oas1a, Irf7, and Ifit1 were not upregulated

after virus infection (Figure 2-5 A, C and D). Although a low-level induction of Oas1b was detected after virus infection, the level was not significantly higher than that in the 24 h mock-infected sample (Figure 2-5 B). Because the previously published data on IFN-independent ISGs in RIG-I-/- and MDA5-/- MEFs were obtained using WNV Eg101 (Pulit-Penaloza *et al.*, 2012b), the RIG-I$^{-/-}$/MDA5$^{-/-}$ MEFs were also infected with WNV Eg101. A similar decrease in the upregulation of the IFN-independent ISGs was observed in WNV Eg101-infected RIG-I$^{-/-}$ /MDA5$^{-/-}$ MEFs (data not shown) as with WNV W956 infection. The data indicate that either RIG-I or MDA5 can activate the IFN-independent antiviral mechanism.

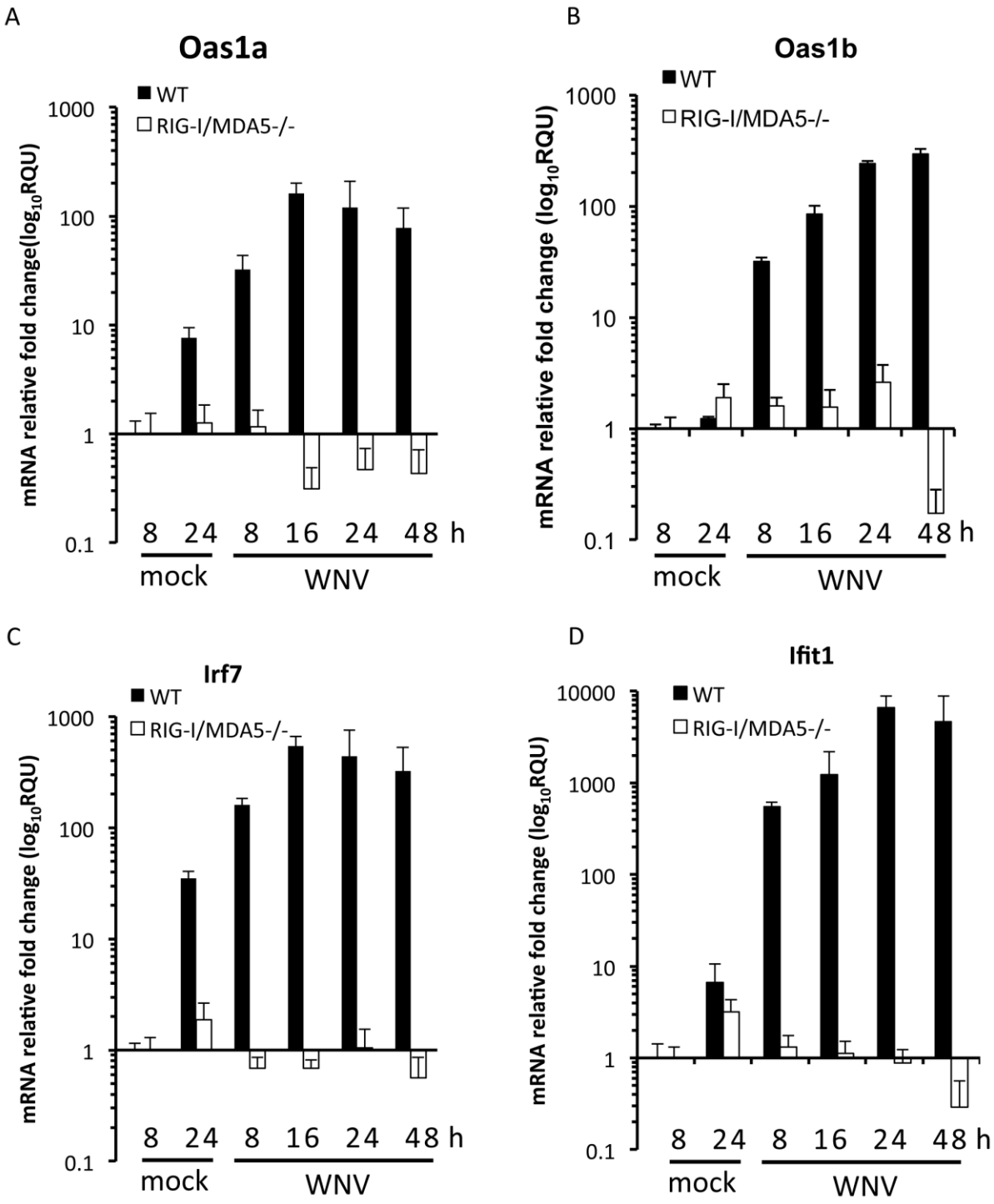

Figure 2.5 At least one of the cytosolic sensors, RIG-I and MDA5, is needed for the induction of the IFN-independent mechanism.

Primary RIG-I$^{-/-}$/MDA5$^{-/-}$ MEFs and wild-type C57BL/6 MEFs were mock-infected or infected with WNV W956 at a MOI of 5. The mRNA expression levels of (A) Oas1a, (B) Oas1b, (C) Irf7, and (D) Ifit1 were measured by real-time qRT-PCR in total cellular RNA samples

collected at the indicated hpi. The transcript level of each gene was normalized to the GAPDH transcript level in the same sample and is shown as relative fold change over the amount in the 8 h mock-infected samples. Each sample was assayed in triplicate, and representative data from one of three independent experiments are shown. The error bars represent SD.

2.3.5 Analysis of the involvement of IRF family transcription factors in the upregulation of the IFN-independent subset of ISGs by a WNV infection

IRF family members were initially identified as transcription factors for genes in the type I IFN pathway. There are nine well-conserved members in the mammalian IRF family: IRF1, IRF2, IRF3, IRF4, IRF5, IRF6, IRF7, IRF8, and IRF9 (also known as ISGF3γ) (Taniguchi *et al.*, 2001). All of the IRF proteins have a helix-turn-helix DNA-binding motif (Ikushima *et al.*, 2013). The DNA binding site for all of the IRFs is called the IRF-binding element (IRF-E), and its consensus sequence is 5′-AANNGAAANNGAAA-3′ (Paun and Pitha, 2007). However, each IRF protein processes slightly different DNA binding specificities within the IRF-E consensus sequence (Schmid *et al.*, 2010).

IRF9 is expressed in a variety of tissues and is essential for the antiviral response induced by type I IFN signaling because it is the DNA-binding subunit of the transcription factor complex ISGF3 (Taniguchi *et al.*, 2001). In a previous study in the Brinton lab, Oas1a and Oas1b were shown to be upregulated in WNV-infected IRF3-/- MEFs but not in IRF3/9-/- MEFs, suggesting the possibility that IRF9 is involved in the upregulation of ISGs by the IFN-independent mechanism (Pulit-Penaloza *et al.*, 2012b). To analyze the role of IRF9 in upregulating the expression of Oas1a, Oas1b, and Irf7 by an IFN-independent mechanism, the transcript levels of these genes were analyzed in primary IRF9-/- MEFs at various times after WNV infection. Oas1a, Oas1b and Irf7 were all induced in WNV-infected IRF9-/- MEFs (Figure

2-6). The data indicate that IRF9 is not required for the upregulation of these ISGs in WNV-infected MEFs and that the IRF3/9-/- MEFs likely had an additional defect(s).

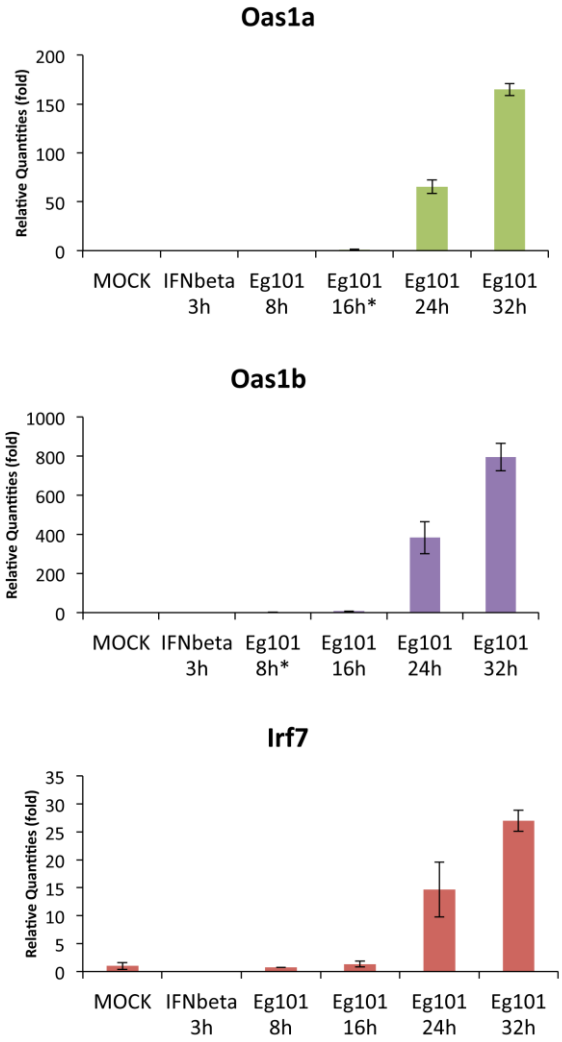

Figure 2.6 The IFN-independent subset of ISGs is upregulated in IRF9-/- MEFs after WNV infection.

Primary IRF9-/- MEFs were mock-infected or infected with WNV Eg101 at a MOI of 5. Cells incubated with IFN-β (1000 U/ml) for 3 h were used as a control. The mRNA expression levels of Oas1a, Oas1b, and Irf7 were measured by real-time qRT-PCR in cellular RNA samples collected at the indicated hpi. The transcript level of each gene was normalized to the GAPDH transcript level in the same sample and is shown as relative fold change over the amount in the 8 h mock-infected samples. The level of Oas1a in 8 h mock-infected sample was too low to be detected, so the amount in 16 h WNV-infected samples was used to calculate relative fold change. Each sample was assayed in triplicate. Representative data from one of three independent experiments are shown. The error bars represent SD.

IRF1, the first discovered member of the IRF family, was shown to induce the expression of many ISGs in the absence of IFN (Pine, 1992). The overexpression of IRF1 in human STAT1-/- MEFs was subsequently shown to transcriptionally activate a subset of ISGs without inducing the expression of IFN (Schoggins *et al.*, 2011). The role of IRF1 in upregulating the expression of the subset of ISGs activated in an IFN-independent manner by a WNV infection was next analyzed. Primary IRF1-/- MEFs and matched wild-type MEFs were infected with WNV W956 at a MOI of 5, and total cellular RNA was collected at the indicated times. The transcript levels of Oas1a, Oas1b, Irf7, and Ifit1 were measured by real-time qRT-PCR. Each of these four genes was efficiently upregulated in IRF1-/- and control cells by both IFN-β and WNV infection (Figure 2-8 A to D). The data suggest that IRF1 alone is not required for the upregulation of the subset of IFN-independent ISGs in WNV-infected MEFs.

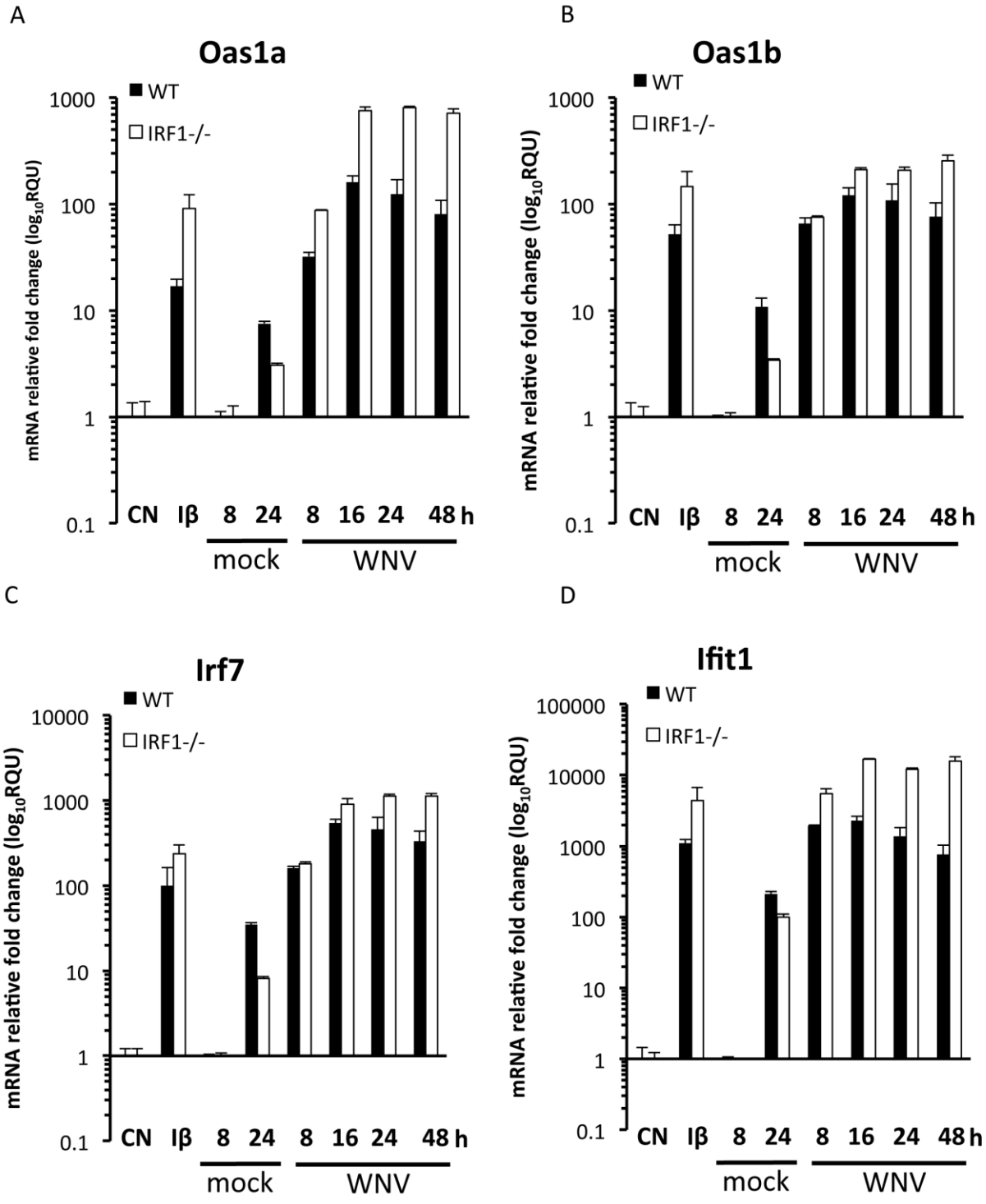

Figure 2.7 The IFN-independent subset of ISGs is upregulated in IRF1-/- MEFsafter WNV infection.

Primary IRF1-/- MEFs and the wild-type C57BL/6 MEFs were mock-infected or infected with WNV W956 at a MOI of 5. Cells treated with IFN-β were used as positive controls. The

mRNA expression levels of (A) Oas1a, (B) Oas1b, (C) Irf7, and (D) Ifit1 were measured by real-time qRT-PCR in cellular RNA samples collected at the indicated hpi. The transcript level for each gene was normalized to the GAPDH transcript level in the same sample and is shown as relative fold change over the amount in the 8 h mock-infected samples. The relative fold change after IFN-β treatment was calculated over the amount in untreated cells. Each sample was assayed in triplicate. Representative data from one of three independent experiments are shown. The error bars represent SD. CN, untreated control. Iβ, IFN-β treatment.

IRF5 is involved in the signaling pathway downstream of the RIG-I/MDA5-IPS-1 pathway for type I IFN production (Ikushima *et al.*, 2013). IRF5 has been reported to be involved in the upregulation of some ISGs as well as in IFN-β gene induction after WNV infection in dendritic cells (Lazear *et al.*, 2013). In WNV-infected mice, IRF5 provided protection through shaping the early innate immune response, which includes controlling the type I IFN response and regulating the expression of other cytokines and chemokines (Thackray *et al.*, 2014). The role of IRF5 in upregulating the IFN-independent subset of ISGs was analyzed in WNV-infected MEFs. Primary IRF5-/- MEFs and matched wild-type MEFs were infected with WNV W956 at a MOI of 5, and total cellular RNA samples were collected at the indicated times. The transcript levels of Oas1a, Oas1b, Irf7, and Ifit1 were assayed by real-time qRT-PCR. All four genes were efficiently upregulated in IRF5-/- and control MEFs by both IFN-β and WNV infection (Figure 2-9 A to D). The data suggest that the IFN-independent subset of ISGs can be upregulated by WNV infection when IRF5 is absent.

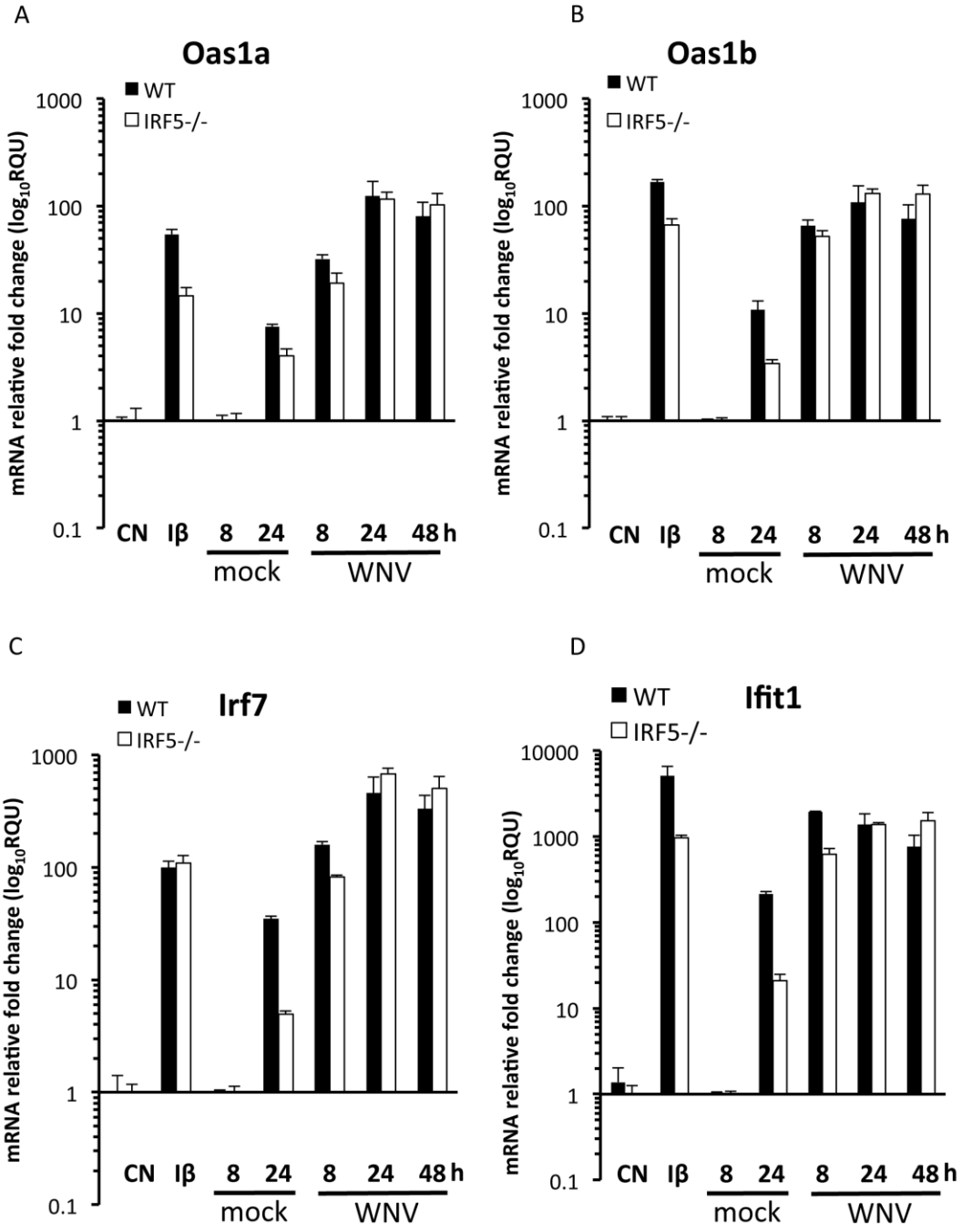

Figure 2.8 The IFN-independent subset of ISGs is upregulated in IRF5-/- MEFs after WNV infection.

Primary IRF5-/- MEFs and wild-type C57BL/6 MEFs were mock-infected or infected with WNV W956 at a MOI of 5. Cells treated with IFN-β for 3 h were used as a positive control. The mRNA expression levels of (A) Oas1a, (B) Oas1b, (C) Irf7, and (D) Ifit1 were measured by real-time qRT-PCR in total cellular RNA samples collected at the indicated times after infection. The transcript level for each gene was normalized to the GAPDH transcript level in the same sample and is shown as relative fold change over the amount in the 8 h mock-infected samples.

The relative fold change after IFN-β treatment is calculated over the amount in control treatment. Each sample was assayed in triplicate. Representative data from one of three independent experiments are shown. The error bars represent SD. CN, untreated. Iβ, IFN-β treatment.

Among all the IRF family members, IRF3 and IRF7 are closely related to each other with respect to their amino acid sequences. Both IRF3 and IRF7 have an N-terminal DNA binding domain and some phosphorylation sites in the C-terminal region (Taniguchi *et al.*, 2001). IRF3 is constitutively expressed and located in the cytoplasm as a latent form. IRF7 is induced by type I IFNs and further regulates the expression of IFN-β. Phosphorylation is required for nuclear translocation and transcription factor activities of IRF3 and IRF7 (Honda and Taniguchi, 2006). Previous data from the Brinton lab showed that Oas1a, Oas1b, and Irf7 are still upregulated in WNV-infected IRF3-/-, IRF7-/- and IRF3/7-/- MEFs (Pulit-Penaloza *et al.*, 2012b). A comparative study of WNV-infected IRF3/7-/- and IRF3/5/7-/- dendritic cells suggested that IRF5, IRF3 and IRF7 are responsible for the induction of IFN-β and some ISGs after virus infection (Lazear *et al.*, 2013).

The induction of Oas1a, Oas1b, and Ifit1 was analyzed in WNV-infected IRF3/5/7-/- MEFs. These cells were infected with WNV Eg101 at a MOI of 5 for consistency with the previous study in IRF3/7-/- MEFs. Oas1a, Oas1b, and Ifit1 mRNA expression levels were induced by IFN-β treatment in the IRF3/5/7-/- MEFs. However, the induction of each of the three genes by WNV infection was less than 10 fold by 8 hpi, and the induction decreased with time (Figure 2-10 A to C). Expression of the IFN-β gene was not induced by WNV infection in these cells, confirming that the IRF3/5/7-/- MEFs do not produce IFN-β in response to WNV infection (Lazear *et al.*, 2013) (Figure 2-10 D). The data suggest that IRF3, IRF5, or IRF7 can function as transcription factors in the IFN-independent ISG upregulation by WNV infection, and that they are functionally redundant.

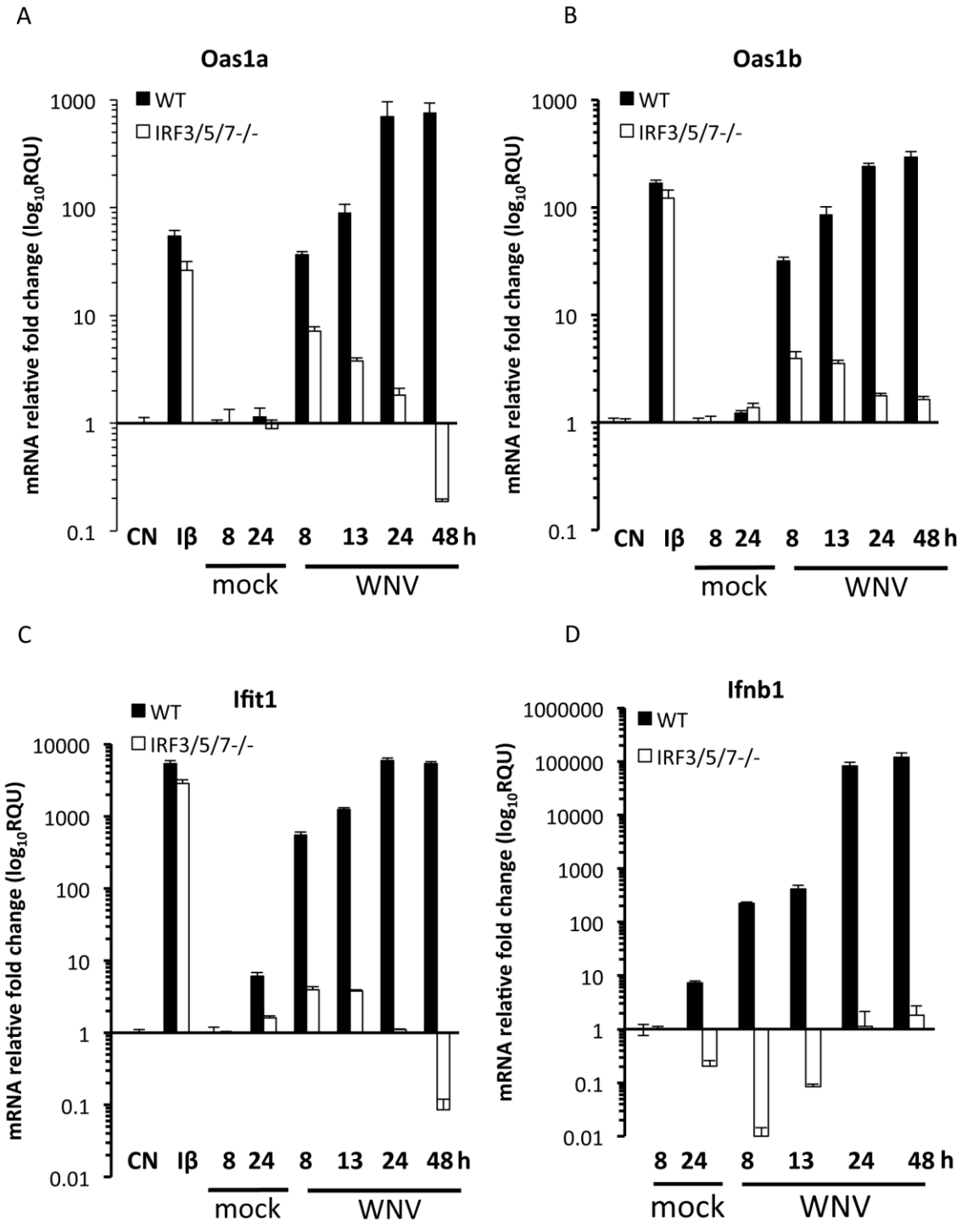

Figure 2.9 IRF3, IRF5, and IRF7 each can function in regulating the IFN-independent mechanism.

Primary IRF3/5/7-/- MEFs and wild-type C57BL/6 MEFs were mock-infected or infected with WNV Eg101 at a MOI of 5. Cells incubated with IFN-β (1000 U/ml) for 3 h were used as

positive controls. The mRNA expression levels of (A) Oas1a, (B) Oas1b, (C) Ifit1, and (D) Ifnb1 were measured by real time qRT-PCR in total cellular RNA samples collected at the indicated times after infection. The transcript level for each gene was normalized to the GAPDH transcript level in the same sample and is shown as relative fold change over the amount in the 8 h mock-infected samples. The relative fold change after IFN-β treatment was calculated over the amount in untreated cells. Each sample was assayed in triplicate. Representative data from one of three independent experiments are shown. The error bars represent SD. CN, untreated control. Iβ, IFN-β treatment.

Ifit1 gene expression was previously reported to be upregulated through the transcription factor IRF3 after activation of cell sensors by viral or bacterial components (Fensterl and Sen, 2011). To determine whether the IFN-independent upregulation of Ifit1 in WNV-infected cells is IRF3-dependent as previously reported, Ifit1 mRNA expression levels in WNV-infected IRF3-/- MEFs were analyzed by real-time qRT-PCR. Ifit1 was upregulated in both IRF3-/- and control MEFs after infection with either WNV W956 or WNV Eg101. However, the induction by WNV W956 reached a higher level at an earlier time after infection (Figure 2-11). The data demonstrate that IRF3 alone does not control the IFN-independent upregulation of Ifit1 after WNV infection.

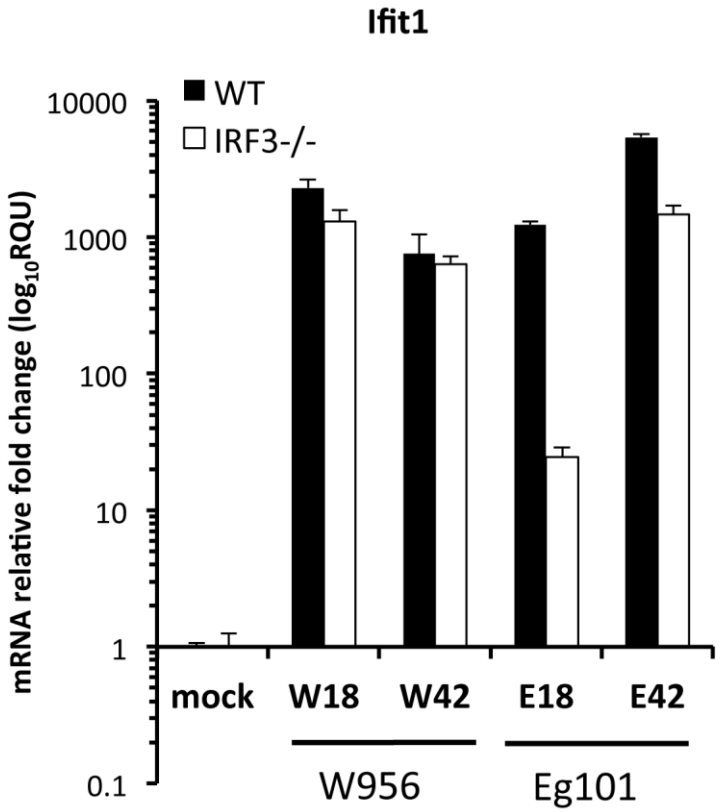

Figure 2.10 Ifit1 is induced by WNV infection in an IRF3-independent manner in MEFs.

Primary IRF3-/- and wild-type C57BL/6 MEFs were mock-infected or infected with WNV W956 or WNV Eg101 at a MOI of 3 for indicated hpi. Ifit1 mRNA expression was assessed by real-time qRT-PCR. The Ifit1 transcript level was normalized to the transcript level of GAPDH in the same sample and is shown as relative fold change over the amount in the 18 h mock-infected samples. Each sample was assayed in triplicate. Shown data are representative of three independent biological repeats. Error bars represent SD.

2.3.6 Mapping alternative response elements in the Ifit1 promoter

As an alternative method for predicting putative transcription factors involved in the IFN-independent ISG upregulation mechanism, functionally important transcription factor binding site (TFBS) regions in the promoters of representative ISGs were mapped. TFBSs are typically 6 to 12 bp in length, while the promoter of a gene is typically more than 1000 bp in length.

Therefore, serially truncated promoter fragments were used for the initial mapping studies using a dual luciferase assay system.

Because of its high level of induction in WNV-infected cells by the IFN-independent mechanism, the Ifit1 gene promoter was chosen for mapping. The longest Ifit1 promoter fragment containing 1000 bp upstream and 66 bp downstream of the transcription start site (TSS) was first cloned into the Nluc luciferase reporter vector pNL4.17. IFNAR-/- MEFs were mock-infected or infected with WNV W956 at a MOI of 3. At 3 hpi, cells were co-transfected with Ifit1 promoter Nluc luciferase construct DNA and a firefly luciferase vector DNA. Cell extracts were harvested at 28 h after infection (25 h after transfection) and assayed for luciferase activity. Basal luciferase activity, which was well distinguished from the background, was detected for the longest Ifit1 (-1000, +66) construct in mock-infected cells. In WNV-infected cells, this construct showed a significant increase in promoter activity, indicating that the promoter was activated by the virus infection (Figure 2-11 A). A set of 5′ sequentially truncated Ifit1 promoter fragments was next cloned into the Nluc luciferase reporter construct and assayed by the dual luciferase assay system. Similar basal activities in mock-infected cells were detected for all of the 5′ truncated promoters except the shortest Ifit1 promoter fragment (-50, +66), which had lower basal activity (Figure 2-11 A). The lower activity of fragment (-50, +66) suggested that the region from -132 to -50 contains elements that enhance basal Ifit1 expression. After WNV infection, the promoter activities of all of the Ifit1 promoter constructs were highly induced. Among them, expression from the longest promoter fragment Ifit1 (-1000, +66) was induced more than 10 fold after the infection. The sequential 5′ truncation constructs Ifit1 (-700, +66) and Ifit1 (-500, +66) showed decreased luciferase activity compared to Ifit1 (-1000, +66), suggesting that the region from -1000 to -500 contains enhancers (Figure 2-11 A). However, the promoter

activities of Ifit1 (-350, +66) and (-192, +66) were higher than that of Ifit1 (-500, +66), indicating that the region from -500 to -192 negatively regulates the promoter activity after virus infection through repressors contained in this region. The promoter activity of Ifit1 (-132, +66) was about 65% of that of Ifit1 (-192, +66), suggesting that the region from -192 to -132 contains enhancers. Comparison of the promoter activities of Ifit1 (-132, +66) and Ifit1 (-50, +66) showed that the deletion of the promoter region from -132 to -50 decreased the promoter activity by about 95%, suggesting that some very strong enhancers are contained in this region (Figure 2-11 A). The mapping data suggest that within the Ifit1 promoter, the regions from -1000 to -500, and from -192 to -50 contain enhancers while the region from -500 to -192 contains repressors (Figure 2-11 B). The promoter activity of the Ifit1 (-192, +66) construct corresponded to about 80% of the promoter activity of the longest Ifit1 promoter construct, which contains both an enhancer region (A1) and a repressor region in the region from -1000 to -192 (Figure 2-11 A), suggesting that the enhancer A1 region can overcome the repressor effects in regulating Ifit1 gene expression after WNV infection.

The ISRE is the TFBS to which the transcription factor complex ISGF3, which is composed of p-STAT1, p-STAT2, and IRF9, binds during the canonical JAK-STAT pathway in response to secreted type I IFNs binding to their cell surface receptors. There are three ISREs on the Ifit1 promoter. One ISRE is located in the enhancer A1 region between -700 and -500. The Ifit1 (-700, +66) construct, which contains this ISRE, showed higher luciferase activity than Ifit1 (-500, +66) construct that does not contain this ISRE (Figure 2-11 A). The other two ISREs on the Ifit1 promoter are located in the enhancer region between -132 and -50. Both of the promoter fragments Ifit1 (-192, +66) and Ifit1 (-132, +66), which contain the two ISREs, showed much higher promoter activities than the Ifit1 (-50, +66) fragment, which does not contain any ISRE

(Figure 2-11 A). The promoter mapping results suggested the possibility that the ISRE may contribute to the increased promoter activity. However, although both promoter fragments Ifit1 (-192, +66) and Ifit1 (-132, +66) contain two ISREs, the lower promoter activity of Ifit1 (-132, +66) compared to that of (-192, +66) suggests that additional elements in the region from -192 to -132 are also involved in upregulating the induction of Ifit1 gene expression in WNV-infected IFNAR-/- MEFs (Figure 2-11 A).

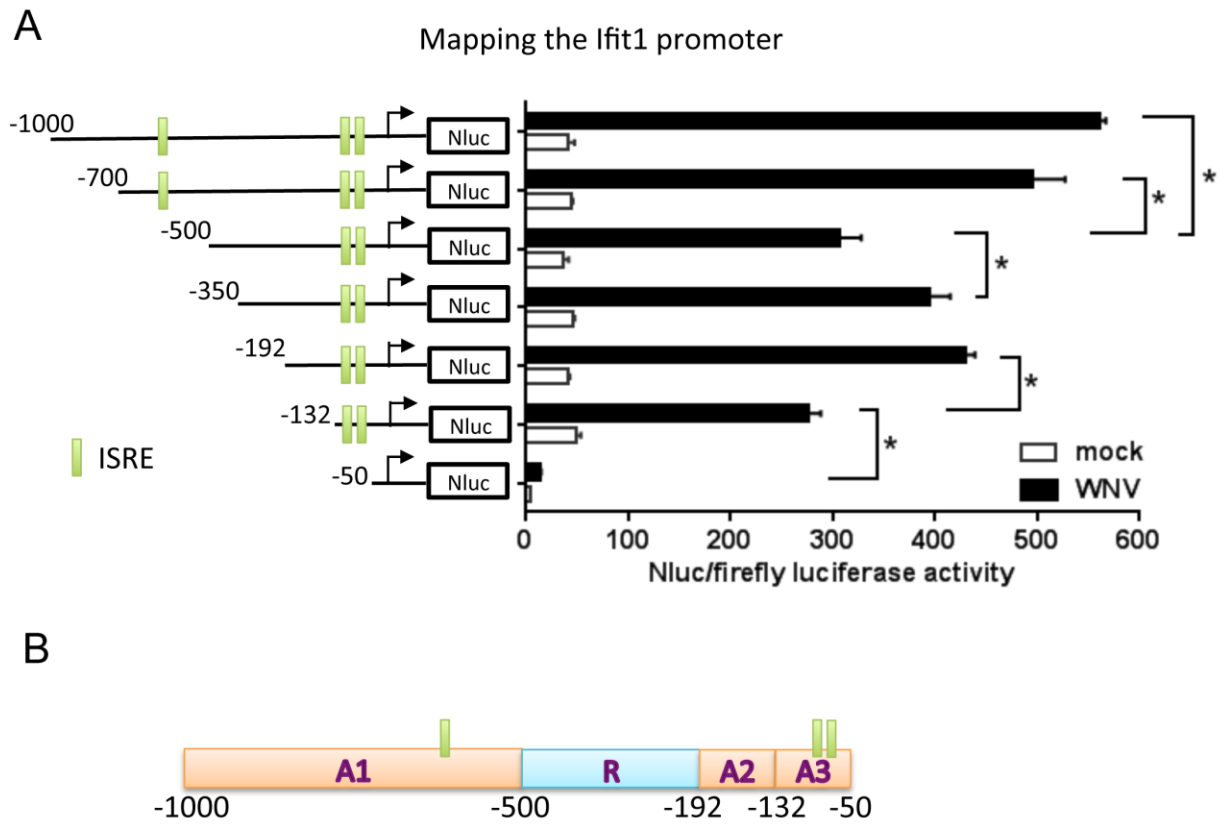

Figure 2.11 Mapping the mouse Ifit1 gene promoter regions that are activated after WNV infection by the IFN-independent mechanism.

Reporter vectors containing Ifit1 promoter fragments of different lengths were constructed. (A) Diagram of the promoter fragments tested (left side) and their luciferase activities (right side). Arrows indicate the position of the TSS. The upstream distances to the TSS are indicated. All promoter fragments terminate 66 bp downstream of the TSS. Transformed (3T3) IFNAR-/- MEFs were mock-infected or infected with WNV W956 at a MOI of 3. At 3 hpi, cells were co-transfected with a Nluc luciferase reporter construct DNA and firefly

luciferase vector pGL4.53 DNA (transfection control) in triplicate. At 28 hpi, cell lysates were prepared, and luciferase activity was measured. The Nluc luciferase activity was normalized to the firefly luciferase activity for each sample. Error bars represent SD. Significant differences were determined with a two-way ANOVA with multi-comparisons across the activities of promoters of different lengths and Tukey's post hoc test (*, $p<0.05$). (B) Diagram of the regulatory regions of the Ifit1 promoter during an IFN-independent response. The upstream distances to the TSS are indicated. A, enhancer. R, repressor.

2.3.7 Mapping alternative response elements in the Oas1b promoter

The promoter of mouse Oas1b was also mapped to locate *cis*-acting elements that respond to IFN-independent signaling in WNV-infected cells using the dual luciferase assay system. An Oas1b promoter fragment that contained 802 bp upstream and 50 bp downstream of the TSS was cloned into the Nluc luciferase vector pNL4.17. A set of 5′ sequentially truncated Oas1b promoter constructs was then made. IFNAR-/- MEFs were mock-infected or infected with WNV W956 at a MOI of 3, and then co-transfected with each Oas1b promoter Nluc luciferase construct DNA and a firefly luciferase vector DNA at 3 hpi. Cell extracts were harvested at 28 hpi (25 h after transfection), and luciferase activity was assayed. The basal activities of the Oas1b constructs were slightly higher and more variable than those found for the Ifit1 promoter constructs, with only the Oas1b (-54, +50) and Oas1b (-28, +50) constructs showing lower basal activities that were still well distinguished from background. The construct Oas1b (-299, +50) produced a higher basal activity than the other constructs that contained either longer or shorter Oas1b promoter fragments. The observation that the basal activity of Oas1b (-28, +50) was 30-fold lower than that of Oas1b (-299, +50) suggested that the region between -299 and -28 contains elements that enhance basal Oas1b expression in IFNAR-/- MEFs (Figure 2-12 A). All of the Oas1b promoter constructs were activated by WNV infection with more than a 3-fold induction. The construct Oas1b (-802, +50) showed higher promoter activity than the constructs Oas1b (-742, +50) and Oas1b (-576, +50), suggesting that in Oas1b promoter, the region from -

802 to -576 contains enhancers (Figure 2-12 A). The observation that the promoter activity of Oas1b (-507, +50) was higher than that of Oas1b (-576, +50) suggested that the region between -576 and -507 contains repressors. The observed decrease in promoter activity between Oas1b (-507, +50) and Oas1b (-394, +50) was subtle and demonstrated no statistical significance, but the deletion of the region from -394 to -299 significantly increased promoter activity as indicated by the promoter activities of constructs Oas1b (-394, +50) and Oas1b (-299, +50), suggesting the region between -394 to -299 contains repressors. Moreover, the promoter activity of Oas1b (-576, +50) was lower than that of Oas1b (-299, +50), indicating that the region between -576 and -299 contains multiple strong negative regulatory elements (Figure 2-12 A). The construct Oas1b (-299, +50) demonstrated the highest WNV-induced promoter activities among all the Oas1b promoter constructs. Multiple 5′ deletions in the region from -299 to -28 decreased the promoter activity, suggesting that this region contains enhancers (Figure 2-12 A). The mapping data suggest that within the Oas1b promoter, the regions from -802 to -576, and from -299 to -28 contain enhancers while the region from -576 to -299 contains repressors (Figure 2-12 C).

The construct Oas1b (-299, +50) showed higher promoter activity than that of the longest promoter construct Oas1b (-802, +50), suggesting that the promoter region in the Oas1b (-299, +50) construct contains all of the key elements needed for IFN-independent upregulation of Oas1b after WNV infection. This region was further mapped using constructs with additional 5′ deletions or internal deletions. Comparison of the promoter activities of Oas1b (-299, +50), Oas1b (-251, +50) and Oas1b (-181, +50) demonstrated that deletion of the region between -251 and -181 significantly decreased promoter activity. In addition, each sequential 5′ deletion of the region from -134 to -28 dramatically decreased the promoter activity as demonstrated by the activities of the Oas1b (-134, +50), Oas1b (-93, +50) and Oas1b (-28, +50) fragments. However,

the deletion of the region from -181 to -134 increased promoter activity as shown by constructs Oas1b (-181, +50) and Oas1b (-134, +50). The data suggest that even in the enhancer region from -299 to -28, there is still a subregion containing repressors. However, the repressors cannot overcome the effect of enhancers in the adjacent subregions (Figure 2-12 B). Comparison of the luciferase activities of the two constructs with internal deletions, Oas1b (-299/-202, -93/+50) and (-299/-144, -93/+50), showed that adding the piece of promoter from -202 to -144 decreased promoter activity, confirming the existence of repressor elements in the -181 to -144 region (Figure 2-12 B). The mapping data suggest that in Oas1b promoter, the regions from -802 to -576, from -299 to -181, and from -134 to -28 contain enhancers while the regions from -576 to -299, and from -181 to -134 contain repressors (Figure 2-13 C). The results indicate that the regulation of the Oas1b promoter is more complicated than that of the Ifit1 promoter in WNV-infected IFNAR-/- MEFs.

There are two ISREs in the Oas1b promoter. When the 5′ ISRE was deleted in the Oas1b promoter [compare fragments (-251, +50) and (-181, +50)], the promoter activity decreased by one-third (Figure 2-12 B), suggesting that this ISRE plays an important role in regulating the IFN-independent induction of Oas1b by WNV infection. Although the shortest Oas1b promoter (-28, +50) contains the 3′ ISRE, it had very low luciferase activity (Figure 2-12 B). The sequential 5′ deletions from -134 to -28 dramatically decreased the promoter activity, suggesting the possibility that enhancers in this region may cooperatively regulate Oas1b gene promoter activation with the 3′ ISRE in WNV-infected IFNAR-/- MEFs.

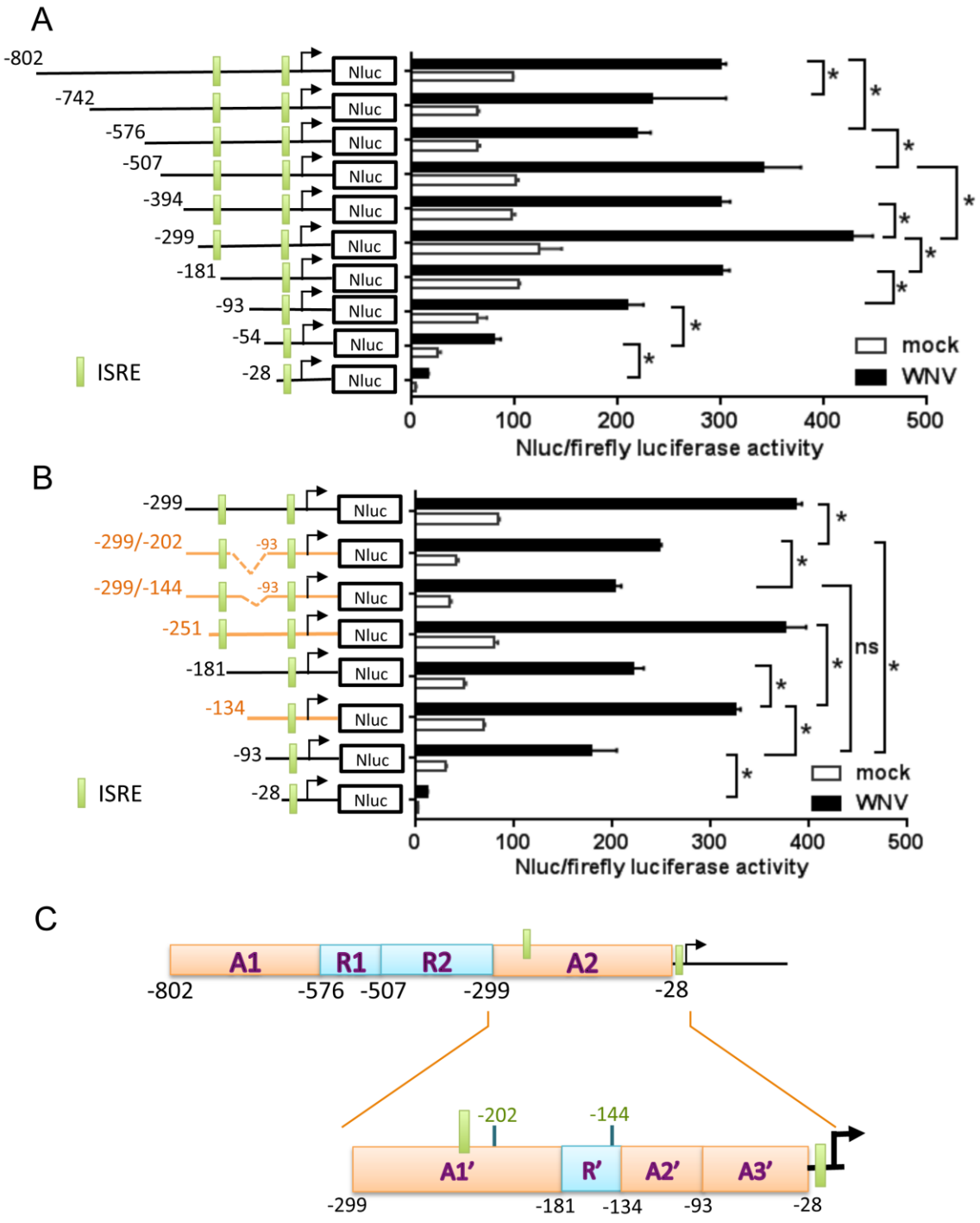

Figure 2.12 Mapping the mouse Oas1b gene promoter regions activated after WNV infection by the IFN-independent mechanism.

Reporter constructs containing Oas1b promoter fragments of different lengths were constructed. (A, B) Diagram of the promoter fragments tested (left side) and their luciferase activities (right side). Arrows indicate the TSS. The upstream distances to the TSS are indicated. All promoter fragments terminate 50 bp downstream of the TSS. Transformed (3T3) IFNAR-/-

MEFs were mock-infected or infected with WNV W956 at a MOI of 3. At 3 hpi, cells were co-transfected with a Nluc luciferase reporter construct DNA and firefly luciferase vector pGL4.53 DNA (transfection control) in triplicate. At 28 hpi, cell lysates were prepared, and luciferase activity was measured. The Nluc luciferase activity was normalized to firefly luciferase activity for each sample. Error bars represent SD. Significant differences were determined with a two-way ANOVA with multi-comparisons across the activities of promoters of different lengths and Tukey's post hoc test (*, $p<0.05$). (C) Diagram of the regulatory regions of the Oas1b promoter. The numbers indicate locations upstream of the TSS. A, enhancer. R, repressor.

2.3.8 ISRE motifs in the Ifit1 and Oas1b promoters are involved in the alternative gene upregulation mechanism

The mapping data obtained for the Oas1b and Ifit1 promoters suggest the involvement of an ISRE in regulating the non-canonical ISG upregulation mechanism. The consensus sequence of the ISRE is 5′A/GNGAAANNGAAACT3′, where the 3′ GAAA (underlined) is the core binding site (Darnell *et al.*, 1994). Both the Ifit1 promoter (Figure 2-11 A) and the Oas1b promoter (Figure 2-12 A and B) contain two ISREs within 350bp upstream of TSS. In the Ifit1 promoter, the two sites are located in the region between -132 and -50 and are separated by 19 nts. In the Oas1b promoter, one ISRE is located between -251 and -181 while the other is between -28 and TSS (206 nts apart). Each of the ISREs in the Oas1b and Ifit1 promoters was individually mutated to change the core binding consensus from GAAA to GTAC. The mutated sequence was analyzed using MatInspector software to confirm that the ISREs had been eliminated and no new TFBSs had been created. The promoter activity of each mutated construct was analyzed.

The ISREs were mutated in the Ifit1 (-192, +66) construct. Mutation of either ISRE in the Ifit1 promoter decreased the luciferase activity by more than 80% (Figure 2-13 A). When both of the ISREs were mutated, the promoter activity was almost completely abolished (Figure 2-13 A). These results suggest that both ISREs contribute to the non-canonical expression of Ifit1 by WNV infection, and they are not redundant.

Because the two ISREs are not close to each other in the Oas1b promoter, the ISREs were separately mutated in two constructs, Oas1b (-251, +50) containing both sites and Oas1b (-93, +50) containing only the 3′ ISRE. Mutation of the ISRE in the Oas1b (-93, +50) construct decreased promoter activity by ~68% (Figure 2-13 B). Mutation of either ISRE in the Oas1b (-251, +50) construct significantly decreased promoter activity, with mutation of the 3′ ISRE having a greater negative effect. When both of the Oas1b ISREs were mutated, the promoter activity was similar to that observed when only the 3′ ISRE was mutated (Figure 2-13 B). These data indicate that the ISREs play a key role in mediating the non-canonical upregulation of Oas1b in WNV-infected cells, and that the 3′ ISRE has a more important role than the 5′ one. However, the data also indicate that the ISREs are not the only sites involved in IFN-independent gene regulation in this promoter. Comparison of the Oas1b (-299, +50) and Oas1b (-299/-202, -93/+50) constructs showed that even when both ISREs were present, deletion of the enhancer region between -202 and -93 decreased the promoter activity by more than 50% (Figure 2-13 B).

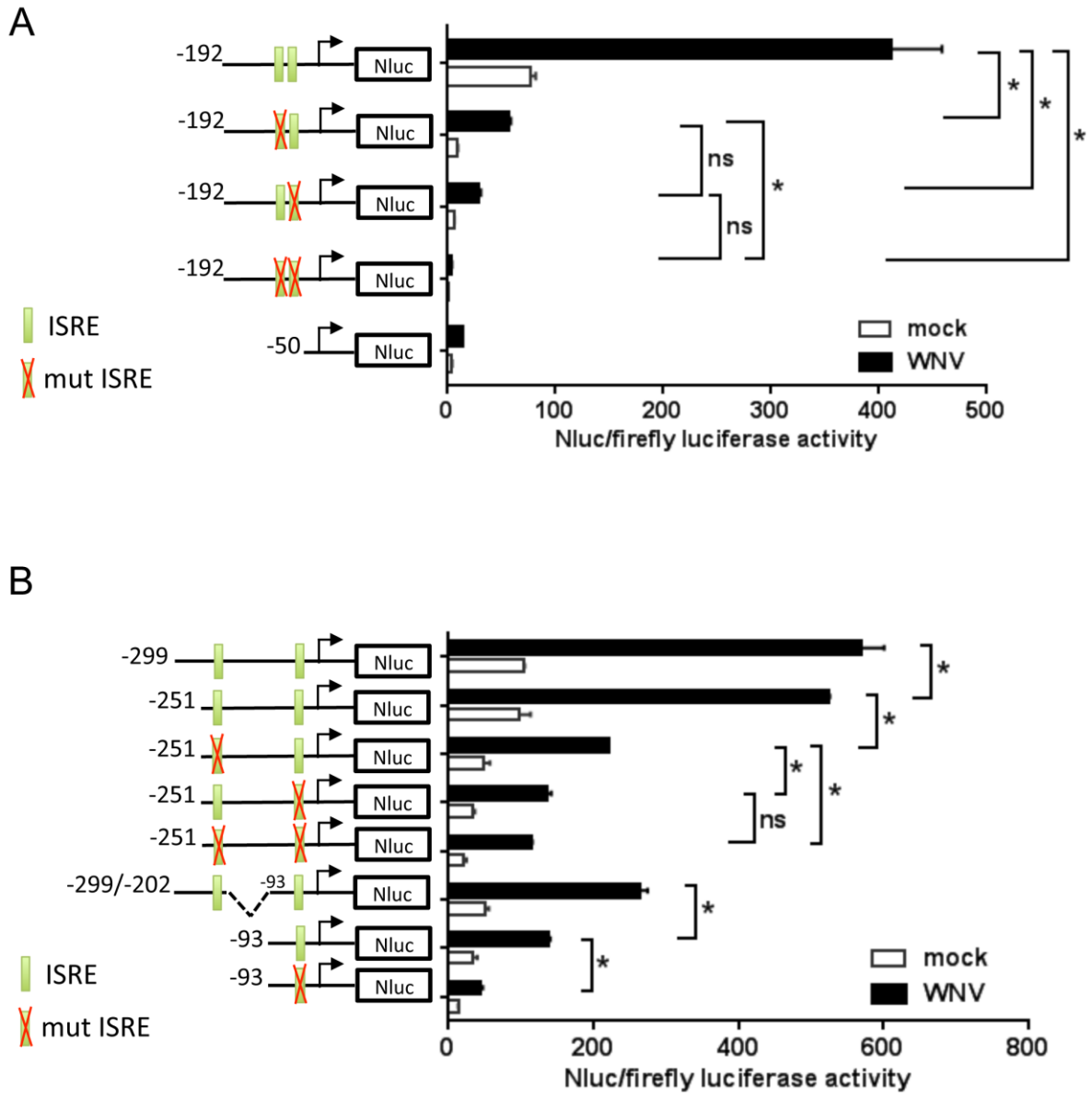

Figure 2.13 Effect of ISRE on the IFN-independent activities of the Ifit1 and Oas1b promoters.

The ISREs in (A) Ifit1 and (B) Oas1b promoter fragments were mutated in reporter constructs as indicated on the left side of the diagram. Transformed (3T3) IFNAR-/- MEFs were mock-infected or infected with WNV W956 at a MOI of 3. At 3 hpi, cells were co-transfected in triplicate with one of the mutant ISRE Nluc luciferase reporter constructs and the firefly luciferase vector pGL4.53 as a transfection control. Cell lysates were prepared at 28 hpi and luciferase activity was measured. Experiments with each construct were repeated three times. The Nluc luciferase activity was normalized to the firefly luciferase activity for each construct sample. Values are mean with SD of a representative experiment from three biological repeats. The significant differences between each sample were determined with two-way ANOVA with Tukey's post hoc test (*, $p<0.05$).

2.3.9 ISREs can be activated in an IFN-independent manner

To further confirm that an ISRE can be activated in an IFN-independent manner, the effect of a WNV infection on the activation of an ISRE luciferase reporter (pISRE-luc) containing three copies of the ISRE consensus sequence was assessed. IFNAR-/- MEFs were mock-infected or infected with WNV W956 at a MOI of 3. At 3 hpi, cells were co-transfected with pISRE-luc and pTK-Rluc (transfection control) construct DNA. The luciferase activity of the ISRE reporter was induced more than 3-fold by WNV infection (Figure 2-14). The data confirm that ISREs can be activated in an IFN-independent manner in WNV-infected cells.

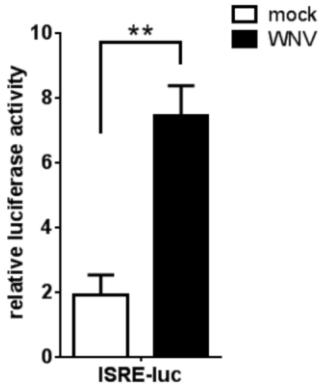

Figure 2.14 Activation of the expression of an ISRE reporter in an IFN-independent manner by WNV infection.

Transformed (3T3) IFNAR-/- MEFs were mock-infected or infected with WNV W956 for 3 h at a MOI of 3 and at 3 hpi, were co-transfected with a 3x ISRE-luc reporter construct DNA and pGL-TK reporter DNA (transfection control) in triplicate. At 28 hpi, cells were lysed, and luciferase activity was measured. Values are mean with SD of a representative experiment from three biological repeats. The statistical significance was evaluated by a student's t-test with $p<0.01$.

2.3.10 Detection of protein complexes binding to the ISREs of Ifit1 promoter by electrophoretic mobility shift (EMSA)

An EMSA was used to directly investigate whether nuclear proteins in WNV-infected IFNAR-/- cells can bind to the ISREs of an Ifit1 promoter fragment. The DNA probe consisted of the Ifit1 promoter region from -103 to -38, which contains two ISREs, was labeled at the 3′

end with biotin. Nuclear extracts were prepared as described in Materials and Methods from mock-infected or WNV W956-infected (MOI of 3) IFNAR-/- MEFs harvested at 21 hpi. The probe was incubated with the nuclear extracts for 1 h, and then the reaction mixtures were subjected to native PAGE. Two complexes were detected in the mock-infected nuclear extracts (Figure 2-15, lane 1) while three complexes were detected in the WNV-infected nuclear extracts (Figure 2-15, lane 7). The unique complex (Complex III) detected in the WNV samples migrated slower than the other two complexes (Complex II and Complex I) that were detected in all of the samples. When the unlabeled probe was titrated into the binding reactions, the Complex III band decreased in intensity in a dose dependent manner in the WNV-infected nuclear extracts and both the Complex II and Complex I band densities decreased in mock-infected and WNV-infected samples (Figure 2-15, lane 2 to 5, lane 8 to 11). A probe that contained both ISRE core sequences mutated from GAAA into GTAC was also tested by EMSA. Complex III was not detected by the mutant probe in the WNV-infected nuclear extract. The formation of Complex I was detected in both mock-infected and WNV-infected nuclear extracts with the mutant probe, but Complex II was not detected in neither mock-infected nor WNV-infected nuclear extracts by the mutant probe. However, an increase of a large slower migrating complex (Complex M) was observed with the mutant probe in both the mock-infected and WNV-infected nuclear extracts (Figure 2-15, lane 6 and lane 12). These data indicate that the ISREs are required for the formation of Complex III in WNV-infected extracts. The formation of Complex II decreased with increasing concentrations of the unlabeled wild-type probe and did not form with the mutant probe (Figure 2-15), suggesting that some cell protein(s) in both infected and uninfected cell nuclear extracts can bind to the ISREs. Complex I formation decreased with increasing concentrations of unlabeled probe, but was still detected with the ISREs mutant probe, indicating

that nuclear proteins can also bind to other regions of the probe and do not require protein-DNA complexes binding at the ISREs to facilitate their binding.

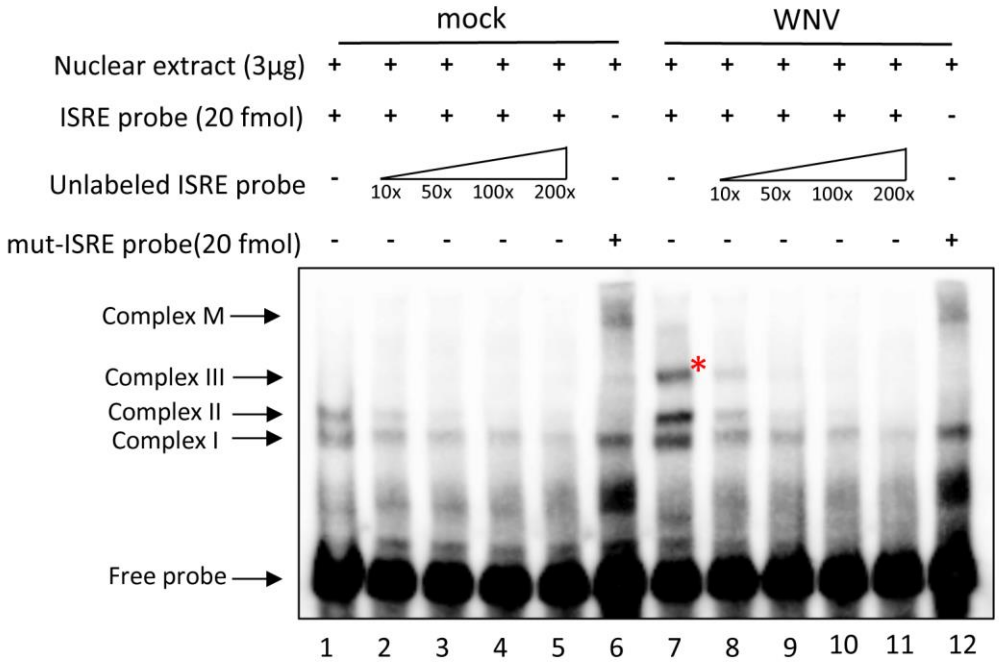

Figure 2.15 Cell proteins in WNV-infected IFNAR-/- MEF nuclear extracts bind to promoter ISRE motifs.

Transformed (3T3) IFNAR-/- MEFs were mock-infected or infected with WNV W956 at a MOI of 3, and at 21 hpi, nuclear extracts were prepared. Nuclear extracts (3 µg) were incubated with biotin-labeled oligonucleotide probes for 1 h at 22°C. The lanes are numbered below the gel. In lanes 1 to 5 and 8 to 11, a 3′ biotinylated Ifit1 probe that contained two ISREs and corresponded to the Ifit1 promoter region from -103 to -38 was used. In lanes 2 to 5 and 8 to 11, increasing concentrations of unlabeled probe was added to the reactions. The excess of the unlabeled probe over labeled probe is indicated. In lanes 6 and 12, labeled probe containing mutant ISREs was used. The reactions were electrophoresed on native 6% polyacrylamide gels. The migration positions of the free probe and protein-DNA complexes are indicated by arrows. The red asterisk indicates the specific complex formed only with the probe containing wild-type ISREs in WNV-infected nuclear extracts. A representative blot from four independent experiments is shown.

2.3.11 One or more NF-κB transcription factors bind to the Ifit1 promoter in IFN-independent ISG upregulation mechanism

During canonical IFN signaling, in response to type I IFN binding to its cell surface receptor, the transcription factor complex ISGF3, which is composed of STAT1, STAT2, and

IRF9, assembles, translocates to the nucleus and binds to the ISREs in ISG promoters resulting in upregulation of their expression. However, WNV infection blocks the nuclear translocation of this complex. Therefore, the proteins found to be binding to the ISRE in WNV-infected, IFNAR-/- extracts are not components of the ISGF3 complex. A recent publication reported that IRF5 could bind to a DNA consensus that is similar to that of the ISRE when assisted by NF-κB RelA (Saliba *et al.*, 2014). The binding of IRF3 to an ISRE after TLR4 activation also requires that RelA forms a complex with IRF3 (Wietek *et al.*, 2003). It was hypothesized that NF-κB RelA is involved in the WNV-induced IFN-independent ISG upregulation mechanism by facilitating the binding of other transcription factors to the ISRE.

The NF-κB family of transcription factors contains five members in mammals: RelA (p65), RelB, c-Rel, NF-κB1 (p105) and NF-κB2 (p100). p105 and p100 are processed into p50 and p52, respectively (Hayden and Ghosh, 2011). In the canonical NF-κB pathway, when cytoplasmic IκBα is phosphorylated, it dissociates from the RelA/p50 heterodimer. The RelA/p50 heterodimer then translocates to the nucleus and binds to NF-κB sites in gene promoters (Oeckinghaus *et al.*, 2011). An NF-κB inhibitor, caffeic acid phenethyl ester (CAPE), inhibits the nuclear translocation of the RelA/p50 complex and suppresses its binding to DNA (Natarajan *et al.*, 1996). The exact mechanism by which CAPE inhibits NF-κB activation is not clear. The observation that the inhibitory effect of CAPE can be reversed by reducing agents suggested that a critical sulfhydryl group in NF-κB complex may be modified by CAPE (Natarajan *et al.*, 1996). As an initial means of studying the possible involvement of NF-κB RelA in the IFN-independent ISG upregulation mechanism, the effect of CAPE on IFN-independent Ifit1 promoter activity was investigated. IFNAR-/- MEFs were mock-infected or infected with WNV W956 at a MOI of 3. Different concentrations of CAPE were added to the culture medium

immediately after virus absorption. At 3 hpi, cells were co-transfected with Ifit1 (-192, +66) Nluc luciferase reporter DNA and pGL 4.53 firefly luciferase reporter DNA (transfection control). At 29 hpi, cells were lysed and luciferase activities were measured. CAPE inhibited the upregulation of Ifit1 promoter activity by WNV infection in the IFNAR-/- MEFs in a dose-dependent manner (Figure 2-16 A). These data suggested that NF-κB plays a role in the alternative ISG upregulation mechanism.

The effect of CAPE on DNA binding complex formation detected by EMSA was next analyzed. Different concentrations of CAPE were first added to nuclear extracts from mock-infected or WNV W956-infected MEFs, and incubated at 37°C for 30 min. A 3′ biotinylated Ifit1 promoter -103 to -38 region probe was then added to the binding mixtures, and after incubation at 22°C for another 1 h, the complexes formed were analyzed by EMSA. Treatment with CAPE reduced the formation of Complexes I and II in the mock-infected nuclear extracts and of Complexes I, II and III in the WNV-infected nuclear extracts in a dose dependent manner (Figure 2-16 B). The data suggest that an NF-κB subunit is involved in each of the three complexes detected. The formation of Complex II and Complex III, which did not form when an ISRE mutant probe was used (Figure 2-15), was reduced by the treatment with CAPE (lane 2 to 5, 8 to 11) (Figure 2-16 B). However, the formation of Complex I, which still formed when an ISRE mutant probe was used (Figure 2-15), was also reduced after the treatment with CAPE (lane 2 to 5, 8 to 11) (Figure 2-16 B). The data suggest that NF-κB subunits are present in protein complexes that bind to the ISRE and to ISRE flanking sequences in mock-infected cells as well as WNV-infected cells. NF-κB subunits also facilitate the upregulation of ISG expression in an IFN-independent manner in WNV-infected cells.

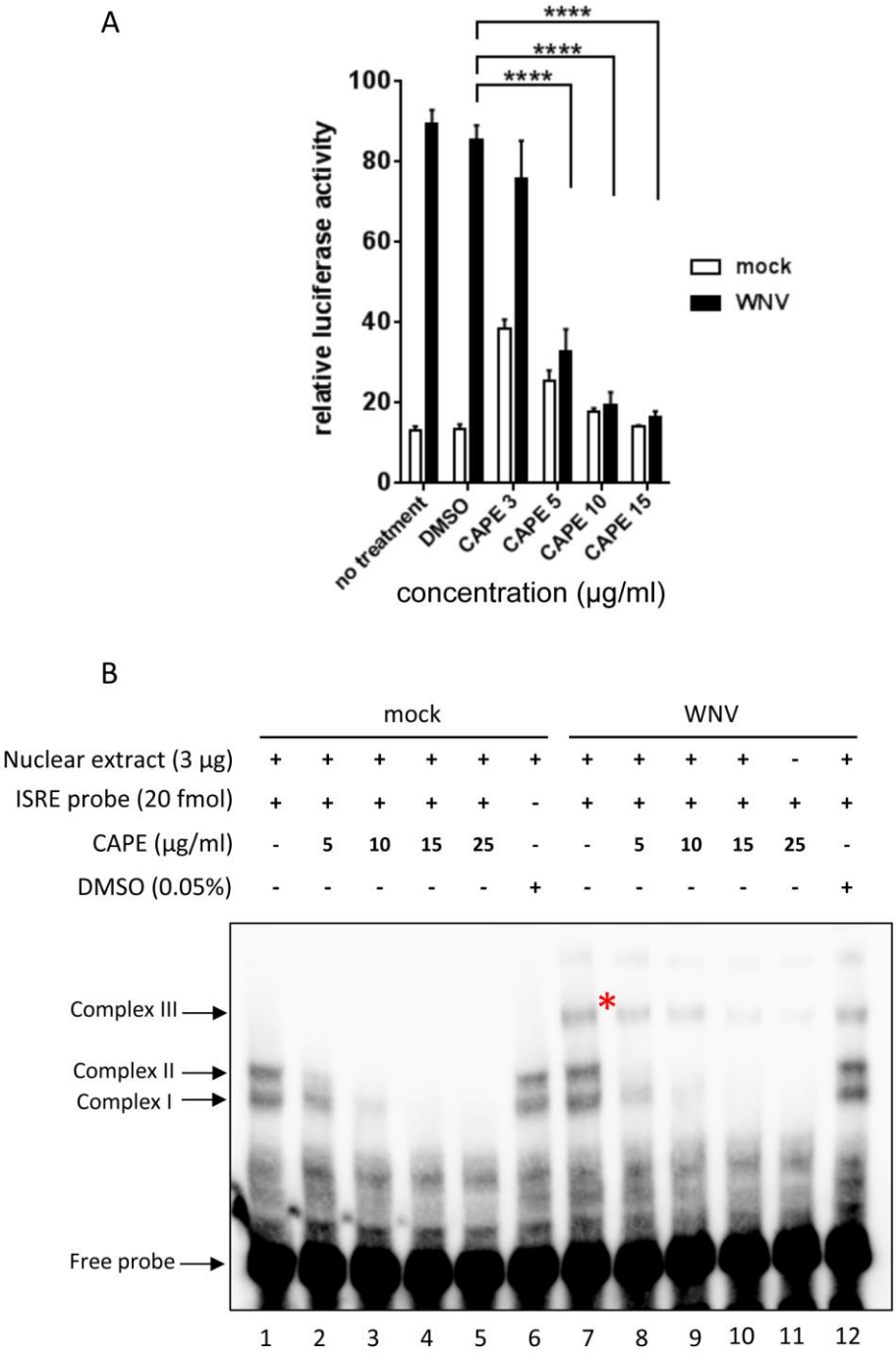

Figure 2.16 An NF-κB transcription factor is involved in regulating the non-canonical ISG upregulation mechanism.

(A) Transformed (3T3) IFNAR-/- MEFs were mock-infected or infected with WNV W956 at a MOI of 3. The NF-κB inhibitor CAPE was added to the culture medium immediately after the virus absorption period. At 3 hpi, cells were co-transfected with Ifit1 (-192, +66) promoter reporter DNA and pGL 4.53 reporter DNA (transfection control) in triplicate. At 29 hpi, cells were lysed, and reporter luciferase activities were measured. The plotted values are the

mean with SD from one representative experiment of three biological repeats. Significant differences were determined with a one-way ANOVA with multi-comparisons to the data for the DMSO treatment sample and Tukey's post hoc test (****, $p<0.0001$). (B) Different concentrations of CAPE were added to the nuclear extract in the binding reaction and incubated at 37°C for 30 min. A 3′ biotinylated Ifit1 promoter -103 to -38 region probe was then added. After incubation for 1 h at 22°C, the DNA-protein complexes were analyzed by EMSA. The data shown are representative of one of two independent repeats.

As an additional means of determining if NF-κB RelA is a component of Complex III, a supershift assay was performed. Different amounts of an anti-RelA antibody were added to the nuclear extracts and after incubation on ice for 30 min, the 3′ biotinylated Ifit1 promoter -103 to -38 region probe was added, and the binding reactions were incubated at 22°C for 1 h. The DNA-protein complexes were separated by native PAGE. A slight decrease in the intensity of the Complex III band was observed when 5 µl of the anti-RelA antibody was added, but lower concentrations of antibody did not cause a detectable decrease in band density (lane 9) (Figure 2-17 A). Quantification of the Complex III band intensities confirmed that there was a statistically significant decrease in the intensity of the Complex III band after incubation with 5 µl anti-RelA antibody compared to the antibody buffer control (Figure 2-17 B). These data suggest that RelA is one of the components of Complex III. The lack of detection of a supershift band may be because of prevention of RelA from binding to the complex due to interaction with the antibody.

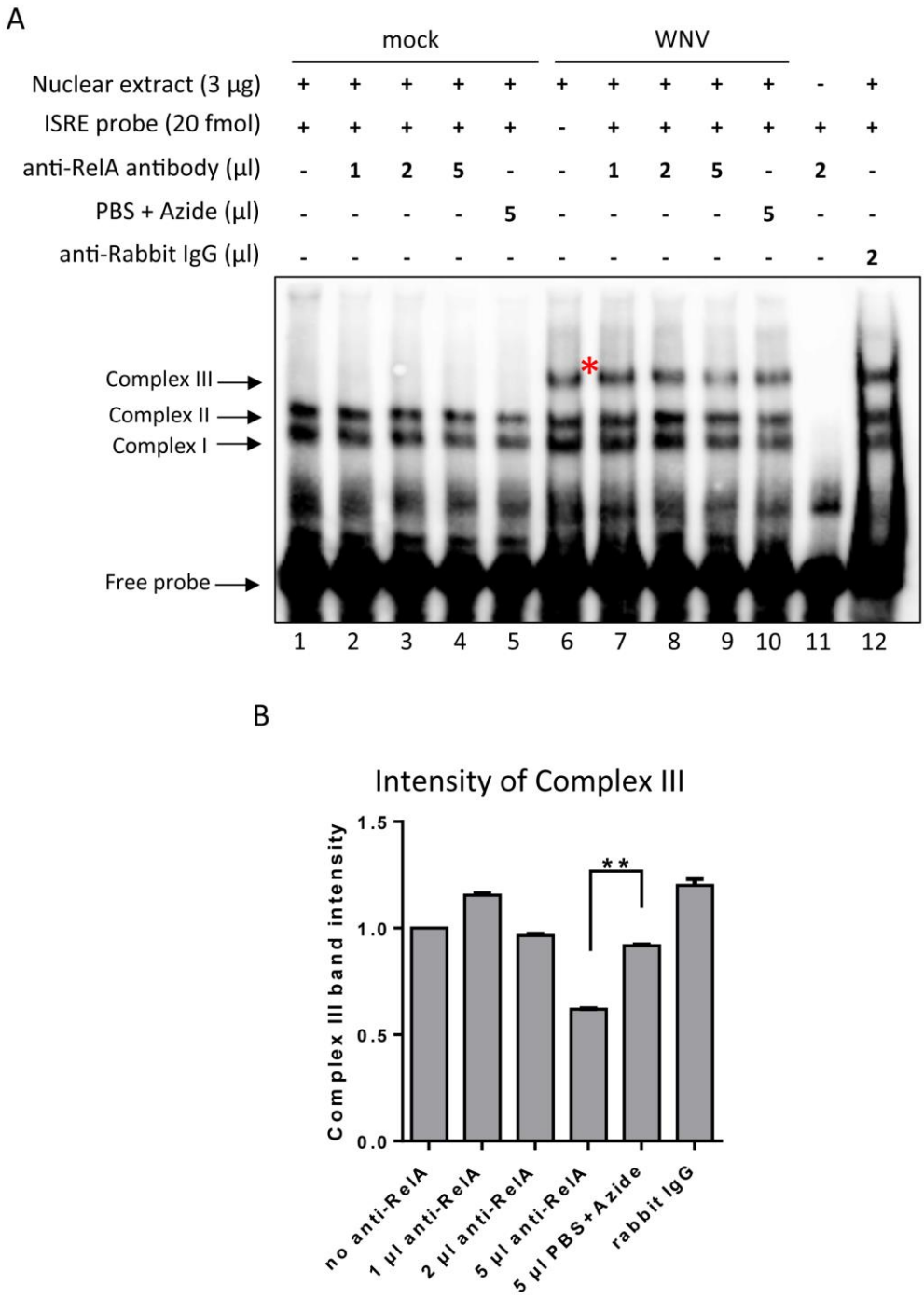

Figure 2.17 NF-κB RelA may be a component of Complex III.

(A) Transformed (3T3) IFNAR-/- MEFs were infected with WNV W956 at a MOI of 3. At 21 hpi, nuclear extracts were prepared and incubated with the indicated amounts of anti-RelA antibody, antibody buffer (PBS plus Azide) or rabbit IgG for 30 min on ice. The wild-type biotin-labeled DNA probe was then added. After incubation for 1 h at 22°C, the DNA-protein complexes were analyzed by EMSA. Arrows indicate the protein-DNA complexes formed. The

red asterisk indicates Complex III that forms only with infected nuclear extracts when the wild-type ISREs are present in the probe. (B) Densitometric quantification of the Complex III bands in the gel shown in panel A.

2.3.12 An IRF protein may interact with NF-κB RelA at ISREs to regulate the IFN-independent ISG upregulation mechanism

The interaction of NF-κB family members with other heterologous transcription factors occurs either through direct interaction or by the different transcription factor occupying neighboring sites on a gene promoter (Oeckinghaus *et al.*, 2011). Transcription factors previously shown to synergistically interact with NF-κB include Sp1, AP-1, STAT3 and CCAAT/enhancer-binding protein beta (CEBP/β) (Oeckinghaus *et al.*, 2011). RelA and IRF3 form a stable complex that can bind to an ISRE in response to TLR4 but not TLR3 activation (Wietek *et al.*, 2003). IRF5 can form a complex with RelA, which is required for IRF5-mediated regulation of tumor necrosis factor (TNF) gene expression at an NF-κB promoter site in dendritic cells (Krausgruber *et al.*, 2010). In macrophages, IRF5 and RelA form a complex that binds to an ISRE-like DNA consensus sequence and regulates the expression of inflammatory genes, including Il-1a, Il-6, and Tnf (Saliba *et al.*, 2014). The sequences of IRF-binding elements (IRF-E) in gene promoters share a high degree of homology with the ISRE (Schmid *et al.*, 2010). In WNV-infected IRF3/5/7-/- MEFs, the level of the IFN-independent ISG response was reduced, and the ISG induction was not sustained. The data suggest the possibility that IRF3, IRF5, and IRF7 may be redundantly involved in the IFN-independent mechanism with any one of these three IRFs being able to function in this role (Figure 2-9).

To directly compare the differences in the proteasome in nuclei of infected and uninfected cells, nuclear extracts of IRFAR-/- MEFs that were mock-infected or infected with W956 at a MOI of 3 were prepared at 23 hpi following the protocol described in the Materials

and Methods. Total amounts of protein in the nuclear extracts were measured with a BCA assay (ThermoFisher Scientific). Approximately 11 µg of each nuclear extract protein sample was loaded onto one lane of a 12% NuPAGE Bis-Tris gel, which was electrophoresed with NuPAGE MOPS SDS buffer (Life Technologies). The electrophoresis was stopped when the samples migrated ~0.5 cm into the gel. The protein gel was then stained with a colloidal blue staining kit (Life Technologies) and shipped to the Wistar Institute Proteomics and Metabolomics Facility (Philadelphia, PA) for MassSpec analysis. The proteins in the mock or WNV infection nuclear extracts on the gel were excised as a single band and digested with trypsin. The tryptic peptides were then analyzed by liquid chromatography-tandem mass spectrometry (LC-MS/MS) on a Q Exactive Plus mass spectrometer (ThermoFisher Scientific). Peptide sequences were identified using MaxQuant 1.5.2.8 (Ref: PMID 19029910). MS/MS spectra were searched against a UniProt *Mus musculus* (September 2016) database. The detected mouse nuclear proteins were quantified based on the identified peptides using the intensity-based absolute quantification (iBAQ) method and normalized using the MaxLFQ algorithm to take into account differences in sample loading (Schwanhausser *et al.*, 2011; Cox *et al.*, 2014). WNV-induced protein fold change was calculated over mock-infected protein level based on the LFQ intensity of each protein. STAT1 and STAT2 proteins, which are components of the transcription factor complex in the canonical JAK-STAT pathway, were not detected by MassSpec in the nuclear extracts of WNV-infected IFNAR-/- MEFs. This observation is consistent with previous data showing blockage of STAT protein nuclear translocation in WNV-infected cells (Pulit-Penaloza *et al.*, 2012b). The levels of RelA in the nucleus were found to be upregulated by WNV infection by 4-fold, but neither p50 nor the IRF1, 3, 5 or 7 proteins were detected in the nucleus or cytoplasm by the MassSpec analysis.

Western blotting of the same nuclear extracts used for EMSA shown in Figure 2-15 was used as an alternative method for analyzing whether the levels of the NF-κB components (p50 and RelA) as well as IRF3, IRF5, and IRF7 increased in the nucleus after WNV infection in IFNAR-/- MEFs. An increase in the nuclear levels of RelA and p50 was observed after WNV infection (Figure 2-18). The data confirm activation of the NF-κB pathway by WNV-infection. The levels of the IRF3, IRF5 and IRF7 proteins were higher in the nucleus than in the cytoplasm in mock-infected cells, and the levels of these proteins in the nucleus increased in the nuclei of IFNAR-/- MEFs after WNV-infection (Figure 2-18). The data indicate that the observed increased nuclear location of the NF-κB and IRF proteins after WNV infection is independent of IFN signaling.

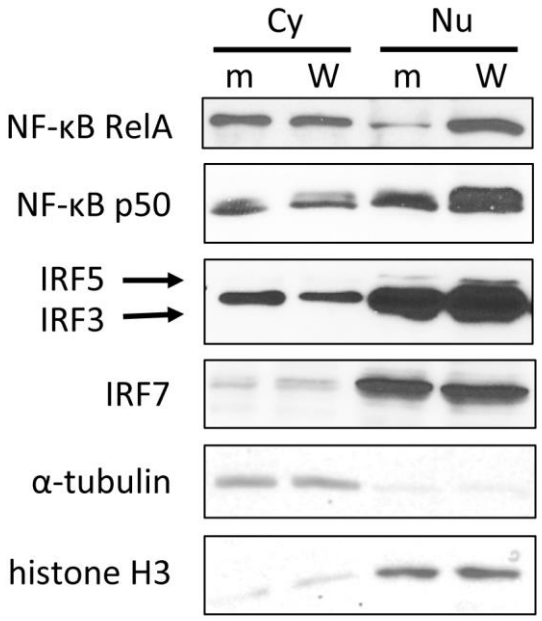

Figure 2.18 The levels of RelA, p50, IRF3, IRF5 and IRF7 proteins increase in the nucleus of WNV-infected IFNAR-/- MEFs.

The same nuclear extracts used in the EMSA (Figure 2-15) were analyzed by Western blotting together with an equivalent amount protein of the corresponding cytoplasmic extracts, which were collected from mock- or WNV-infected IFNAR-/- MEFs (3T3-transformed) at 21 hpi. Protein samples (45 µg) were separated in 10% and 15% SDS-PAGE gel. After transfer, the proteins on the membrane were detected with corresponding antibodies.

2.4 Discussion

2.4.1 Cell sensors involved in the alternative ISG upregulation mechanism

After WNV infection, multiple cell sensors, including RIG-I, MDA5, TLR3, TLR7, TLR8, and DNA sensor cGAS, are activated by viral pathogen-associated molecular patterns (PAMPs), thus leading to the induction of type I IFN (Suthar *et al.*, 2013; Gack and Diamond, 2016). Among these sensors, RIG-I and MDA5 are considered necessary for detection of a WNV infection and have nonredundant roles (Errett *et al.*, 2013). This conclusion was reached from data obtained in studies performed with cells that have a functional IFN-dependent innate immune system. Data obtained in the present study showed that only basal expression of ISGs was observed in WNV-infected RIG-I$^{-/-}$/MDA5$^{-/-}$ MEFs at early and late times after infection, indicating that either RIG-I or MDA5 sensing is also required to initiate the WNV-induced IFN-independent ISG upregulation mechanism. The data also suggest that other cell sensors are not required for the alternative antiviral mechanism in WNV-infected cells. The previously reported data showing that the IFN-independent ISG upregulation mechanism is also reduced in WNV-infected IPS-1-/- MEFs (Pulit-Penaloza *et al.*, 2012b), confirmed the essential role of RIG-I and MDA5 in detecting WNV infection and IPS-1 in mediating downstream signaling in both the IFN-dependent and IFN-independent ISG upregulation mechanisms.

The RIG-I$^{-/-}$/MDA5$^{-/-}$ MEFs and IPS-1-/- MEFs do not produce type I IFN after WNV infection (Pulit-Penaloza *et al.*, 2012b; Errett *et al.*, 2013), providing a “clean system” for studying the effect of these factors on the IFN-independent antiviral mechanism. However, the kinetics of ISG induction in these two types of MEFs after WNV infection differed. In cells lacking IPS-1, the ISGs are upregulated at 8 hpi, and then the levels progressively decrease (Pulit-Penaloza *et al.*, 2012b), while ISGs are not upregulated at any time after infection in WNV

infected RIG-I$^{-/-}$/MDA5$^{-/-}$ MEFs (Figure 2-5). IPS-1 is currently considered to be the only adaptor for RIG-I and MDA5 downstream signaling. The inconsistency in ISG expression between RIG-I$^{-/-}$/MDA5$^{-/-}$ MEFs and IPS-1-/- MEFs suggests the possibility that another unknown adaptor protein(s) can also transduce signaling downstream of RIG-I or MDA5.

The data obtained from the comparison of the WNV W956- and Eg101-induced ISG expression levels in IFNAR-/- MEFs also support the role of the cell RNA sensors in initiating the alternative antiviral mechanism. A WNV W956 infection produces higher levels of "unprotected" viral RNA at early times after infection, which activate the cell RNA sensors leading to higher induction levels of ISGs than a WNV Eg101 infection (Figure 2-3). The induced ISGs then work cooperatively to limit the virus yield produced by WNV W956 (Figure 2-4). Interestingly, in W956-infected cells, the mRNA expression levels of Oas1a and Oas1b progressively decrease after 24 hpi, while no decrease in Oas1a and Oas1b levels is observed in WNV Eg101-infected cells (Figure 2-3), suggesting that additional factors in WNV-infected cells are involved in maintaining the activation of the cell sensors.

2.4.2 ISREs are involved in both the IFN-dependent and -independent mechanisms

During the canonical IFN-dependent ISG upregulation mechanism, activation of the JAK-STAT pathway leads to the transcription factor complex ISGF3 binding to ISREs on the promoters of ISGs, which activates their expression. However, data obtained in the present study showed that the ISREs also mediate non-canonical, IFN-independent ISG expression by interacting with a different transcription factor complex. The finding that the same DNA element can bind to two distinct sets of proteins in response to a virus infection suggests transcriptional regulation redundancy that ensures an efficient antiviral system being activated by either the

IFN-dependent or -independent mechanism. This finding also provides new insights about the eukaryotic gene regulatory network.

Data obtained in the present study show that Oas1a, Oas1b, Irf7, Ifit1, and Mx1 belong to the subset of ISGs that are upregulated by WNV-induced IFN-independent mechanism but Mx2 and Rsad2 do not. The numbers and locations of ISREs in the promoters of these ISGs were compared. The promoters of each of the IFN-independently upregulated ISGs, Oas1a, Oas1b, Irf7, and Mx1, contain one or two ISREs while the Ifit1 promoter contains three ISREs. The promoters of Mx2 and Rsad2 also contain one and two ISREs, respectively. Concerning ISRE location, the promoters of each of these ISGs contain at least one ISRE within 350 bp upstream of the TSS except for Irf7, which belongs to the IFN-independently upregulated subset of ISGs (Table 2-5). Differences in the number or locations of the ISREs in the promoters of the ISGs did not correlate with the ability of the ISG to be upregulated in response to only the IFN-dependent upregulation mechanism or both the IFN-dependent and IFN-independent upregulation mechanisms. In the present study, individual mutation of the two ISREs in the Ifit1 and Oas1b promoters that are located within 350 bp upstream of TSS shows that each of these ISREs is critical for the IFN-independent upregulation (Figure 2-13). The two ISREs in Ifit1 promoter that are close to the TSS are 19 nts apart, while the two ISREs in the Oas1b promoter are 219 nts apart. It is interesting that no matter whether the ISREs are close or not, they both contribute to the gene upregulation in the IFN-independent mechanism.

Table 2.5 Locations of the ISREs on the promoters of some ISGs

Gene[a]	ISRE site amount	ISRE site upstream of TSS[b]
Oas1a	one	-15
Oas1b	two	-235, -16
Irf7	one	-661
Ifit1	three	-613, -79, -60
Mx1	two	-912, -318
Mx2	one	-165

Rsad2	two	-817, -103

[a] The rows shaded pink indicate genes that are upregulated by the IFN-independent mechanism, while the rows shaded blue indicate genes that are not.
[b] The location of the N site, which is next to the 3′GAAA (underlined) in the 5′A/GNGAAANNGAAACT3′ consensus, relative to the TSS of the gene.

The finding that not all of the ISREs can be activated by the non-canonical mechanism suggests that the nts contained in the different ISREs, including the variation of the 5′ GAAA site and the N nts in the ISRE consensus, may determine the binding partners of the ISRE and the sequences flanking the ISRE may also play a role. Analysis of additional ISREs, which are activated by the WNV-induced IFN-independent mechanism, is needed to further investigate the consensus of the ISREs that can mediate this non-canonical mechanism as well as the sequence differences between ISREs that can and cannot respond to IFN-independent signaling.

2.4.3 Additional promoter regions are involved in mediating the IFN-independent mechanism

Although ISREs mediate IFN-independent ISG expression, the present study demonstrated that regulation mediated by the ISRE works together with other enhancers. Both constructs Oas1b (-28, +50) and Oas1b (-93, +50) contain the 3′ ISRE. However, the promoter activity of Oas1b (-28, +50) was quite low, while the enhancer region located from -93 to -28 significantly increased the promoter activity of Oas1b (-93, +50) (Figure 2-12 B). On the other hand, mutation of this 3′ ISRE decreased the promoter activity of Oas1b (-93, +50) by about 67% [comparison of Oas1b (-93, +50)-mut ISRE and Oas1b (-93, +50)] (Figure 2-13 B). The data suggest that the high promoter activity of Oas1b (-93, +50) is due to the effect of the ISRE as well as the enhancers in the adjacent upstream region between -93 to -28. In another example, although both of the ISREs in the Oas1b promoter are present in the construct Oas1b (-299/-202, -93/+50), its promoter activity was still less than 50% of the promoter activity of Oas1b (-299,

+50) (Figure 2-13 B), demonstrating that the enhancers in the region between -202 to -93 are also involved in regulating the IFN-independent induction of Oas1b by WNV infection together with the two ISREs. Similar data were also obtained with the Ifit1 promoter constructs. Although the two 3′ ISREs contributed more than 80% of the promoter activity of Ifit1 (-192, +66) [comparison of Ifit1 (-192, +50)-mutate-both-ISRE and Ifit1 (-192, +50)], the enhancers in the region between -192 to -132 contributed nearly 40% of the promoter activity of Ifit1 (-192, +50) [comparison of Ifit1 (-192, +50) and Ifit1 (-132, +50)] (Figure 2-11 A, Figure 2-12 A). TFBS prediction in the enhancer regions of both the Oas1b and Ifit1 promoters, which coordinately work with the ISREs, revealed a CEBP/β binding site. The transcription factor CEBP/β is has been shown to synergistically interact with NF-κB (Oeckinghaus *et al.*, 2011). Data obtained in the present study suggested that NF-κB transcription factors bind to the ISREs in the IFN-independent ISG upregulation mechanism.

2.4.4 The additional promoter regions involved in mediating the IFN-dependent and -independent ISG upregulation mechanisms differ

ISREs mediate both IFN-dependent and -independent ISG induction after WNV infection, but the additional promoter regions involved in these two ISG upregulation mechanisms are different. In previous study of mapping the Oas1b promoter regions required for induction by IFN-β, the region from -576 to +50 was shown to have the highest induction activity, the region from -814 to -576 to contain repressors and the region from -576 to -181 to contain enhancers (Pulit-Penaloza *et al.*, 2012a). In contrast, data from the present study showed that for the IFN-independent WNV-induced ISG expression mechanism, the Oas1b promoter construct containing promoter regions from -299 to +50 showed the highest induction activity, and the region from -802 to -576 to contain enhancers and the region from -576 to -181 to

contain enhancers as well as repressors (Figure 2-12). These data demonstrate that the same promoter regions have opposite function in response to different cell signaling pathways (Figure 2-19). These opposite regulatory effects are likely due to different repressors and activators binding to the various DNA elements present.

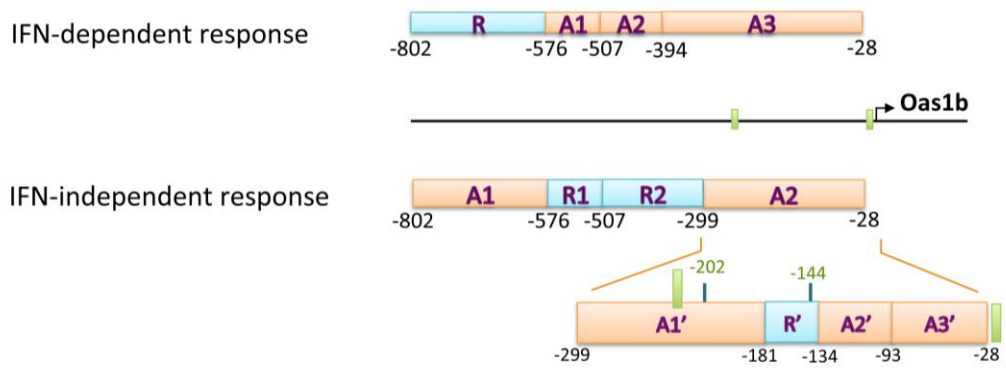

Figure 2.19 Oas1b promoter regions function differently in response to IFN-dependent and IFN-independent signaling.

The regulatory regions of Oas1b promoter for IFN-dependent signaling were summarized from previously published data (Pulit-Penaloza *et al.*, 2012a), while the regulatory regions for WNV-induced IFN-independent signaling were summarized from the data in Figure 2-12. Green rectangle, ISRE. A, enhancer. R, repressor.

2.4.5 NF-κB and either IRF3, IRF5 or IRF7 work together with additional TFs on ISG promoters to facilitate IFN-independent gene upregulation

Data obtained in the present study suggested a working model at the transcriptional regulation level for the non-canonical ISG upregulation mechanism in WNV-infected cells. In mock-infected IFNAR-/- cells, a particular set of transcription factors, including one or more NF-κB proteins, bind to the ISREs and flanking regions but only maintain basal levels of promoter activation. WNV infection activates an additional protein complex binds to the ISREs, thus inducing higher levels of ISG expression. This new protein complex could form through replacing either some or all of the proteins already bound to the ISRE under basal conditions, and could form through recruiting additional proteins to the enhancer regions.

Data from the present study suggested that the WNV-induced, ISRE-binding protein complex may include RelA. A crystal structure of IRF proteins bound to a targeted DNA sequences demonstrated that the GAAA consensus of DNA is critical for IRF3 and IRF7 binding (Panne *et al.*, 2004; 2007). The mutated ISRE used in the present study contains a disrupted GAAA consensus. The observation that the unique WNV-induced complex does not form with a mutated ISRE (Figure 2-15) suggested that IRF3 or IRF7 may also be part of the complex. IRF3 and IRF5 were previously shown to be able to form a complex with RelA (Wietek *et al.*, 2003; Krausgruber *et al.*, 2010). The observation that the cells lacking IRF3, IRF5 and IRF7 showed decreased ISG upregulation after WNV infection suggests that IRF3, IRF5, and IRF7 may redundantly regulate the expression of the ISGs (Figure 2-9). The three IRF proteins, IRF3, IRF5, and IRF7, as well as RelA, were all shown to be present in the nucleus after WNV infection (Figure 2-18). Either IRF3, IRF5 or IRF7 may be contained in the unique WNV-induced complex that binds to the ISREs, but whether these IRFs are present as monomers or dimers is not known.

The data obtained suggest that RelA and an IRF protein may be present in the promoters of responsive ISGs, but additional enhancer regions identified suggest other proteins are involved. Transcription co-activator proteins CREB-binding protein (CBP) and its homolog p300 are possible candidates. Phosphorylated IRF3 forms a strong association with CBP and p300 that facilitates its transcription activation of type I IFN genes (Weaver *et al.*, 1998; Clement *et al.*, 2008). In Newcastle disease virus-infected cells, IRF5 interacts with CBP and p300, which were specifically recruited to the IFN-α promoter (Feng *et al.*, 2010). In a study of Sendai virus infected cells, a virus-activated factor (VAF) complex, which contains IRF3, IRF7, and p300, bind to ISRE and IRF-E in the IRF7 promoter (Ning *et al.*, 2005).

3 FUTURE DIRECTIONS

Although the majority of WNV infections in humans are asymptomatic, about 20% of infected humans experience fever and mild disease symptoms while one in every 150 develops severe neuroinvasive diseases. Typically mild flu-like disease symptoms resolve after 1 week of infection, but fatigue, muscle weakness, joint pain and headache can persist for more than 30 days. In the neuroinvasive cases, WNV infection can cause irreversible damage to the central neuron system (Murray *et al.*, 2011). No approved vaccines or specific therapies for WNV infections in human are currently commercially available. WNV-host interactions are being studied to gain additional knowledge to facilitate future development of effective treatments. The expression of hundreds of ISGs activated by virus-induced IFN constitutes the first line of host antiviral defense. Although WNV has evolved effective ways of counteracting the host IFN response, the Brinton lab previously discovered that there is an alternative backup mechanism in host cells for establishing an antiviral state. In the present study, the WNV-induced IFN-independent antiviral mechanism was further characterized in mouse cells. After a WNV infection, the host cell cytosolic sensors, RIG-I and MDA5, redundantly detect viral RNA and signal through their adaptor IPS-1 to downstream transcription factors. In the nucleus, WNV-induced transcription factor complexes bind to ISREs and flanking regions, mediating the expression of a subset of ISGs. The data obtained in the present study suggest that the WNV-induced ISRE-binding complex contains NF-κB components and either IRF3, IRF5 or IRF7 (Figure 3-1).

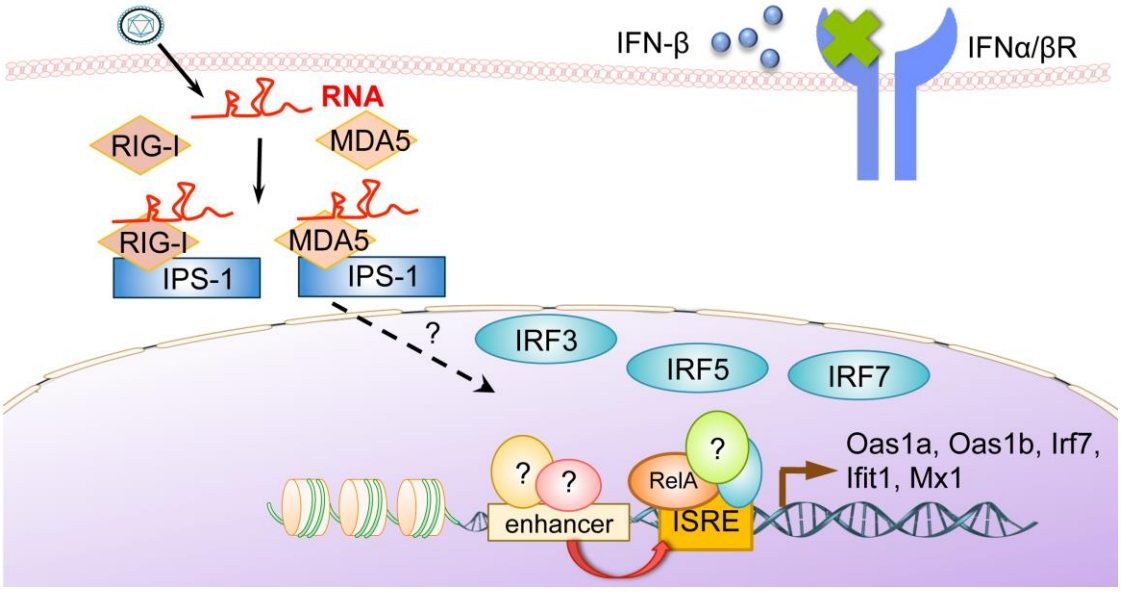

Figure 3.1 Working model for the IFN-independent ISG upregulation mechanism in WNV-infected cells.

After WNV infection, viral RNAs are detected by host cytosolic sensors, RIG-I and MDA5. The activated sensors signal through their adaptor molecule IPS-1, which ultimately activates transcription factors. In the nucleus, a unique WNV-induced transcription factor complex binds to the ISRE on the promoters of a subset of ISGs, thereby activating expression of these ISGs in an IFN-independent manner. The proteins binding to flanking enhancers of ISREs also contribute to the IFN-independent upregulation of ISGs.

3.1 Cell signaling pathways that are activated downstream of IPS-1 in WNV-infected IFNAR-/- MEFs

After WNV infection, cell cytosolic receptors RIG-I and MDA5 are both essential for detecting virus infection, and transduce signaling through IPS-1 to induce IFN gene expression (Errett *et al.*, 2013). Data from the present study suggest that the RIG-I/MDA5-IPS-1 pathway is also used to activate downstream transcription factors, including IRF3, IRF5, or IRF7, and NF-κB p50 and RelA, to initiate the WNV-induced IFN-independent antiviral mechanism. However, the molecules involved in this downstream signaling in WNV-infected IFNAR-/- MEFs are not known.

It was shown in previous studies that upon RIG-I or MDA5 activation, IPS-1 recruits TNFR1-associated death domain protein (TRADD), which coordinates interactions with relevant downstream molecules. The IPS-1/TRADD complex recruits TNF receptor-associated factor 3 (TRAF3), TRAF-associated NF-κB activator (TANK), and IKKγ, thereby initiating the activation of TBK1 and IKKε (Saha *et al.*, 2006). The interaction of TRADD with IPS-1 also orchestrates the formation of a multimeric complex containing Fas-associated death domain containing protein (FADD), receptor interacting protein 1 (RIP1) that initiates NF-κB activation (Michallet *et al.*, 2008; Jensen and Thomsen, 2012). The kinases TANK-binding kinase 1 (TBK1) and IκB kinase ε (IKKε) are known to be activated downstream of IPS-1, and they phosphorylate IRF3 and IRF7, which is required for nuclear translocation of IRF3 and IRF7 (Fitzgerald *et al.*, 2003; Sharma *et al.*, 2003). In addition, TBK1 and IKKε have been implicated in NF-κB activation. Both of these kinases can catalyze RelA phosphorylation that is essential for RelA transactivation function (Peters and Maniatis, 2001; Fitzgerald *et al.*, 2003). Future studies could analyze the involvement of these known IPS-1 downstream molecules and posttranslational modifications in the WNV-induced IFN-independent ISG upregulation mechanism.

The involvement of kinases TBK1 and IKKε in upregulating the IFN-independent ISG expression could be investigated first. Dominant negative mutants of TBK1 and IKKε or specific kinase inhibitors could be used to knock down these kinases. Alternatively, the two proteins could be overexpressed from transfected vectors. The effect of knocking down or overexpressing TBK1 and IKKε could be assayed in the dual luciferase assay system established in the present study in WNV W956-infected IFNAR-/- MEFs using the Ifit1 (-192, +66) and the Oas1b (-299, +50) Nluc reporter constructs.

If TBK1 and/or IKKε are found to be involved in signaling downstream of IPS-1 during activation of the IFN-independent ISG upregulation mechanism, additional studies could be done to investigate which molecules are associated with IPS-1 in this mechanism. The candidates are TRADD, TRAF3, TANK, IKKγ, FADD, and RIP1. The association of each of these proteins with endogenous IPS-1 could be investigated by immunoprecipitation using an antibody to IPS-1 and immunoblotting with antibodies for each candidate in cell lysates of WNV W956-infected IFNAR-/- MEFs. The involvement of these proteins in IPS-1 downstream signaling could also be studied by overexpressing each protein together with the IPS-1 protein and evaluating the effect in the dual luciferase system established in the present study.

3.2 The subgroup of ISREs and other DNA regulatory elements that can be activated by the IFN-independent ISG upregulation mechanism

The WNV-induced IFN-independent ISG upregulation mechanism is mediated through the ISRE on the promoters of the ISGs that are upregulated. However, only a subset of ISGs can be upregulated by this mechanism, indicating that only this subset contains the ISREs that can be activated by the IFN-independent as well as the IFN-dependent mechanism. The subgroup of ISREs could be studied to try to identify possible unique characteristics that are functionally relevant. In the present study, the ISRE sequences analyzed were from only five ISGs, including Oas1a, Oas1b, Irf7, Ifit1, and Mx1. Among these, only the five ISRE sites that are on the promoters of Ifit1 and Oas1b were functionally tested during the IFN-independent activation. To obtain a more accurate sequence consensus of this subgroup of ISREs, additional ISGs responsive to the IFN-independent mechanism would need to be identified to compare a larger number of the functional ISRE sequences. A microarray analysis was previously performed on the samples collected from WNV-infected, wild-type MEFs (Scherbik *et al.*, 2007b), which

detected both IFN-dependent and IFN-independent upregulated ISGs and therefore did not allow unambiguous detection of ISGs upregulated by the IFN-independent mechanism. To obtain a complete list of the ISGs upregulated by WNV in IFNAR-/- MEFs, an RNA-seq analysis could be performed. The ISREs of these ISGs could then be tested to confirm their ability to respond to the IFN-independent induction mechanism by a mutation in promoter constructs used in the luciferase reporter system. Next, the core and flanking sequences of all the ISREs that respond to the IFN-independent mechanism could be subjected to bioinformatics analysis to obtain a consensus sequence. If a characteristic consensus can be found, this information would be added to TFBS databases as well as to the gene regulation network databases to provide foundational information for other studies.

The data obtained in the present study suggested that additional regulatory elements on the ISG promoters besides the ISREs are involved in the IFN-independent ISG upregulation mechanism in WNV-infected MEFs. These additional regulatory elements could be studied to obtain a complete picture of the factors involved in IFN-independent ISG upregulation. The Assay for Transposase-Accessible Chromatin with high-throughput sequencing (ATAC-seq) could be used to investigate genome-wide accessible regions and to map regions of transcription-factor binding and nucleosome positioning on responsive ISG promoters in WNV-infected IFNAR-/- MEFs (Buenrostro *et al.*, 2013). The derived sequences of transcription-factor binding regions of the upregulated ISGs would be analyzed by computational motif discovery methods to search for potential transcriptional regulatory elements mediating the WNV-induced IFN-independent ISG upregulation. The Oas1b and Ifit1 promoter mapping data obtained in the present this study could be used to confirm the ATAC-seq analysis and computational analysis results.

3.3 A novel WNV-induced ISRE-binding protein complex involved in the IFN-independent mechanism

During IFN-dependent ISG upregulation, activation of the JAK-STAT pathway leads to the transcription factor complex ISGF3 that consists of p-STAT1, p-STAT2, and IRF9, binding to the ISREs on the promoters of ISGs and upregulating their expression. However, the nuclear translocation of the transcription factor complex ISGF3 is blocked in WNV-infected human and mouse cells (Keller *et al.*, 2006; Laurent-Rolle *et al.*, 2010; Pulit-Penaloza *et al.*, 2012b). Moreover, STAT1, STAT2, and IRF9 were not detected in the nuclear extracts of WNV-infected IFNAR-/- MEFs by MassSpec in the present study and STAT1 and STAT2 were not previously detected in nuclei of WNV-infected, wild-type MEFs by immunofluorescence assay (IFA) or in nuclear extracts by Western blotting (Pulit-Penaloza *et al.*, 2012b). Therefore, the WNV-induced ISRE-binding protein complex in the IFN-independent mechanism does not contain STAT1, STAT2 or IRF9. Data from the present study suggest that NF-κB RelA and IRF proteins are present in the novel virus-induced complex that binds to the ISREs in the promoters of responsive ISGs. Previous studies suggested that a RelA/IRF3 or RelA/IRF5 complex can bind to an ISRE after bacterial LPS treatment of cells (Wietek *et al.*, 2003; Saliba *et al.*, 2014). In the present study, NF-κB components were shown to mediate ISRE-driven ISG expression in the context of virus infection. It was suggested that NF-κB RelA, either IRF3, IRF5 and IRF7, and some other transcription co-activator proteins, such as CBP and p300, are present in this WNV-induced ISRE-binding complex. The components of this complex could be elucidated by a pull-down assay using the biotin/streptavidin affinity system in combination with MassSpec analysis of the pulled down proteins. The DNA probes containing ISREs that were used in the EMSA assay in this present study would be biotin-labeled, mixed with the nuclear extracts of WNV-

infected IFNAR-/- MEFs. Next, the protein-DNA complex formed will be pulled down with streptavidin magnetic beads making use of the high affinity biotin-streptavidin bond. The proteins associated with the ISREs can then be identified with MassSpec. The probe with mutated ISREs would be used as a negative control to eliminate non-specific binding proteins in the MassSpec results. After the components of the WNV-induced ISRE-binding complex are identified, their roles in regulating the IFN-independent ISG upregulation could be confirmed by Chromatin immunoprecipitation (ChIP) assay in WNV-infected IFNAR-/- MEFs if ChIP grade antibodies are available.

After the components of the WNV-induced ISRE binding complex are identified, how this complex is assembled could next be investigated. The domains of individual components of the complex would be studied first. All IRF proteins share a common DNA-binding domain (DBD) while they each contain a unique IRF association domain (IAD) that is responsible for interacting with other IRF proteins and other factors (Taniguchi *et al.*, 2001). RelA has a dimerization domain (DD), a carboxy-terminal transactivation domain (TAD), and a Rel homology domain (RHD) that is conserved among all NF-κB proteins and is responsible for DNA binding and interaction with IκB (Oeckinghaus and Ghosh, 2009). When forming a complex with a heterologous transcription factor, RelA can provide its TAD for regulating gene expression (Yang *et al.*, 2007). IRF3 has been shown to bind to the RHD of RelA, whereas the IAD of IRF5 and the DD of RelA are critical for the interaction of IRF5 and RelA (Ogawa *et al.*, 2005; Saliba *et al.*, 2014). RelA has been found to interact with CBP/p300 via its DBD and TAD (Mukherjee *et al.*, 2013). The domains of IRFs, RelA and other components that are important for the formation of the WNV-induced ISRE binding complex could be identified by coimmunoprecipitation assays with each truncated protein exogenously expressed in WNV-

infected mouse IFNAR-/- cells. The conformation of the ISRE-binding complex could be studied using structural approaches. In the canonical NF-κB pathway, the NF-κB heterodimer RelA/p50 binds to the NF-κB site containing the consensus sequence 5′-GGGRNYYYCC-3′ (R = A or G, Y = C or T, N = any base) (Chen and Ghosh, 1999). Notably, although RelA may be involved in the ISRE-binding complex, this consensus sequence was not found in the ISRE-containing probe used in the EMSA experiments of the present study. It is possible that RelA adopts a novel conformation and binds to a DNA sequence that is different from the NF-κB consensus sequence. A previous crystallization study suggested that one of the RelA monomers in the RelA homodimer can bind to te DNA sequence 5′-NGGAA-3′ (Chen *et al.*, 2000), which is also a portion of the ISRE consensus. IRF3 and IRF7 usually bind to DNA as a homodimer or heterodimer, and each IRF interacts with a GAAA consensus sequence. It is not clear how many IRF proteins are present in the WNV-induced, ISRE-binding complex. The structure of the complex binding to the ISRE-containing DNA probe could be studied by co-crystallization.

3.4 The antiviral effect of the alternative ISG upregulation mechanism

The expression of hundreds of ISGs establishes an antiviral state in virus-infected IFN-competent cells. The ISGs, which have diverse antiviral functions, can work together to negatively affect each step of a virus life cycle in infected host cells. The antiviral activities of each ISG are not equal, with some being strong antiviral inhibitors while many being modest inhibitors. The magnitude of the antiviral activity of two ISGs expressed together is usually greater than that of either gene expressed alone (Schoggins and Rice, 2011; Schoggins *et al.*, 2011). Moreover, the antiviral activities of each ISG vary for different viruses. The present study demonstrated that when the subset of ISGs upregulated by the IFN-independent antiviral mechanism is induced to a higher level at early times after WNV W956 infection than that after

WNV Eg101 infection, the antiviral activities of the ISGs work cooperatively to limit the yield of WNV W956. Although the inhibition effect on WNV W956 virus yield of the IFN-independent antiviral mechanism is not as significant as the IFN-dependent antiviral state (Scherbik *et al.*, 2013), the antiviral function of the alternative antiviral response could be studied.

Both the IFN-dependent and IFN-independent antiviral responses are not activated in WNV-infected RIG-I$^{-/-}$/MDA5$^{-/-}$ MEFs, and only the IFN-dependent antiviral response is not activated in WNV-infected IFNAR-/- MEFs. Therefore, virus yields that are produced by WNV W956 in RIG-I$^{-/-}$/MDA5$^{-/-}$ MEFs and IFNAR-/- MEFs could be compared to evaluate the function of the backup IFN-independent antiviral response. If the key transcription factor of the IFN-independent antiviral mechanism is identified, this protein could be knocked down or knocked out in IFNAR-/- MEFs to eliminate the IFN-independent mechanism, and WNV virus yield could be used to evaluate the antiviral effect of the IFN-independent mechanism.

Whether the alternative ISG upregulation mechanism responds to other virus infections could also be investigated. JEV could be used to investigate to see if the IFN-independent mechanism could be induced by another flavivirus through assaying its ability to induce the subset of ISGs in IFNAR-/- MEFs. The IFN-independent mechanism could also be investigated in IFNAR-/- MEFs infected with other RNA viruses, including Sendai virus and vesicular stomatitis virus (with a negative-sensed single-stranded RNA genome), as well as Sindbis virus (with a positive-sensed single-stranded RNA genome). In addition, the alternative ISG upregulation mechanism could be investigated in human cells. A human cell line that only has the IFN-independent antiviral response could be obtained by knocking out the type I IFN receptor using CRISPR. The upregulation of human orthologs of the subset of ISGs could be

investigated in human IFNAR-/- cells infected with WNV, JEV and other RNA viruses that could induce this alternative antiviral response in IFNAR-/- MEFs.

SIGNIFICANCE

The results of the present study extend knowledge of host antiviral mechanisms. Analysis of the host cellular factors and TFBS involved in a non-canonical ISG upregulation mechanism furthers the understanding of host antiviral responses against WNV infection. The findings of this study extend knowledge about viral detection, signaling activation and gene induction during the innate immune responses against virus infections. Many flaviviruses cause significant human morbidity and mortality around the world, but there are no effective antiviral therapies. Because most viruses have evolved ways to counteract the host IFN system, the knowledge gained in this study about an alternative host cell “backup” response provides new insights for future studies on host antiviral mechanisms and for the development of future antiviral therapies that target WNV and possibly, also other flaviviruses.

REFERENCES

Aaronson DS, Horvath CM. 2002. A road map for those who don't know JAK-STAT. Science 296(5573):1653-1655.

Aguirre S, Maestre AM, Pagni S, Patel JR, Savage T, Gutman D, Maringer K, Bernal-Rubio D, Shabman RS, Simon V et al. . 2012. DENV inhibits type I IFN production in infected cells by cleaving human STING. PLoS Pathog 8(10):e1002934.

Akira S, Uematsu S, Takeuchi O. 2006. Pathogen recognition and innate immunity. Cell 124(4):783-801.

Andrejeva J, Childs KS, Young DF, Carlos TS, Stock N, Goodbourn S, Randall RE. 2004. The V proteins of paramyxoviruses bind the IFN-inducible RNA helicase, mda-5, and inhibit its activation of the IFN-beta promoter. Proc Natl Acad Sci U S A 101(49):17264-9.

Andrejeva J, Poole E, Young DF, Goodbourn S, Randall RE. 2002. The p127 subunit (DDB1) of the UV-DNA damage repair binding protein is essential for the targeted degradation of STAT1 by the V protein of the paramyxovirus simian virus 5. J Virol 76(22):11379-86.

Anglero-Rodriguez YI, Pantoja P, Sariol CA. 2014. Dengue virus subverts the interferon induction pathway via NS2B/3 protease-IkappaB kinase epsilon interaction. Clin Vaccine Immunol 21(1):29-38.

Arjona A, Ledizet M, Anthony K, Bonafe N, Modis Y, Town T, Fikrig E. 2007. West Nile virus envelope protein inhibits dsRNA-induced innate immune responses. J Immunol 179(12):8403-9.

Ashour J, Morrison J, Laurent-Rolle M, Belicha-Villanueva A, Plumlee CR, Bernal-Rubio D, Williams KL, Harris E, Fernandez-Sesma A, Schindler C et al. . 2010. Mouse STAT2 restricts early dengue virus replication. Cell Host Microbe 8(5):410-21.

Austin BA, James C, Silverman RH, Carr DJ. 2005. Critical role for the oligoadenylate synthetase/RNase L pathway in response to IFN-beta during acute ocular herpes simplex virus type 1 infection. J Immunol 175(2):1100-6.

Bakonyi T, Hubalek Z, Rudolf I, Nowotny N. 2005. Novel flavivirus or new lineage of West Nile virus, central Europe. Emerg Infect Dis 11(2):225-31.

Barber GN. 2015. STING: infection, inflammation and cancer. Nat Rev Immunol 15(12):760-70.

Barnes BJ, Richards J, Mancl M, Hanash S, Beretta L, Pitha PM. 2004. Global and distinct targets of IRF-5 and IRF-7 during innate response to viral infection. J Biol Chem 279(43):45194-207.

Barral PM, Sarkar D, Su ZZ, Barber GN, DeSalle R, Racaniello VR, Fisher PB. 2009. Functions of the cytoplasmic RNA sensors RIG-I and MDA-5: key regulators of innate immunity. Pharmacol Ther 124(2):219-34.

Basler CF, Amarasinghe GK. 2009. Evasion of interferon responses by Ebola and Marburg viruses. J Interferon Cytokine Res 29(9):511-20.

Basu M, Brinton MA. 2011. West Nile virus (WNV) genome RNAs with up to three adjacent mutations that disrupt long distance 5'-3' cyclization sequence basepairs are viable. Virology 412(1):220-32.

Beasley DW, Whiteman MC, Zhang S, Huang CY, Schneider BS, Smith DR, Gromowski GD, Higgs S, Kinney RM, Barrett AD. 2005. Envelope protein glycosylation status influences mouse neuroinvasion phenotype of genetic lineage 1 West Nile virus strains. J Virol 79(13):8339-47.

Berthet F, Zeller H, Drouet M, Rauzier J, Digoutte J, Deubel V. 1997. Extensive nucleotide changes and deletions within the envelope glycoprotein gene of Euro-African West Nile viruses. Journal of General Virology 78(9):2293-2297.

Blaszczyk K, Olejnik A, Nowicka H, Ozgyin L, Chen YL, Chmielewski S, Kostyrko K, Wesoly J, Balint BL, Lee CK et al. . 2015. STAT2/IRF9 directs a prolonged ISGF3-like transcriptional response and antiviral activity in the absence of STAT1. Biochem J 466(3):511-24.

Bondre VP, Jadi RS, Mishra AC, Yergolkar PN, Arankalle VA. 2007. West Nile virus isolates from India: evidence for a distinct genetic lineage. J Gen Virol 88(Pt 3):875-84.

Borden EC, Sen GC, Uze G, Silverman RH, Ransohoff RM, Foster GR, Stark GR. 2007. Interferons at age 50: past, current and future impact on biomedicine. Nature Reviews Drug Discovery 6(12):975-990.

Bowen JR, Quicke KM, Maddur MS, O'Neal JT, McDonald CE, Fedorova NB, Puri V, Shabman RS, Pulendran B, Suthar MS. 2017. Zika Virus Antagonizes Type I Interferon Responses during Infection of Human Dendritic Cells. PLoS Pathog 13(2):e1006164.

Brass AL, Huang IC, Benita Y, John SP, Krishnan MN, Feeley EM, Ryan BJ, Weyer JL, van der Weyden L, Fikrig E et al. . 2009. The IFITM proteins mediate cellular resistance to influenza A H1N1 virus, West Nile virus, and dengue virus. Cell 139(7):1243-54.

Brehin AC, Casademont I, Frenkiel MP, Julier C, Sakuntabhai A, Despres P. 2009. The large form of human 2',5'-Oligoadenylate Synthetase (OAS3) exerts antiviral effect against Chikungunya virus. Virology 384(1):216-22.

Brennan K, Bowie AG. 2010. Activation of host pattern recognition receptors by viruses. Curr Opin Microbiol 13(4):503-7.

Brierley MM, Fish EN. 2005. Stats: multifaceted regulators of transcription. J Interferon Cytokine Res 25(12):733-44.

Brierley MM, Marchington KL, Jurisica I, Fish EN. 2006. Identification of GAS-dependent interferon-sensitive target genes whose transcription is STAT2-dependent but ISGF3-independent. Febs Journal 273(7):1569-1581.

Brinton MA. 2002. The molecular biology of West Nile Virus: a new invader of the western hemisphere. Annu Rev Microbiol 56:371-402.

Brinton MA. 2014. Replication cycle and molecular biology of the West Nile virus. Viruses 6(1):13-53.

Brinton MA, Basu M. 2015. Functions of the 3' and 5' genome RNA regions of members of the genus Flavivirus. Virus Res 206:108-19.

Bruns AM, Horvath CM. 2012. Activation of RIG-I-like receptor signal transduction. Crit Rev Biochem Mol Biol 47(2):194-206.

Buenrostro JD, Giresi PG, Zaba LC, Chang HY, Greenleaf WJ. 2013. Transposition of native chromatin for fast and sensitive epigenomic profiling of open chromatin, DNA-binding proteins and nucleosome position. Nat Methods 10(12):1213-8.

Caignard G, Guerbois M, Labernardiere JL, Jacob Y, Jones LM, Infectious Mapping Project IM, Wild F, Tangy F, Vidalain PO. 2007. Measles virus V protein blocks Jak1-mediated phosphorylation of STAT1 to escape IFN-alpha/beta signaling. Virology 368(2):351-62.

Chan YK, Gack MU. 2016. A phosphomimetic-based mechanism of dengue virus to antagonize innate immunity. Nat Immunol 17(5):523-30.

Chan YL, Chang TH, Liao CL, Lin YL. 2008. The cellular antiviral protein viperin is attenuated by proteasome-mediated protein degradation in Japanese encephalitis virus-infected cells. J Virol 82(21):10455-64.

Chapman EG, Costantino DA, Rabe JL, Moon SL, Wilusz J, Nix JC, Kieft JS. 2014. The structural basis of pathogenic subgenomic flavivirus RNA (sfRNA) production. Science 344(6181):307-10.

Chen FE, Ghosh G. 1999. Regulation of DNA binding by Rel/NF-kappaB transcription factors: structural views. Oncogene 18(49):6845-52.

Chen YQ, Sengchanthalangsy LL, Hackett A, Ghosh G. 2000. NF-kappaB p65 (RelA) homodimer uses distinct mechanisms to recognize DNA targets. Structure 8(4):419-28.

Cheon H, Stark GR. 2009. Unphosphorylated STAT1 prolongs the expression of interferon-induced immune regulatory genes. Proc Natl Acad Sci U S A 106(23):9373-8.

Cheon H, Yang J, Stark GR. 2011. The functions of signal transducers and activators of transcriptions 1 and 3 as cytokine-inducible proteins. J Interferon Cytokine Res 31(1):33-40.

Chiang JJ, Davis ME, Gack MU. 2014. Regulation of RIG-I-like receptor signaling by host and viral proteins. Cytokine Growth Factor Rev 25(5):491-505.

Clement JF, Bibeau-Poirier A, Gravel SP, Grandvaux N, Bonneil E, Thibault P, Meloche S, Servant MJ. 2008. Phosphorylation of IRF-3 on Ser 339 generates a hyperactive form of IRF-3 through regulation of dimerization and CBP association. J Virol 82(8):3984-96.

Cox J, Hein MY, Luber CA, Paron I, Nagaraj N, Mann M. 2014. Accurate proteome-wide label-free quantification by delayed normalization and maximal peptide ratio extraction, termed MaxLFQ. Mol Cell Proteomics 13(9):2513-26.

Daep CA, Muñoz-Jordán JL, Eugenin EA. 2014. Flaviviruses, an expanding threat in public health: focus on dengue, West Nile, and Japanese encephalitis virus. Journal of neurovirology 20(6):539-560.

Daffis S, Samuel MA, Suthar MS, Gale M, Jr., Diamond MS. 2008. Toll-like receptor 3 has a protective role against West Nile virus infection. J Virol 82(21):10349-58.

Daffis S, Szretter KJ, Schriewer J, Li J, Youn S, Errett J, Lin TY, Schneller S, Zust R, Dong H et al. . 2010. 2'-O methylation of the viral mRNA cap evades host restriction by IFIT family members. Nature 468(7322):452-6.

Dalrymple NA, Cimica V, Mackow ER. 2015. Dengue Virus NS Proteins Inhibit RIG-I/MAVS Signaling by Blocking TBK1/IRF3 Phosphorylation: Dengue Virus Serotype 1 NS4A Is a Unique Interferon-Regulating Virulence Determinant. MBio 6(3):e00553-15.

Damoc E, Fraser CS, Zhou M, Videler H, Mayeur GL, Hershey JW, Doudna JA, Robinson CV, Leary JA. 2007. Structural characterization of the human eukaryotic initiation factor 3 protein complex by mass spectrometry. Mol Cell Proteomics 6(7):1135-46.

Darnell JE, Jr., Kerr IM, Stark GR. 1994. Jak-STAT pathways and transcriptional activation in response to IFNs and other extracellular signaling proteins. Science 264(5164):1415-21.

Dauphin G, Zientara S. 2007. West Nile virus: recent trends in diagnosis and vaccine development. Vaccine 25(30):5563-76.

de Veer MJ, Holko M, Frevel M, Walker E, Der S, Paranjape JM, Silverman RH, Williams BRG. 2001. Functional classification of interferon-stimulated genes identified using microarrays. Journal of Leukocyte Biology 69(6):912-920.

Decroly E, Ferron F, Lescar J, Canard B. 2011. Conventional and unconventional mechanisms for capping viral mRNA. Nat Rev Microbiol 10(1):51-65.

Der SD, Zhou A, Williams BR, Silverman RH. 1998. Identification of genes differentially regulated by interferon α, β, or γ using oligonucleotide arrays. Proceedings of the National Academy of Sciences 95(26):15623-15628.

Diamond MS. 2014. IFIT1: A dual sensor and effector molecule that detects non-2'-O methylated viral RNA and inhibits its translation. Cytokine Growth Factor Rev 25(5):543-50.

Donelan NR, Basler CF, Garcia-Sastre A. 2003. A recombinant influenza A virus expressing an RNA-binding-defective NS1 protein induces high levels of beta interferon and is attenuated in mice. J Virol 77(24):13257-66.

Elbahesh H, Jha BK, Silverman RH, Scherbik SV, Brinton MA. 2011. The Flvr-encoded murine oligoadenylate synthetase 1b (Oas1b) suppresses 2-5A synthesis in intact cells. Virology 409(2):262-70.

Emara MM, Liu H, Davis WG, Brinton MA. 2008. Mutation of mapped TIA-1/TIAR binding sites in the 3' terminal stem-loop of West Nile virus minus-strand RNA in an infectious clone negatively affects genomic RNA amplification. J Virol 82(21):10657-70.

Errett JS, Suthar MS, McMillan A, Diamond MS, Gale M, Jr. 2013. The essential, nonredundant roles of RIG-I and MDA5 in detecting and controlling West Nile virus infection. J Virol 87(21):11416-25.

Escalante CR, Yie J, Thanos D, Aggarwal AK. 1998. Structure of IRF-1 with bound DNA reveals determinants of interferon regulation. Nature 391(6662):103-6.

Eskildsen S, Justesen J, Schierup MH, Hartmann R. 2003. Characterization of the 2'-5'-oligoadenylate synthetase ubiquitin-like family. Nucleic Acids Res 31(12):3166-73.

Evans JD, Crown RA, Sohn JA, Seeger C. 2011. West Nile virus infection induces depletion of IFNAR1 protein levels. Viral Immunol 24(4):253-63.

Evans JD, Seeger C. 2007. Differential effects of mutations in NS4B on West Nile virus replication and inhibition of interferon signaling. J Virol 81(21):11809-16.

Feng D, Sangster-Guity N, Stone R, Korczeniewska J, Mancl ME, Fitzgerald-Bocarsly P, Barnes BJ. 2010. Differential requirement of histone acetylase and deacetylase activities for IRF5-mediated proinflammatory cytokine expression. J Immunol 185(10):6003-12.

Fensterl V, Sen GC. 2011. The ISG56/IFIT1 gene family. J Interferon Cytokine Res 31(1):71-8.

Fensterl V, Sen GC. 2015. Interferon-induced Ifit proteins: their role in viral pathogenesis. J Virol 89(5):2462-8.

Fields BN, Knipe DM, Howley PM. 2013. Fields virology. Philadelphia :: Wolters Kluwer Health/Lippincott Williams & Wilkins. p. 2 volumes (xx, 2456, I-82 pages) : illustrations (some color) ; 29 cm.

Fink K, Grandvaux N. 2013. STAT2 and IRF9: Beyond ISGF3. JAKSTAT 2(4):e27521.

Fitzgerald KA, McWhirter SM, Faia KL, Rowe DC, Latz E, Golenbock DT, Coyle AJ, Liao SM, Maniatis T. 2003. IKKepsilon and TBK1 are essential components of the IRF3 signaling pathway. Nat Immunol 4(5):491-6.

Fox BA, Sheppard PO, O'Hara PJ. 2009. The role of genomic data in the discovery, annotation and evolutionary interpretation of the interferon-lambda family. PLoS One 4(3):e4933.

Fredericksen BL, Keller BC, Fornek J, Katze MG, Gale M, Jr. 2008. Establishment and maintenance of the innate antiviral response to West Nile Virus involves both RIG-I and MDA5 signaling through IPS-1. J Virol 82(2):609-16.

Fujii Y, Shimizu T, Kusumoto M, Kyogoku Y, Taniguchi T, Hakoshima T. 1999. Crystal structure of an IRF-DNA complex reveals novel DNA recognition and cooperative binding to a tandem repeat of core sequences. EMBO J 18(18):5028-41.

Funk A, Truong K, Nagasaki T, Torres S, Floden N, Balmori Melian E, Edmonds J, Dong H, Shi PY, Khromykh AA. 2010. RNA structures required for production of subgenomic flavivirus RNA. J Virol 84(21):11407-17.

Gack MU. 2014. Mechanisms of RIG-I-like receptor activation and manipulation by viral pathogens. J Virol 88(10):5213-6.

Gack MU, Albrecht RA, Urano T, Inn KS, Huang IC, Carnero E, Farzan M, Inoue S, Jung JU, Garcia-Sastre A. 2009. Influenza A virus NS1 targets the ubiquitin ligase TRIM25 to evade recognition by the host viral RNA sensor RIG-I. Cell Host Microbe 5(5):439-49.

Gack MU, Diamond MS. 2016. Innate immune escape by Dengue and West Nile viruses. Curr Opin Virol 20:119-128.

Garcia-Alvarez M, Berenguer J, Jimenez-Sousa MA, Pineda-Tenor D, Aldamiz-Echevarria T, Tejerina F, Diez C, Vazquez-Moron S, Resino S. 2017. Mx1, OAS1 and OAS2 polymorphisms are associated with the severity of liver disease in HIV/HCV-coinfected patients: A cross-sectional study. Sci Rep 7:41516.

Garcia-Sastre A. 2011. Induction and evasion of type I interferon responses by influenza viruses. Virus Res 162(1-2):12-8.

Ghislain JJ, Wong T, Nguyen M, Fish EN. 2001. The interferon-inducible Stat2 : Stat1 heterodimer preferentially binds in vitro to a consensus element found in the promoters of a subset of interferon-stimulated genes. Journal of Interferon and Cytokine Research 21(6):379-388.

Gillespie LK, Hoenen A, Morgan G, Mackenzie JM. 2010. The endoplasmic reticulum provides the membrane platform for biogenesis of the flavivirus replication complex. J Virol 84(20):10438-47.

Goodbourn S, Randall RE. 2009. The regulation of type I interferon production by paramyxoviruses. J Interferon Cytokine Res 29(9):539-47.

Gotoh B, Takeuchi K, Komatsu T, Yokoo J. 2003. The STAT2 activation process is a crucial target of Sendai virus C protein for the blockade of alpha interferon signaling. Journal of Virology 77(6):3360-3370.

Grandvaux N, Servant MJ, tenOever B, Sen GC, Balachandran S, Barber GN, Lin R, Hiscott J. 2002. Transcriptional profiling of interferon regulatory factor 3 target genes: direct involvement in the regulation of interferon-stimulated genes. J Virol 76(11):5532-9.

Grant A, Ponia SS, Tripathi S, Balasubramaniam V, Miorin L, Sourisseau M, Schwarz MC, Sanchez-Seco MP, Evans MJ, Best SM et al. . 2016. Zika Virus Targets Human STAT2 to Inhibit Type I Interferon Signaling. Cell Host Microbe 19(6):882-90.

Gupta S, Jiang M, Pernis AB. 1999. IFN-α activates Stat6 and leads to the formation of Stat2: Stat6 complexes in B cells. The Journal of Immunology 163(7):3834-3841.

Haller O, Staeheli P, Kochs G. 2007. Interferon-induced Mx proteins in antiviral host defense. Biochimie 89(6-7):812-8.

Hayden MS, Ghosh S. 2011. NF-kappaB in immunobiology. Cell Res 21(2):223-44.

Helbig KJ, Beard MR. 2014. The role of viperin in the innate antiviral response. J Mol Biol 426(6):1210-9.

Hida S, Ogasawara K, Sato K, Abe M, Takayanagi H, Yokochi T, Sato T, Hirose S, Shirai T, Taki S et al. . 2000. CD8(+) T cell-mediated skin disease in mice lacking IRF-2, the transcriptional attenuator of interferon-alpha/beta signaling. Immunity 13(5):643-55.

Hoenen A, Gillespie L, Morgan G, van der Heide P, Khromykh A, Mackenzie J. 2014. The West Nile virus assembly process evades the conserved antiviral mechanism of the interferon-induced MxA protein. Virology 448:104-16.

Hoffmann HH, Schneider WM, Rice CM. 2015. Interferons and viruses: an evolutionary arms race of molecular interactions. Trends Immunol 36(3):124-38.

Holm CK, Jensen SB, Jakobsen MR, Cheshenko N, Horan KA, Moeller HB, Gonzalez-Dosal R, Rasmussen SB, Christensen MH, Yarovinsky TO et al. . 2012. Virus-cell fusion as a trigger of innate immunity dependent on the adaptor STING. Nat Immunol 13(8):737-43.

Honda K, Mizutani T, Taniguchi T. 2004. Negative regulation of IFN-alpha/beta signaling by IFN regulatory factor 2 for homeostatic development of dendritic cells. Proc Natl Acad Sci U S A 101(8):2416-21.

Honda K, Taniguchi T. 2006. IRFs: master regulators of signalling by Toll-like receptors and cytosolic pattern-recognition receptors. Nat Rev Immunol 6(9):644-58.

Honda K, Yanai H, Negishi H, Asagiri M, Sato M, Mizutani T, Shimada N, Ohba Y, Takaoka A, Yoshida N et al. . 2005. IRF-7 is the master regulator of type-I interferon-dependent immune responses. Nature 434(7034):772-777.

Hornung V, Hartmann R, Ablasser A, Hopfner KP. 2014. OAS proteins and cGAS: unifying concepts in sensing and responding to cytosolic nucleic acids. Nat Rev Immunol 14(8):521-8.

Horvath CM. 2004. Silencing STATs: lessons from paramyxovirus interferon evasion. Cytokine Growth Factor Rev 15(2-3):117-27.

Hui DJ, Terenzi F, Merrick WC, Sen GC. 2005. Mouse p56 blocks a distinct function of eukaryotic initiation factor 3 in translation initiation. J Biol Chem 280(5):3433-40.

Hyde JL, Gardner CL, Kimura T, White JP, Liu G, Trobaugh DW, Huang C, Tonelli M, Paessler S, Takeda K et al. . 2014. A viral RNA structural element alters host recognition of nonself RNA. Science 343(6172):783-7.

Ikushima H, Negishi H, Taniguchi T. 2013. The IRF family transcription factors at the interface of innate and adaptive immune responses. Cold Spring Harb Symp Quant Biol 78:105-16.

Isaacs A, Lindenmann J. 1957. Virus interference. I. The interferon. Proc R Soc Lond B Biol Sci 147(927):258-67.

Ishikawa H, Ma Z, Barber GN. 2009. STING regulates intracellular DNA-mediated, type I interferon-dependent innate immunity. Nature 461(7265):788-92.

Itsui Y, Sakamoto N, Kurosaki M, Kanazawa N, Tanabe Y, Koyama T, Takeda Y, Nakagawa M, Kakinuma S, Sekine Y et al. . 2006. Expressional screening of interferon-stimulated genes for antiviral activity against hepatitis C virus replication. J Viral Hepat 13(10):690-700.

Jensen S, Thomsen AR. 2012. Sensing of RNA viruses: a review of innate immune receptors involved in recognizing RNA virus invasion. J Virol 86(6):2900-10.

Jiang D, Guo HT, Xu CX, Chang JH, Gu BH, Wang LJ, Block TM, Guo JT. 2008. Identification of three interferon-inducible cellular enzymes that inhibit the replication of hepatitis C virus. Journal of Virology 82(4):1665-1678.

Jiang D, Weidner JM, Qing M, Pan XB, Guo HT, Xu CX, Zhang XC, Birk A, Chang JH, Shi PY et al. . 2010. Identification of Five Interferon-Induced Cellular Proteins That Inhibit West Nile Virus and Dengue Virus Infections. Journal of Virology 84(16):8332-8341.

Justesen J, Hartmann R, Kjeldgaard NO. 2000. Gene structure and function of the 2'-5'-oligoadenylate synthetase family. Cell Mol Life Sci 57(11):1593-612.

Kakuta S, Shibata S, Iwakura Y. 2002. Genomic structure of the mouse 2',5'-oligoadenylate synthetase gene family. J Interferon Cytokine Res 22(9):981-93.

Kalvakolanu DV. 2003. Alternate interferon signaling pathways. Pharmacol Ther 100(1):1-29.

Katibah GE, Lee HJ, Huizar JP, Vogan JM, Alber T, Collins K. 2013. tRNA binding, structure, and localization of the human interferon-induced protein IFIT5. Molecular cell 49(4):743-750.

Kell AM, Gale M, Jr. 2015. RIG-I in RNA virus recognition. Virology 479-480:110-21.

Keller BC, Fredericksen BL, Samuel MA, Mock RE, Mason PW, Diamond MS, Gale M, Jr. 2006. Resistance to alpha/beta interferon is a determinant of West Nile virus replication fitness and virulence. J Virol 80(19):9424-34.

Kim MS, Kim S-Y, Yoon JK, Lee Y-W, Bahn Y-S. 2009. An efficient gene-disruption method in Cryptococcus neoformans by double-joint PCR with NAT-split markers. Biochemical and biophysical research communications 390(3):983-988.

Kimura T, Katoh H, Kayama H, Saiga H, Okuyama M, Okamoto T, Umemoto E, Matsuura Y, Yamamoto M, Takeda K. 2013. Ifit1 inhibits Japanese encephalitis virus replication through binding to 5' capped 2'-O unmethylated RNA. J Virol 87(18):9997-10003.

Knapp S, Yee LJ, Frodsham AJ, Hennig BJ, Hellier S, Zhang L, Wright M, Chiaramonte M, Graves M, Thomas HC et al. . 2003. Polymorphisms in interferon-induced genes and the

outcome of hepatitis C virus infection: roles of MxA, OAS-1 and PKR. Genes Immun 4(6):411-9.

Komar N. 2003. West Nile virus: epidemiology and ecology in North America. Adv Virus Res 61:185-234.

Komatsu T, Takeuchi K, Yokoo J, Gotoh B. 2002. Sendai virus C protein impairs both phosphorylation and dephosphorylation processes of Stat1. Febs Letters 511(1-3):139-144.

Kong KF, Delroux K, Wang X, Qian F, Arjona A, Malawista SE, Fikrig E, Montgomery RR. 2008. Dysregulation of TLR3 impairs the innate immune response to West Nile virus in the elderly. J Virol 82(15):7613-23.

Kramer LD, Styer LM, Ebel GD. 2008. A global perspective on the epidemiology of West Nile virus. Annu Rev Entomol 53:61-81.

Kraus TA, Lau JF, Parisien JP, Horvath CM. 2003. A hybrid IRF9-STAT2 protein recapitulates interferon-stimulated gene expression and antiviral response. J Biol Chem 278(15):13033-8.

Krausgruber T, Saliba D, Ryzhakov G, Lanfrancotti A, Blazek K, Udalova IA. 2010. IRF5 is required for late-phase TNF secretion by human dendritic cells. Blood 115(22):4421-4430.

Kuo TC, Calame KL. 2004. B lymphocyte-induced maturation protein (Blimp)-1, IFN regulatory factor (IRF)-1, and IRF-2 can bind to the same regulatory sites. Journal of Immunology 173(9):5556-5563.

Lanciotti RS, Roehrig JT, Deubel V, Smith J, Parker M, Steele K, Crise B, Volpe KE, Crabtree MB, Scherret JH et al. . 1999. Origin of the West Nile virus responsible for an outbreak of encephalitis in the northeastern United States. Science 286(5448):2333-7.

Laurent-Rolle M, Boer EF, Lubick KJ, Wolfinbarger JB, Carmody AB, Rockx B, Liu W, Ashour J, Shupert WL, Holbrook MR et al. . 2010. The NS5 protein of the virulent West Nile virus NY99 strain is a potent antagonist of type I interferon-mediated JAK-STAT signaling. J Virol 84(7):3503-15.

Lazear HM, Diamond MS. 2015. New insights into innate immune restriction of West Nile virus infection. Curr Opin Virol 11:1-6.

Lazear HM, Lancaster A, Wilkins C, Suthar MS, Huang A, Vick SC, Clepper L, Thackray L, Brassil MM, Virgin HW et al. . 2013. IRF-3, IRF-5, and IRF-7 coordinately regulate the type I IFN response in myeloid dendritic cells downstream of MAVS signaling. PLoS Pathog 9(1):e1003118.

Lee MS, Kim B, Oh GT, Kim YJ. 2013. OASL1 inhibits translation of the type I interferon-regulating transcription factor IRF7. Nat Immunol 14(4):346-55.

Levy DE, Darnell JE, Jr. 2002. Stats: transcriptional control and biological impact. Nat Rev Mol Cell Biol 3(9):651-62.

Levy DE, Marie IJ, Durbin JE. 2011. Induction and function of type I and III interferon in response to viral infection. Curr Opin Virol 1(6):476-86.

Li SH, Dong H, Li XF, Xie X, Zhao H, Deng YQ, Wang XY, Ye Q, Zhu SY, Wang HJ et al. . 2013. Rational design of a flavivirus vaccine by abolishing viral RNA 2'-O methylation. J Virol 87(10):5812-9.

Lin RJ, Chang BL, Yu HP, Liao CL, Lin YL. 2006. Blocking of interferon-induced Jak-Stat signaling by Japanese encephalitis virus NS5 through a protein tyrosine phosphatase-mediated mechanism. J Virol 80(12):5908-18.

Liu WJ, Chen HB, Wang XJ, Huang H, Khromykh AA. 2004. Analysis of adaptive mutations in Kunjin virus replicon RNA reveals a novel role for the flavivirus nonstructural protein NS2A in inhibition of beta interferon promoter-driven transcription. J Virol 78(22):12225-35.

Liu WJ, Wang XJ, Clark DC, Lobigs M, Hall RA, Khromykh AA. 2006. A single amino acid substitution in the West Nile virus nonstructural protein NS2A disables its ability to inhibit alpha/beta interferon induction and attenuates virus virulence in mice. J Virol 80(5):2396-404.

Mackenzie JM, Khromykh AA, Parton RG. 2007. Cholesterol manipulation by West Nile virus perturbs the cellular immune response. Cell Host Microbe 2(4):229-39.

Maher SG, Romero-Weaver AL, Scarzello AJ, Gamero AM. 2007. Interferon: cellular executioner or white knight? Curr Med Chem 14(12):1279-89.

Majoros A, Platanitis E, Kernbauer-Holzl E, Rosebrock F, Muller M, Decker T. 2017. Canonical and Non-Canonical Aspects of JAK-STAT Signaling: Lessons from Interferons for Cytokine Responses. Front Immunol 8:29.

Malur M, Gale M, Jr., Krug RM. 2012. LGP2 downregulates interferon production during infection with seasonal human influenza A viruses that activate interferon regulatory factor 3. J Virol 86(19):10733-8.

Manokaran G, Finol E, Wang C, Gunaratne J, Bahl J, Ong EZ, Tan HC, Sessions OM, Ward AM, Gubler DJ et al. . 2015. Dengue subgenomic RNA binds TRIM25 to inhibit interferon expression for epidemiological fitness. Science 350(6257):217-21.

Mansfield KL, Johnson N, Cosby SL, Solomon T, Fooks AR. 2010. Transcriptional upregulation of SOCS 1 and suppressors of cytokine signaling 3 mRNA in the absence of suppressors of cytokine signaling 2 mRNA after infection with West Nile virus or tick-borne encephalitis virus. Vector Borne Zoonotic Dis 10(7):649-53.

Maringer K, Fernandez-Sesma A. 2014. Message in a bottle: lessons learned from antagonism of STING signalling during RNA virus infection. Cytokine Growth Factor Rev 25(6):669-79.

Mazzon M, Jones M, Davidson A, Chain B, Jacobs M. 2009. Dengue virus NS5 inhibits interferon-alpha signaling by blocking signal transducer and activator of transcription 2 phosphorylation. J Infect Dis 200(8):1261-70.

Michallet MC, Meylan E, Ermolaeva MA, Vazquez J, Rebsamen M, Curran J, Poeck H, Bscheider M, Hartmann G, Koenig M et al. . 2008. TRADD protein is an essential component of the RIG-like helicase antiviral pathway. Immunity 28(5):651-661.

Mori M, Yoneyama M, Ito T, Takahashi K, Inagaki F, Fujita T. 2004. Identification of Ser-386 of interferon regulatory factor 3 as critical target for inducible phosphorylation that determines activation. Journal of Biological Chemistry 279(11):9698-9702.

Moritoh K, Yamauchi H, Asano A, Yoshii K, Kariwa H, Takashima I, Isoda N, Sakoda Y, Kida H, Sasaki N et al. . 2009. Generation of congenic mouse strains by introducing the virus-resistant genes, Mx1 and Oas1b, of feral mouse-derived inbred strain MSM/Ms into the common strain C57BL/6J. Jpn J Vet Res 57(2):89-99.

Morrow AN, Schmeisser H, Tsuno T, Zoon KC. 2011. A novel role for IFN-stimulated gene factor 3II in IFN-gamma signaling and induction of antiviral activity in human cells. J Immunol 186(3):1685-93.

Muir AJ, Shiffman ML, Zaman A, Yoffe B, de la Torre A, Flamm S, Gordon SC, Marotta P, Vierling JM, Lopez-Talavera JC et al. . 2010. Phase 1b study of pegylated interferon lambda 1 with or without ribavirin in patients with chronic genotype 1 hepatitis C virus infection. Hepatology 52(3):822-32.

Mukherjee SP, Behar M, Birnbaum HA, Hoffmann A, Wright PE, Ghosh G. 2013. Analysis of the RelA:CBP/p300 interaction reveals its involvement in NF-kappaB-driven transcription. PLoS Biol 11(9):e1001647.

Munoz-Jordan JL, Fredericksen BL. 2010. How Flaviviruses Activate and Suppress the Interferon Response. Viruses-Basel 2(2):676-691.

Munoz-Jordan JL, Laurent-Rolle M, Ashour J, Martinez-Sobrido L, Ashok M, Lipkin WI, Garcia-Sastre A. 2005. Inhibition of alpha/beta interferon signaling by the NS4B protein of flaviviruses. J Virol 79(13):8004-13.

Murray KO, Walker C, Gould E. 2011. The virology, epidemiology, and clinical impact of West Nile virus: a decade of advancements in research since its introduction into the Western Hemisphere. Epidemiol Infect 139(6):807-17.

Natarajan K, Singh S, Burke TR, Grunberger D, Aggarwal BB. 1996. Caffeic acid phenethyl ester is a potent and specific inhibitor of activation of nuclear transcription factor NF-kappa B. Proceedings of the National Academy of Sciences of the United States of America 93(17):9090-9095.

Ng SL, Friedman BA, Schmid S, Gertz J, Myers RM, Tenoever BR, Maniatis T. 2011. IkappaB kinase epsilon (IKK(epsilon)) regulates the balance between type I and type II interferon responses. Proc Natl Acad Sci U S A 108(52):21170-5.

Ning S, Huye LE, Pagano JS. 2005. Regulation of the transcriptional activity of the IRF7 promoter by a pathway independent of interferon signaling. J Biol Chem 280(13):12262-70.

Oeckinghaus A, Ghosh S. 2009. The NF-kappaB family of transcription factors and its regulation. Cold Spring Harb Perspect Biol 1(4):a000034.

Oeckinghaus A, Hayden MS, Ghosh S. 2011. Crosstalk in NF-kappaB signaling pathways. Nat Immunol 12(8):695-708.

Ogawa S, Lozach J, Benner C, Pascual G, Tangirala RK, Westin S, Hoffmann A, Subramaniam S, David M, Rosenfeld MG et al. . 2005. Molecular determinants of crosstalk between nuclear receptors and toll-like receptors. Cell 122(5):707-21.

Panne D, Maniatis T, Harrison SC. 2004. Crystal structure of ATF-2/c-Jun and IRF-3 bound to the interferon-beta enhancer. EMBO J 23(22):4384-93.

Panne D, Maniatis T, Harrison SC. 2007. An atomic model of the interferon-beta enhanceosome. Cell 129(6):1111-23.

Parisien JP, Lau JF, Rodriguez JJ, Sullivan BM, Moscona A, Parks GD, Lamb RA, Horvath CM. 2001. The V protein of human parainfluenza virus 2 antagonizes type I interferon responses by destabilizing signal transducer and activator of transcription 2. Virology 283(2):230-9.

Paun A, Pitha P. 2007. The IRF family, revisited. Biochimie 89(6):744-753.

Perelygin AA, Zharkikh AA, Scherbik SV, Brinton MA. 2006. The mammalian 2'-5' oligoadenylate synthetase gene family: evidence for concerted evolution of paralogous Oas1 genes in Rodentia and Artiodactyla. J Mol Evol 63(4):562-76.

Perry ST, Buck MD, Lada SM, Schindler C, Shresta S. 2011. STAT2 mediates innate immunity to Dengue virus in the absence of STAT1 via the type I interferon receptor. PLoS Pathog 7(2):e1001297.

Perwitasari O, Cho H, Diamond MS, Gale M, Jr. 2011. Inhibitor of kappaB kinase epsilon (IKK(epsilon)), STAT1, and IFIT2 proteins define novel innate immune effector pathway against West Nile virus infection. J Biol Chem 286(52):44412-23.

Peters RT, Maniatis T. 2001. A new family of IKK-related kinases may function as I kappa B kinase kinases. Biochim Biophys Acta 1471(2):M57-62.

Pichlmair A, Lassnig C, Eberle CA, Gorna MW, Baumann CL, Burkard TR, Burckstummer T, Stefanovic A, Krieger S, Bennett KL et al. . 2011. IFIT1 is an antiviral protein that recognizes 5 '-triphosphate RNA. Nature Immunology 12(7):624-U177.

Pine R. 1992. Constitutive expression of an ISGF2/IRF1 transgene leads to interferon-independent activation of interferon-inducible genes and resistance to virus infection. J Virol 66(7):4470-8.

Pulit-Penaloza JA, Scherbik SV, Brinton MA. 2012a. Activation of Oas1a gene expression by type I IFN requires both STAT1 and STAT2 while only STAT2 is required for Oas1b activation. Virology 425(2):71-81.

Pulit-Penaloza JA, Scherbik SV, Brinton MA. 2012b. Type 1 IFN-independent activation of a subset of interferon stimulated genes in West Nile virus Eg101-infected mouse cells. Virology 425(2):82-94.

Reid SP, Leung LW, Hartman AL, Martinez O, Shaw ML, Carbonnelle C, Volchkov VE, Nichol ST, Basler CF. 2006. Ebola virus VP24 binds karyopherin alpha1 and blocks STAT1 nuclear accumulation. J Virol 80(11):5156-67.

Reid SP, Valmas C, Martinez O, Sanchez FM, Basler CF. 2007. Ebola virus VP24 proteins inhibit the interaction of NPI-1 subfamily karyopherin alpha proteins with activated STAT1. J Virol 81(24):13469-77.

Reisen WK. 2013. Ecology of West Nile virus in North America. Viruses 5(9):2079-105.

Richardson RJ, Dixon J, Malhotra S, Hardman MJ, Knowles L, Boot-Handford RP, Shore P, Whitmarsh A, Dixon MJ. 2006. Irf6 is a key determinant of the keratinocyte proliferation-differentiation switch. Nature Genetics 38(11):1329-1334.

Roby JA, Pijlman GP, Wilusz J, Khromykh AA. 2014. Noncoding subgenomic flavivirus RNA: multiple functions in West Nile virus pathogenesis and modulation of host responses. Viruses 6(2):404-27.

Rodriguez JJ, Parisien JP, Horvath CM. 2002. Nipah virus V protein evades alpha and gamma interferons by preventing STAT1 and STAT2 activation and nuclear accumulation. J Virol 76(22):11476-83.

Rodriguez JJ, Wang LF, Horvath CM. 2003. Hendra virus V protein inhibits interferon signaling by preventing STAT1 and STAT2 nuclear accumulation. J Virol 77(21):11842-5.

Rutherford MN, Hannigan GE, Williams BR. 1988. Interferon-induced binding of nuclear factors to promoter elements of the 2-5A synthetase gene. EMBO J 7(3):751-9.

Saha SK, Pietras EM, He JQ, Kang JR, Liu SY, Oganesyan G, Shahangian A, Zarnegar B, Shiba TL, Wang Y et al. . 2006. Regulation of antiviral responses by a direct and specific interaction between TRAF3 and Cardif. Embo Journal 25(14):3257-3263.

Saito T, Owen DM, Jiang F, Marcotrigiano J, Gale M, Jr. 2008. Innate immunity induced by composition-dependent RIG-I recognition of hepatitis C virus RNA. Nature 454(7203):523-7.

Saliba DG, Heger A, Eames HL, Oikonomopoulos S, Teixeira A, Blazek K, Androulidaki A, Wong D, Goh FG, Weiss M et al. . 2014. IRF5:RelA interaction targets inflammatory genes in macrophages. Cell Rep 8(5):1308-17.

Sato M, Hata N, Asagiri M, Nakaya T, Taniguchi T, Tanaka N. 1998. Positive feedback regulation of type I IFN genes by the IFN-inducible transcription factor IRF-7. FEBS Lett 441(1):106-10.

Satoh T, Kato H, Kumagai Y, Yoneyama M, Sato S, Matsushita K, Tsujimura T, Fujita T, Akira S, Takeuchi O. 2010. LGP2 is a positive regulator of RIG-I- and MDA5-mediated antiviral responses. Proc Natl Acad Sci U S A 107(4):1512-7.

Scherbik SV, Kluetzman K, Perelygin AA, Brinton MA. 2007a. Knock-in of the Oas1b(r) allele into a flavivirus-induced disease susceptible mouse generates the resistant phenotype. Virology 368(2):232-7.

Scherbik SV, Paranjape JM, Stockman BM, Silverman RH, Brinton MA. 2006. RNase L plays a role in the antiviral response to West Nile virus. J Virol 80(6):2987-99.

Scherbik SV, Pulit-Penaloza JA, Basu M, Courtney SC, Brinton MA. 2013. Increased Early RNA Replication by Chimeric West Nile Virus W956IC Leads to IPS-1-Mediated Activation of NF-kappaB and Insufficient Virus-Mediated Counteraction of the Resulting Canonical Type I Interferon Signaling. J Virol 87(14):7952-65.

Scherbik SV, Stockman BM, Brinton MA. 2007b. Differential expression of interferon (IFN) regulatory factors and IFN-stimulated genes at early times after West Nile virus infection of mouse embryo fibroblasts. J Virol 81(21):12005-18.

Schlee M. 2013. Master sensors of pathogenic RNA - RIG-I like receptors. Immunobiology 218(11):1322-35.

Schmid S, Mordstein M, Kochs G, Garcia-Sastre A, Tenoever BR. 2010. Transcription factor redundancy ensures induction of the antiviral state. J Biol Chem 285(53):42013-22.

Schneider WM, Chevillotte MD, Rice CM. 2014. Interferon-Stimulated Genes: A Complex Web of Host Defenses. Annu Rev Immunol.

Schoggins JW, MacDuff DA, Imanaka N, Gainey MD, Shrestha B, Eitson JL, Mar KB, Richardson RB, Ratushny AV, Litvak V et al. . 2014. Pan-viral specificity of IFN-induced genes reveals new roles for cGAS in innate immunity. Nature 505(7485):691-5.

Schoggins JW, Rice CM. 2011. Interferon-stimulated genes and their antiviral effector functions. Curr Opin Virol 1(6):519-25.

Schoggins JW, Wilson SJ, Panis M, Murphy MY, Jones CT, Bieniasz P, Rice CM. 2011. A diverse range of gene products are effectors of the type I interferon antiviral response. Nature 472(7344):481-5.

Schomacker H, Hebner RM, Boonyaratanakornkit J, Surman S, Amaro-Carambot E, Collins PL, Schmidt AC. 2012. The C proteins of human parainfluenza virus type 1 block IFN signaling by binding and retaining Stat1 in perinuclear aggregates at the late endosome. PLoS One 7(2):e28382.

Schroder K, Hertzog PJ, Ravasi T, Hume DA. 2004. Interferon-gamma: an overview of signals, mechanisms and functions. J Leukoc Biol 75(2):163-89.

Schwanhausser B, Busse D, Li N, Dittmar G, Schuchhardt J, Wolf J, Chen W, Selbach M. 2011. Global quantification of mammalian gene expression control. Nature 473(7347):337-42.

Severa M, Coccia EM, Fitzgerald KA. 2006. Toll-like receptor-dependent and -independent viperin gene expression and counter-regulation by PRDI-binding factor-1/BLIMP1. J Biol Chem 281(36):26188-95.

Sharma S, tenOever BR, Grandvaux N, Zhou GP, Lin RT, Hiscott J. 2003. Triggering the interferon antiviral response through an IKK-related pathway. Science 300(5622):1148-1151.

Shaw ML, Cardenas WB, Zamarin D, Palese P, Basler CF. 2005. Nuclear localization of the Nipah virus W protein allows for inhibition of both virus- and toll-like receptor 3-triggered signaling pathways. J Virol 79(10):6078-88.

Shipley JG, Vandergaast R, Deng L, Mariuzza RA, Fredericksen BL. 2012. Identification of multiple RIG-I-specific pathogen associated molecular patterns within the West Nile virus genome and antigenome. Virology 432(1):232-8.

Shiryaev SA, Kozlov IA, Ratnikov BI, Smith JW, Lebl M, Strongin AY. 2007. Cleavage preference distinguishes the two-component NS2B-NS3 serine proteinases of Dengue and West Nile viruses. Biochem J 401(3):743-52.

Silverman RH. 2007. Viral encounters with 2',5'-oligoadenylate synthetase and RNase L during the interferon antiviral response. J Virol 81(23):12720-9.

Sommereyns C, Paul S, Staeheli P, Michiels T. 2008. IFN-lambda (IFN-lambda) is expressed in a tissue-dependent fashion and primarily acts on epithelial cells in vivo. PLoS Pathog 4(3):e1000017.

Sparrer KM, Pfaller CK, Conzelmann KK. 2012. Measles virus C protein interferes with Beta interferon transcription in the nucleus. J Virol 86(2):796-805.

Stark GR, Darnell JE, Jr. 2012. The JAK-STAT pathway at twenty. Immunity 36(4):503-14.

Suthar MS, Diamond MS, Gale M, Jr. 2013. West Nile virus infection and immunity. Nat Rev Microbiol 11(2):115-28.

Suthar MS, Ma DY, Thomas S, Lund JM, Zhang N, Daffis S, Rudensky AY, Bevan MJ, Clark EA, Kaja MK et al. . 2010. IPS-1 is essential for the control of West Nile virus infection and immunity. PLoS Pathog 6(2):e1000757.

Suthar MS, Ramos HJ, Brassil MM, Netland J, Chappell CP, Blahnik G, McMillan A, Diamond MS, Clark EA, Bevan MJ et al. . 2012. The RIG-I-like receptor LGP2 controls CD8(+) T cell survival and fitness. Immunity 37(2):235-48.

Szretter KJ, Brien JD, Thackray LB, Virgin HW, Cresswell P, Diamond MS. 2011. The interferon-inducible gene viperin restricts West Nile virus pathogenesis. J Virol 85(22):11557-66.

Szretter KJ, Daffis S, Patel J, Suthar MS, Klein RS, Gale M, Jr., Diamond MS. 2010. The innate immune adaptor molecule MyD88 restricts West Nile virus replication and spread in neurons of the central nervous system. J Virol 84(23):12125-38.

Szretter KJ, Daniels BP, Cho H, Gainey MD, Yokoyama WM, Gale M, Jr., Virgin HW, Klein RS, Sen GC, Diamond MS. 2012. 2'-O methylation of the viral mRNA cap by West Nile virus evades ifit1-dependent and -independent mechanisms of host restriction in vivo. PLoS Pathog 8(5):e1002698.

Takaoka A, Yanai H. 2006. Interferon signalling network in innate defence. Cell Microbiol 8(6):907-22.

Taniguchi T, Ogasawara K, Takaoka A, Tanaka N. 2001. IRF family of transcription factors as regulators of host defense. Annual Review of Immunology 19:623-655.

Tenoever BR, Ng SL, Chua MA, McWhirter SM, Garcia-Sastre A, Maniatis T. 2007. Multiple functions of the IKK-related kinase IKKepsilon in interferon-mediated antiviral immunity. Science 315(5816):1274-8.

Terenzi F, Hui DJ, Merrick WC, Sen GC. 2006. Distinct induction patterns and functions of two closely related interferon-inducible human genes, ISG54 and ISG56. J Biol Chem 281(45):34064-71.

Terenzi F, Pal S, Sen GC. 2005. Induction and mode of action of the viral stress-inducible murine proteins, P56 and P54. Virology 340(1):116-24.

Terenzi F, Saikia P, Sen GC. 2008. Interferon-inducible protein, P56, inhibits HPV DNA replication by binding to the viral protein E1. EMBO J 27(24):3311-21.

Thackray LB, Shrestha B, Richner JM, Miner JJ, Pinto AK, Lazear HM, Gale M, Jr., Diamond MS. 2014. Interferon regulatory factor 5 (IRF5)-dependent immune responses in the draining lymph node protect against West Nile virus infection. J Virol.

Titus RG, Bishop JV, Mejia JS. 2006. The immunomodulatory factors of arthropod saliva and the potential for these factors to serve as vaccine targets to prevent pathogen transmission. Parasite Immunol 28(4):131-41.

Town T, Bai F, Wang T, Kaplan AT, Qian F, Montgomery RR, Anderson JF, Flavell RA, Fikrig E. 2009. Toll-like receptor 7 mitigates lethal West Nile encephalitis via interleukin 23-dependent immune cell infiltration and homing. Immunity 30(2):242-53.

Uematsu S, Akira S. 2007. Toll-like receptors and Type I interferons. J Biol Chem 282(21):15319-23.

Valmas C, Basler CF. 2011. Marburg virus VP40 antagonizes interferon signaling in a species-specific manner. J Virol 85(9):4309-17.

Valmas C, Grosch MN, Schumann M, Olejnik J, Martinez O, Best SM, Krahling V, Basler CF, Muhlberger E. 2010. Marburg virus evades interferon responses by a mechanism distinct from ebola virus. PLoS Pathog 6(1):e1000721.

van Boxel-Dezaire AH, Rani MR, Stark GR. 2006. Complex modulation of cell type-specific signaling in response to type I interferons. Immunity 25(3):361-72.

van Boxel-Dezaire AH, Zula JA, Xu Y, Ransohoff RM, Jacobberger JW, Stark GR. 2010. Major differences in the responses of primary human leukocyte subsets to IFN-beta. J Immunol 185(10):5888-99.

Venter M, Swanepoel R. 2010. West Nile Virus Lineage 2 as a Cause of Zoonotic Neurological Disease in Humans and Horses in Southern Africa. Vector-Borne and Zoonotic Diseases 10(7):659-664.

Verhelst J, Hulpiau P, Saelens X. 2013. Mx proteins: antiviral gatekeepers that restrain the uninvited. Microbiol Mol Biol Rev 77(4):551-66.

Vladimer GI, Gorna MW, Superti-Furga G. 2014. IFITs: Emerging Roles as Key Anti-Viral Proteins. Front Immunol 5:94.

Wang T, Town T, Alexopoulou L, Anderson JF, Fikrig E, Flavell RA. 2004. Toll-like receptor 3 mediates West Nile virus entry into the brain causing lethal encephalitis. Nature Medicine 10(12):1366-1373.

Wang Y, Swiecki M, McCartney SA, Colonna M. 2011. dsRNA sensors and plasmacytoid dendritic cells in host defense and autoimmunity. Immunol Rev 243(1):74-90.

Weaver BK, Kumar KP, Reich NC. 1998. Interferon regulatory factor 3 and CREB-binding protein/p300 are subunits of double-stranded RNA-activated transcription factor DRAF1. Mol Cell Biol 18(3):1359-68.

Weber M, Gawanbacht A, Habjan M, Rang A, Bomer C, Schmidt AM, Veitinger S, Jacob R, Devignot S, Kochs G et al. . 2013. Incoming RNA Virus Nucleocapsids Containing a 5 '-Triphosphorylated Genome Activate RIG-I and Antiviral Signaling. Cell Host & Microbe 13(3):336-346.

Welsch S, Miller S, Romero-Brey I, Merz A, Bleck CK, Walther P, Fuller SD, Antony C, Krijnse-Locker J, Bartenschlager R. 2009. Composition and three-dimensional architecture of the dengue virus replication and assembly sites. Cell Host Microbe 5(4):365-75.

White LK, Sali T, Alvarado D, Gatti E, Pierre P, Streblow D, Defilippis VR. 2011. Chikungunya virus induces IPS-1-dependent innate immune activation and protein kinase R-independent translational shutoff. J Virol 85(1):606-20.

Wietek C, Miggin SM, Jefferies CA, O'Neill LA. 2003. Interferon regulatory factor-3-mediated activation of the interferon-sensitive response element by Toll-like receptor (TLR) 4 but not TLR3 requires the p65 subunit of NF-kappa. J Biol Chem 278(51):50923-31.

Wilkins C, Gale M, Jr. 2010. Recognition of viruses by cytoplasmic sensors. Curr Opin Immunol 22(1):41-7.

Yamshchikov VF, Wengler G, Perelygin AA, Brinton MA, Compans RW. 2001. An infectious clone of the West Nile flavivirus. Virology 281(2):294-304.

Yan W, Ma L, Stein P, Pangas SA, Burns KH, Bai Y, Schultz RM, Matzuk MM. 2005. Mice deficient in oocyte-specific oligoadenylate synthetase-like protein OAS1D display reduced fertility. Mol Cell Biol 25(11):4615-24.

Yang J, Liao X, Agarwal MK, Barnes L, Auron PE, Stark GR. 2007. Unphosphorylated STAT3 accumulates in response to IL-6 and activates transcription by binding to NFkappaB. Genes Dev 21(11):1396-408.

You F, Wang P, Yang L, Yang G, Zhao YO, Qian F, Walker W, Sutton R, Montgomery R, Lin R et al. . 2013. ELF4 is critical for induction of type I interferon and the host antiviral response. Nat Immunol 14(12):1237-46.

Yu C-Y, Chang T-H, Liang J-J, Chiang R-L, Lee Y-L, Liao C-L, Lin Y-L. 2012a. Dengue virus targets the adaptor protein MITA to subvert host innate immunity. PLoS Pathog 8(6):e1002780.

Yu CY, Chang TH, Liang JJ, Chiang RL, Lee YL, Liao CL, Lin YL. 2012b. Dengue virus targets the adaptor protein MITA to subvert host innate immunity. PLoS Pathog 8(6):e1002780.

Zhang YG, Burke CW, Ryman KD, Klimstra WB. 2007. Identification and characterization of interferon-induced proteins that inhibit alphavirus replication. Journal of Virology 81(20):11246-11255.

Zhu JZ, Zhang YG, Ghosh A, Cuevas RA, Forero A, Dhar J, Ibsen MS, Schmid-Burgk JL, Schmidt T, Ganapathiraju MK et al. . 2014. Antiviral Activity of Human OASL Protein Is Mediated by Enhancing Signaling of the RIG-I RNA Sensor. Immunity 40(6):936-948.